DEVELOPMENT OF A METHODOLOGY FOR POSTING LOAD LIMITS ON LOAD-ZONED PAVEMENTS: INTERIM REPORT

PB98-141013

by

Seong-wan Park
Graduate Assistant Research
Texas Transportation Institute

and

Emmanuel G. Fernando
Associate Research Engineer
Texas Transportation Institute

Research Report 1701-1
Research Study Number 0-1701
Research Study Title: Develop a Method for Determining Allowable Loads on Load-Zoned Pavements

Sponsored by the
Texas Department of Transportation
In Cooperation with
U. S. Department of Transportation
Federal Highway Administration

December 1997

TEXAS TRANSPORTATION INSTITUTE
The Texas A&M University System
College Station, Texas 77843-3135

REPRODUCED BY: NTIS
U.S. Department of Commerce
National Technical Information Service
Springfield, Virginia 22161

Technical Report Documentation Page

1. Report No.	2. Government Accession No.	3. Recipient's Catalog No.
FHWA/TX-98/1701-1		

4. Title and Subtitle	5. Report Date
DEVELOPMENT OF A METHODOLOGY FOR POSTING LOAD LIMITS ON LOAD-ZONED PAVEMENTS: INTERIM REPORT	December 1997
	6. Performing Organization Code
7. Author(s) Seong-wan Park and Emmanuel G. Fernando	8. Performing Organization Report No. Research Report 1701-1
9. Performing Organization Name and Address Texas Transportation Institute The Texas A&M University System College Station, Texas 77843-3135	10. Work Unit No. (TRAIS) 11. Contract or Grant No. Study No. 0-1701
12. Sponsoring Agency Name and Address Texas Department of Transportation Research and Technology Transfer Office P. O. Box 5080 Austin, Texas 78763-5080	13. Type of Report and Period Covered Research: September 1996 - August 1997 14. Sponsoring Agency Code

15. Supplementary Notes

Research performed in cooperation with the Texas Department of Transportation and the U.S. Department of Transportation, Federal Highway Administration.
Research Study Title: Develop a Method for Determining Allowable Loads on Load-Zoned Pavements

16. Abstract

Load-zoned pavements in Texas are presently posted using gross vehicle weight (GVW) limits to prevent or minimize the development of permanent deformation due to excessive truck loads. In reality, pavement damage is more related to axle loads and axle configuration rather than GVW. Thus, load restrictions need to be related to axle loads, axle type, pavement structure, and material characteristics. To address this need, the Texas Department of Transportation (TxDOT) initiated a study with the Texas Transportation Institute (TTI) to develop a procedure for posting or removing load limits based on predicted pavement performance. For this purpose, non-linear elastic and non-linear elasto-plastic programs were developed to predict the structural adequacy of pavements using the Mohr-Coulomb failure criterion. The stress-dependent behavior of pavement materials is considered based on the Universal Soil Model.

This research report presents the results of the work conducted during the first year of the study. Initially, researchers undertook a review of the current practice in Texas to identify the needs that should be addressed in this development work. In addition, a review of load-zoning practices in other agencies was conducted. Findings from the literature survey are summarized herein. Using the programs developed and existing performance models, researchers conducted a sensitivity analysis to identify the factors that significantly influence predicted pavement response and performance. By evaluating the changes in the predicted plastic strains, yield function, and service life with changes in the factors considered, their influence on predicted pavement response and performance was established.

To evaluate the permanent deformation behavior of pavement materials under repeated loadings, researchers also conducted repeated load-permanent deformation tests on a number of base and subgrade materials at various moisture contents and stress conditions. Observations from the laboratory tests were reviewed in relation to known physical behavior and engineering experience. The data from the permanent deformation tests will be used in developing a model to predict rutting in flexible pavements for evaluating load restrictions. This development work is still on-going.

17. Key Words	18. Distribution Statement
Load-Zoning, Flexible Pavements, Load Limits, Permanent Deformation	No restrictions. This document is available to the public through NTIS: National Technical Information Service 5285 Port Royal Road Springfield, Virginia 22161

19. Security Classif.(of this report)	20. Security Classif.(of this page)	21. No. of Pages	22. Price
Unclassified	Unclassified	164	

Form DOT F 1700.7 (8-72) Reproduction of completed page authorized

DISCLAIMER

The contents of this report reflect the views of the authors, who are responsible for the facts and the accuracy of the data presented herein. The contents do not necessarily reflect the official view or policies of the Texas Department of Transportation, or the Federal Highway Administration (FHWA). This report does not constitute a standard, specification, or regulation, nor is it intended for construction, bidding, or permit purposes. The engineer in charge of the project is Dr. Emmanuel G. Fernando, P.E. # 69614.

ACKNOWLEDGMENT

The work reported herein was conducted as part of an ongoing study sponsored by the Texas Department of Transportation (TxDOT) and the Federal Highway Administration, U.S. Department of Transportation. The objective of the study is to develop a procedure for evaluating the need for load restrictions on the basis of predicted pavement performance. The researchers gratefully acknowledge the support and guidance of Mr. Joe Leidy, project director, and Mr. Michael Murphy of the advisory committee who provided detailed information on the current practice of load zoning in Texas. A note of appreciation is also extended to Ms. Cindy Estakhri who surveyed the districts to identify current procedures used to evaluate the need for load restrictions.

TABLE OF CONTENTS

Page

LIST OF FIGURES ix

LIST OF TABLES xviii

CHAPTER 1 INTRODUCTION 1

BACKGROUND 1

PROBLEM STATEMENT 3

RESEARCH OBJECTIVE AND SCOPE OF REPORT 3

CHAPTER 2 LITERATURE REVIEW ON LOAD-ZONING PROCEDURES 5

THE STATE OF PRACTICE OF LOAD-ZONING IN TEXAS 5

Load Restrictions in Texas 5

Survey of TxDOT Districts 6

LOAD-ZONING PRACTICES IN OTHER HIGHWAY AGENCIES 16

U.S. Federal Law 16

Pennsylvania 17

Minnesota 17

Indiana Study 17

Seasonal Load Restrictions 20

Washington DOT 20

Finland Practice 25

Canadian Practice 26

U.K. and E.C. Practices on Load Limits 27

South African Study 28

Permit Fee and Enforcement 29

Summary 37

CHAPTER 3 SENSITIVITY ANALYSIS OF PREDICTED PAVEMENT RESPONSE AND PERFORMANCE 39

BACKGROUND 39

Page

SENSITIVITY OF PREDICTED PLASTIC STRAIN 49
SENSITIVITY OF THE MOHR-COULOMB YIELD FUNCTION VALUE 54
SENSITIVITY OF PREDICTED SERVICE LIFE 57
SUMMARY OF FINDINGS 65
CHAPTER 4 EVALUATION OF PERMANENT DEFORMATION BEHAVIOR 67
LABORATORY TESTS 68
TEST RESULTS 77
REFERENCES 85
APPENDIX A SUMMARY OF TXDOT DISTRICT SURVEY RESPONSES 91
APPENDIX B FORMULATION OF FINITE ELEMENT MODEL 97
APPENDIX C PERMANENT DEFORMATION DATA 109

LIST OF FIGURES

Figures Page

1 Sign for a Load Zoned Segment of FM 362 (GVW 260 kN) 2

2 Thin Pavement Structure and Evaluation Points for Sensitivity Analysis 40

3 Thick Pavement Structure and Evaluation Points for Sensitivity Analysis 40

4 Finite Element Mesh for Pavement Structure 41

5 Variation in Resilient Modulus With Parameter, k_1 (Jooste and Fernando, 1995) 43

6 Illustration of the Hardening Effect Due to θ and the Softening Effect Due to τ_{oct} (Jooste and Fernando, 1995) 44

7 Illustration of the Effect of Load on θ and τ_{oct} 46

8 Illustration of the Effect of Base Thickness on θ and τ_{oct} 46

9 Component of Stresses Under Axisymmetric Loading 48

10 Sensitivity of the Plastic Strain to Changes in k1 and k2 Parameters of the Asphalt Concrete (Center of Load, Thin Pavement) 50

11 Sensitivity of the Plastic Strain to Changes in Cohesion of the Asphalt Concrete (Center of Load, Thin Pavement) 50

12 Sensitivity of the Plastic Strain to Changes in k1, k2, and k3 Parameters of the Base (Center of Load, Thin Pavement) 51

13 Sensitivity of the Plastic Strain to Changes in Cohesion and Angle of Friction of the Base (Center of Load, Thin Pavement) 51

14 Sensitivity of the Plastic Strain to Changes in k1 and k3 Parameters of the Subgrade (Center of Load, Thin Pavement) 52

15 Sensitivity of the Yield Function to Changes in k1 and k2 Parameters of the Asphalt Concrete (Center of Load, Thick Pavement) 55

16 Sensitivity of the Yield Function to Changes in k1, k2, and k3 Parameters of the Base (Center of Load Thick Pavement) 55

LIST OF FIGURES (Continued)

Figures Page

17 Sensitivity of the Yield Function to Changes in k1 and k3 Parameters of the Subgrade (Center of Load, Thick Pavement) 56

18 Sensitivity of the Service Life Based on Rutting to Changes in k1 and k2 Parameters of the Asphalt Concrete (Center of Load, Thin Pavement) 59

19 Sensitivity of the Service Life Based on Rutting to Changes in k1, k2, and k3 Parameters of the Base (Center of Load, Thin Pavement) 59

20 Sensitivity of the Service Life Based on Rutting to Changes in k1 and k3 Parameters of the Subgrade (Center of Load, Thin Pavement) 60

21 Sensitivity of the Service Life Based on Rutting to Changes in k1 and k2 Parameters of the Asphalt Concrete (Center of Load, Thick Pavement) 60

22 Sensitivity of the Service Life Based on Rutting to Changes in k1, k2, and k3 Parameters of the Base (Center of Load, Thick Pavement) 61

23 Sensitivity of the Service Life Based on Rutting to Changes in k1 and k3 Parameters of the Subgrade (Center of Load, Thick Pavement) 61

24 Sensitivity of the Fatigue Life to Changes in k1 and k2 Parameters of the Asphalt Concrete (Center of Load, Thin Pavement) 62

25 Sensitivity of the Fatigue Life to Changes in k1, k2, and k3 Parameters of the Base (Center of Load Thin Pavement) 62

26 Sensitivity of the Fatigue Life to Changes in k1 and k3 Parameters of the Subgrade (Center of Load, Thin Pavement) 63

27 Sensitivity of the Fatigue Life to Changes in k1 and k2 Parameters of the Asphalt Concrete (Center of Load, Thick Pavement) 63

28 Sensitivity of the Fatigue Life to Changes in k1, k2, and k3 Parameters of the Base (Center of Load, Thick Pavement) 64

29 Sensitivity of the Fatigue Life to Changes in k1 and k3 Parameters of the Subgrade (Center of Load, Thick Pavement) 64

LIST OF FIGURES (Continued)

Figures Page

30 Conceptual Pavement Behavior under Traffic (redrawn from CSRA, 1985) 67

31 Environmental Control Chamber and Testing Apparatus of SST 70

32 Test Specimen with Latex Membrane and Platens 72

33 Vertical and Radial LVDTs on Sample 73

34 Conceptual Illustration of Test Results from Repeated Load-Permanent Deformation Testing (Hoyt et al. 1987) 75

35 Effect of Moisture Content on Accumulated Plastic Strain in Clay (13.8 kPa Confining Pressure and 48.3 kPa Deviatoric Stress) 78

36 Effect of Moisture Content on Accumulated Plastic Strain in Clay (13.8 kPa Confining Pressure and 96.6 kPa Deviatoric Stress) 78

37 Effect of Confining Pressure on Accumulated Plastic Strain in Clay (48.3 kPa Deviatoric Stress and at Wet of Optimum Moisture Content) 79

38 Effect of Confining Pressure on Accumulated Plastic Strain in Clay (96.6 kPa Deviatoric Stress and at Wet of Optimum Moisture Content) 79

39 Effect of Deviatoric Stress on Accumulated Plastic Strain in Clay (13.8 kPa Confining Pressure and at Wet of Optimum Moisture Content) 80

40 Effect of Deviatoric Stress on Accumulated Plastic Strain in Clay (41.4 kPa Confining Pressure and at Wet of Optimum Moisture Content) 80

41 Effect of Moisture Content on Accumulated Plastic Strain in Limestone (34.5 kPa Confining Pressure and 172.5 kPa Deviatoric Stress) 81

42 Effect of Moisture Content on Accumulated Plastic Strain in Limestone (103.5 kPa Confining Pressure and 345.0 kPa Deviatoric Stress) 81

43 Effect of Confining Pressure on Accumulated Plastic Strain in Limestone (172.5 kPa Deviatoric Stress and at Wet of Optimum Moisture Content) 82

LIST OF FIGURES (Continued)

Figures Page

44 Effect of Confining Pressure on Accumulated Plastic Strain in Limestone (345.0 kPa Deviatoric Stress and at Optimum Moisture Content) 82

45 Effect of Deviatoric Stress on Accumulated Plastic Strain in Limestone (34.5 kPa Confining Pressure and at Dry of Optimum Moisture Content) 83

46 Effect of Deviatoric Stress on Accumulated Plastic Strain in Limestone (103.5 kPa Confining Pressure and at Wet of Optimum Moisture Content) 83

B1 Gaussian Points in the Eight-Node Element 101

B2 Program Structure for Two-Dimensional Elasto-Plastic Finite Element Analysis Using Stress-Dependency 102

C1 Influence of Moisture Content on Accumulated Plastic Strain in Clay (13.8kPa Confining Pressure, 48.3 kPa Deviatoric Stress) 113

C2 Influence of Moisture Content on Accumulated Plastic Strain in Clay (13.8 kPa Confining Pressure, 96.6 kPa Deviatoric Stress) 113

C3 Influence of Moisture Content on Accumulated Plastic Strain in Clay (41.4 kPa Confining Pressure, 48.3 kPa Deviatoric Stress) 114

C4 Influence of Moisture Content on Accumulated Plastic Strain in Clay (41.4 kPa Confining Pressure, 96.6 kPa Deviatoric Stress) 114

C5 Effect of Confining Pressure on Accumulated Plastic Strain in Clay (48.3 kPa Deviatoric Stress and at Wet of Optimum Moisture Content) 115

C6 Effect of Confining Pressure on Accumulated Plastic Strain in Clay (48.3 kPa Deviatoric Stress and at Optimum Moisture Content) 115

C7 Effect of Confining Pressure on Accumulated Plastic Strain in Clay (48.3 kPa Deviatoric Stress and at Dry of Optimum Moisture Content) 116

C8 Effect of Confining Pressure on Accumulated Plastic Strain in Clay (96.6 kPa Deviatoric Stress and at Wet of Optimum Moisture Content) 116

LIST OF FIGURES (Continued)

Figures Page

C9 Effect of Confining Pressure on Accumulated Plastic Strain in Clay (96.6 kPa Deviatoric Stress and at Optimum Moisture Content) 117

C10 Effect of Confining Pressure on Accumulated Plastic Strain in Clay (96.6 kPa Deviatoric Stress and at Dry of Optimum Moisture Content) 117

C11 Effect of Deviatoric Stress on Accumulated Plastic Strain in Clay (13.8 kPa Confining Pressure and at Wet of Optimum Moisture Content) 118

C12 Effect of Deviatoric Stress on Accumulated Plastic Strain in Clay (13.8 kPa Confining Pressure and at Optimum Moisture Content) 118

C13 Effect of Deviatoric Stress on Accumulated Plastic Strain in Clay (13.8 kPa Confining Pressure and at Dry of Optimum Moisture Content) 119

C14 Effect of Deviatoric Stress on Accumulated Plastic Strain in Clay (41.4 kPa Confining Pressure and at Wet of Optimum Moisture Content) 119

C15 Effect of Deviatoric Stress on Accumulated Plastic Strain in Clay (41.4 kPa Confining Pressure and at Optimum Moisture Content) 120

C16 Effect of Deviatoric Stress on Accumulated Plastic Strain in Clay (41.4 kPa Confining Pressure and at Dry of Optimum Moisture Content) 120

C17 Effect of Deviatoric Stress on Accumulated Plastic Strain in Limestone (34.5 kPa Confining Pressure and 172.5 kPa Deviatoric Stress) 121

C18 Effect of Moisture Content on Accumulated Plastic Strain in Limestone (34.5 kPa Confining Pressure and 345.0 kPa Deviatoric Stress) 121

C19 Effect of Moisture Content on Accumulated Plastic Strain in Limestone (103.5 kPa Confining Pressure and 172.5 kPa Deviatoric Stress) 122

C20 Effect of Moisture Content on Accumulated Plastic Strain in Limestone (103.5 kPa Confining Pressure and 345.0 kPa Deviatoric Stress) 122

LIST OF FIGURES (Continued)

Figures Page

C21 Effect of Confining Pressure on Accumulated Plastic Strain in Limestone (172.5 kPa Deviatoric Stress and at Wet of Optimum Moisture Content) 123

C22 Effect of Confining Pressure on Accumulated Plastic Strain in Limestone (172.5 kPa Deviatoric Stress and at Wet of Optimum Moisture Content) 123

C23 Effect of Confining Pressure on Accumulated Plastic Strain in Limestone (172.5 kPa Deviatoric Stress and at Dry of Optimum Moisture Content) 124

C24 Effect of Confining Pressure on Accumulated Plastic Strain in Limestone (345.0 kPa Deviatoric Stress and at Wet of Optimum Moisture Content) 124

C25 Effect of Confining Pressure on Accumulated Plastic Strain in Limestone (345.0 kPa Deviatoric Stress and at Optimum Moisture Content) 125

C26 Effect of Confining Pressure on Accumulated Plastic Strain in Limestone (345.0 kPa Deviatoric Stress and at Dry of Optimum Moisture Content) 125

C27 Effect of Deviatoric Stress on Accumulated Plastic Strain in Limestone (34.5 kPa Confining Pressure and at Wet of Optimum Moisture Content) 126

C28 Effect of Deviatoric Stress on Accumulated Plastic Strain in Limestone (34.5 kPa Confining Pressure and at Optimum Moisture Content) 126

C29 Effect of Deviatoric Stress on Accumulated Plastic Strain in Limestone (34.5 kPa Confining Pressure and at Dry of Optimum Moisture Content) 127

C30 Effect of Deviatoric Stress on Accumulated Plastic Strain in Limestone (103.5 kPa Confining Pressure and at Wet of Optimum Moisture Content) 127

C31 Effect of Deviatoric Stress on Accumulated Plastic Strain in Limestone (103.5 kPa Confining Pressure and at Optimum Moisture Content) 128

C32 Effect of Deviatoric Stress on Accumulated Plastic Strain in Limestone (103.5 kPa Confining Pressure and at Dry of Optimum Moisture Content) 128

LIST OF FIGURES (Continued)

Figures Page

C33 Effect of Moisture Content on Accumulated Plastic Strain in Caliche (34.5 kPa Confining Pressure and 172.5 kPa Deviatortic Stress) 129

C34 Effect of Moisture Content on Accumulated Plastic Strain in Caliche (34.5 kPa Confining Pressure and 345.0 kPa Deviatortic Stress) 129

C35 Effect of Moisture Content on Accumulated Plastic Strain in Caliche (103.5 kPa Confining Pressure and 172.5 kPa Deviatortic Stress) 130

C36 Effect of Moisture Content on Accumulated Plastic Strain in Caliche (103.5 kPa Confining Pressure and 345.0 kPa Deviatortic Stress) 130

C37 Effect of Confining Pressure on Accumulated Plastic Strain in Caliche (172.5 kPa Deviatoric Stress and at Wet of Optimum Moisture) 131

C38 Effect of Confining Pressure on Accumulated Plastic Strain in Caliche (172.5 kPa Deviatoric Stress and at Optimum Moisture Content) 131

C39 Effect of Confining Pressure on Accumulated Plastic Strain in Caliche (172.5 kPa Deviatoric Stress and at Dry of Optimum Moisture Content) 132

C40 Effect of Confining Pressure on Accumulated Plastic Strain in Caliche (345.0 kPa Deviatoric Stress and at Optimum Moisture Content) 132

C41 Effect of Confining Pressure on Accumulated Plastic Strain in Caliche (345.0 kPa Deviatoric Stress and at Dry of Optimum Moisture Content) 133

C42 Effect of Deviatoric Stress on Accumulated Plastic Strain in Caliche (34.5 kPa Confining Pressure and at Optimum Moisture Content) 133

C43 Effect of Deviatoric Stress on Accumulated Plastic Strain in Caliche (34.5 kPa Confining Pressure and at Dry of Optimum Moisture Content) 134

C44 Effect of Deviatoric Stress on Accumulated Plastic Strain in Caliche (103.5 kPa Confining Pressure and at Wet of Optimum Moisture Content) 134

LIST OF FIGURES (Continued)

Figures Page

C45 Effect of Deviatoric Stress on Accumulated Plastic Strain in Caliche (103.5 kPa Confining Pressure and at Optimum Moisture Content) 135

C46 Effect of Deviatoric Stress on Accumulated Plastic Strain in Caliche (103.5 kPa Confining Pressure and at Dry of Optimum Moisture Content) 135

C47 Effect of Moisture Content on Accumulated Plastic Strain in Iron Ore Gravel (34.5 kPa Confining Pressure and 172.5.0 kPa Deviatoric Stress) 136

C48 Effect of Moisture Content on Accumulated Plastic Strain in Iron Ore Gravel (34.5 kPa Confining Pressure and 3415.0 kPa Deviatoric Stress) 136

C49 Effect of Moisture Content on Accumulated Plastic Strain in Iron Ore Gravel (103.5 kPa Confining Pressure and 172.5 kPa Deviatoric Stress) 137

C50 Effect of Moisture Content on Accumulated Plastic Strain in Iron Ore Gravel (103.5 kPa Confining Pressure and 345.0 kPa Deviatoric Stress) 137

C51 Effect of Confining Pressure on Accumulated Plastic Strain in Iron Ore Gravel (172.5 kPa Deviatoric Stress and at Wet of Optimum Moisture) 138

C52 Effect of Confining Pressure on Accumulated Plastic Strain in Iron Ore Gravel (172.5 kPa Deviatoric Stress and at Optimum Moisture Content) 138

C53 Effect of Confining Pressure on Accumulated Plastic Strain in Iron Ore Gravel (172.5 kPa Deviatoric Stress and at Dry of Optimum Moisture Content) 139

C54 Effect of Confining Pressure on Accumulated Plastic Strain in Iron Ore Gravel (345.0 kPa Deviatoric Stress and at Wet of Optimum Moisture Content) 139

C55 Effect of Confining Pressure on Accumulated Plastic Strain in Iron Ore Gravel (345.0 kPa Deviatoric Stress and at Optimum Moisture Content) 140

C56 Effect of Confining Pressure on Accumulated Plastic Strain in Iron Ore Gravel (345.0 kPa Deviatoric Stress and at Dry of Optimum Moisture Content) 140

LIST OF FIGURES (Continued)

Figures Page

C57 Effect of Deviatoric Stress on Accumulated Plastic Strain in Iron Ore Gravel (34.5 kPa Confining Pressure and at Wet of Optimum Moisture Content) 141

C58 Effect of Deviatoric Stress on Accumulated Plastic Strain in Iron Ore Gravel (34.5 kPa Confining Pressure and at Optimum Moisture Content) 141

C59 Effect of Deviatoric Stress on Accumulated Plastic Strain in Iron Ore Gravel (34.5 kPa Confining Pressure and at Dry of Optimum Moisture Content) 142

C60 Effect of Deviatoric Stress on Accumulated Plastic Strain in Iron Ore Gravel (103.5 kPa Confining Pressure and at Wet of Optimum Moisture Content) 142

C61 Effect of Deviatoric Stress on Accumulated Plastic Strain in Iron Ore Gravel (103.5 kPa Confining Pressure and at Optimum Moisture Content) 143

C59 Effect of Deviatoric Stress on Accumulated Plastic Strain in Iron Ore Gravel (103.5 kPa Confining Pressure and at Dry of Optimum Moisture Content) 143

LIST OF TABLES

Table Page

1 Load-Zoned Roads per District (TxDOT 1996) 7

2 Roadways Analyzed in the Last Few Years for Load Zoning 14

3 The Benefits of Using Load Restrictions (Mahoney et al. 1987) 21

4 Timing for Load Restrictions (Mahoney and Jackson 1990) 22

5 Example Freeze and Thaw Data (Mahoney and Jackson 1990) 23

6 Example Freeze and Thaw Data (Mahoney et al. 1987) 24

7 Threshold Values for Weight Restrictions in Finland (Isotalo 1996) 25

8 Axle Weight Limits in Canada and the U.S. (Nix et al. 1992) 27

9 Gross Vehicle Weight and Size Restrictions in Canada and the U.S. (Nix et al. 1992) 27

10 Axle Weight Limits in the E.C. and the U.K. (Nix et al. 1992) 27

11 Gross Vehicle Weight and Size Restrictions in the E.C. and the U.K. (Nix et al. 1992) 28

12 Axle Load Limits in South Africa (Vantonder et al. 1992) 28

13 Annual Overweight Permit Fees for Those States Who Base Their Fees on Vehicle Weight and Distance Traveled (Moffett and Whitford 1995) 32

14 Annual Overweight Permit Fees for Those States Who Charge Flat-Fee Independent of Vehicle Configuration, Distance Traveled, and Commodity Shipped (Moffett and Whitford 1995) 32

15 Annual Overweight Permit Fees for Those States Who Base Fees on Vehicle Configuration (Moffett and Whitford 1995) 33

16 Maximum Weight That Each State Will Issue an Annual Overweight Permit (Moffett and Whitford 1995) 33

LIST OF TABLES (Continued)

Table Page

17 States Who Issue a Blanket Annual Overweight Permit with an Accompanying Official Route Map that Must Always be Attrached to the Permit (Moffett and Whitford 1995) 34

18 States Who Issue a Blanket Annual Overweight Permit Without Any Type of Accompanying Official Route Map (Moffett and Whitford 1995) 34

19 States Who Issue Annual Overweight Permits that Restrict Movements to Either Specific Loads or Specific Routes (Moffett and Whitford 1995) 35

20 States Who Issue Annual Overweight Permits and Still Require a Company to Call-in or a Specific Route Authorization for Each Trip (Moffett and Whitford 1995) 35

21 Summary of Load-Zoning Information from DOT Web Sites 36

22 Summary of Internet Addresses of the DOT Web Sites 37

23 Base Levels of Resilient Parameters Used in Sensitivity Analysis 47

24 Base Levels of Strength Parameters Used in Sensitivity Analysis 47

25 Gradation of Materials Tested (Percent Passing Under Sieve Size) 71

26 Atterberg Limits of Materials Tested 71

27 Moisture Content at Which Samples Were Prepared 76

28 The Level of Test Loads for Materials 76

C1 Moisture Content and Measured Stress Level for Crushed Limestone and Clay 111

C2 Moisture Content and Measured Stress Level for Iron Ore Gravel and Caliche 112

CHAPTER 1
INTRODUCTION

BACKGROUND

Overweight and oversized vehicles play an important role in the economic development of a given region. The productivity in the movement of goods can certainly be enhanced if trucks are allowed to use highways at their peak operating capacities. However, the consequent increase in the truck loadings will accelerate the deterioration of highways and bridges. Unless additional funds are available to upgrade existing highways to higher standards or to pay for the increased maintenance and resurfacing costs due to the accelerated deterioration, the highway network will deteriorate to an unacceptable condition. Consequently, states have established load restrictions to maintain and preserve the highway infrastructure.

Current regulations restrict the gross vehicle weight (GVW) to prevent or minimize the development of permanent deformation due to excessive truck loads. Figure 1 shows the posted gross vehicle weight limit on a load-zoned segment of FM 362. However, pavement performance is much more associated with axle loads and axle configuration rather than GVW (Fernando et al. 1987). Crockford (1993) showed that a vehicle with a GVW of 356 kN can cause five times more pavement damage than a vehicle weighing 260 kN, the legal load limit on load-zoned roads in Texas. In addition, a truck with a GVW of 260 kN can induce serious pavement damage if the pavement is not designed to carry that load. Further, the gross vehicle weight may be within 356 kN, but significant pavement damage can still be induced because of higher axle loads. Thus, load restrictions need to be related to axle loads, axle type, pavement layer thicknesses, and material characteristics.

Permit fees are generally inadequate to pay for roadway maintenance and repair due to pavement damage from overweight vehicles. Clearly, a permit fee schedule that is tied to predicted pavement damage would be more equitable in terms of assigning cost responsibility to road users. This development will require a quantitative study on the relationships between vehicle loadings and pavement damage.

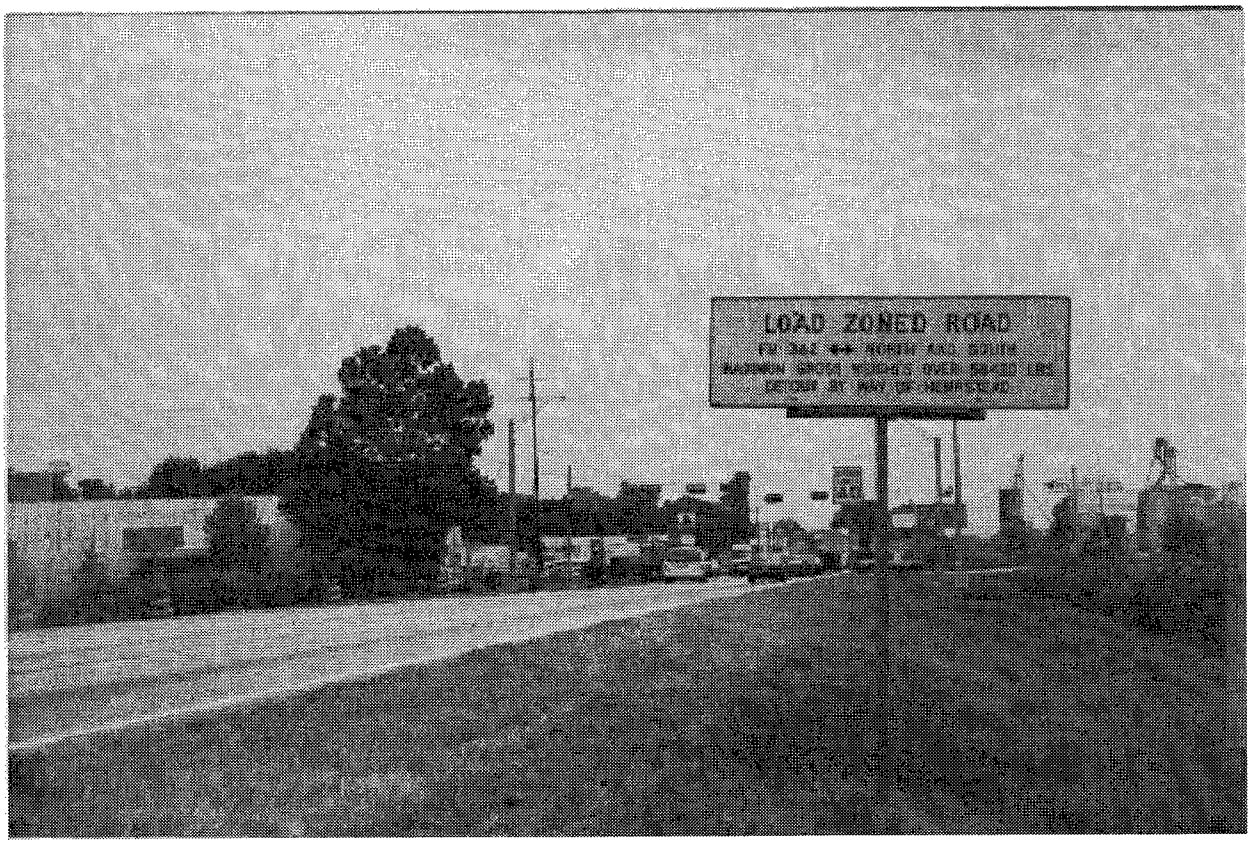

Figure 1. Sign for a Load Zoned Segment of FM 362 (GVW 260 kN).

Permit fees and types of permits issued vary from state to state. Moffett and Whitford (1995) showed that issuing annual overweight permits may lead to significant revenue loss compared with single-trip permits. Fees for annual permits are difficult to assess on the basis of vehicle configuration and distance traveled. The issuance of annual overweight permits without route control was not recommended either. Other alternatives identified by Moffett and Whitford are permit fees based on weight and distance traveled and trip-by-trip permits. However, the types of permits issued and the fees assessed should depend on the trucking business and be tied to pavement management objectives. The study recommends the development and use of a route map to implement overweight and oversized regulations. This map will identify roadways in terms of required gross vehicle and axle weights and axle spacing.

Numerous factors need to be considered in developing load-zoning procedures. Among these are vehicle-related factors such as gross vehicle and axle weights, tire contact

pressure, wheel configuration and axle spacing, vehicle configuration, and vehicle dynamics. Route-related factors such as bridge capacity and pavement structure must logically be considered in determining load restrictions. Relationships between vehicle loadings and pavement damage are important in assigning cost responsibility and developing a permit fee schedule. Implementation is also a valid concern.

PROBLEM STATEMENT

Texas has approximately 28,200 km of load-zoned pavements. About 98 percent of these are posted with a gross vehicle weight (GVW) restriction of 260 kN. While easy to implement, it is recognized that the gross load from a vehicle is transmitted through the axle tires. Thus, the tire loads and the geometric arrangement of the tires comprising the axle are the factors that more directly influence the response of the pavement to the vehicle rather than its gross weight. Indeed, a vehicle may be in compliance with the GVW limit but still be damaging because of axle loads that exceed the pavement's structural capacity. Load restrictions need to be related to axle loads, axle type, pavement structure, and material characteristics. A need therefore exists within the Texas Department of Transportation (TxDOT) for a methodology of determining load limits on the basis of axle load and axle configuration.

RESEARCH OBJECTIVE AND SCOPE OF REPORT

The objective of this study is to develop a methodology for posting or removing load limits on Texas highways. To accomplish this objective, a work plan consisting of the following major tasks was established.

1. Review previously published literature on load-zoning procedures and establish the state of the practice of load zoning in Texas;
2. Identify factors important for load zoning;
3. Develop the load zoning procedure; and
4. Submit recommendations for implementation.

This interim report presents the results of tasks 1 and 2 above. Researchers conducted a survey of the different districts to establish the current practice of load zoning in the state. Because of recent legislation allowing the operation of trucks with higher than allowable gross vehicle weights and axle loads, this survey established the need for a methodology that TxDOT can use to post or lift load restrictions, and to determine requirements for upgrading existing roadways to carry the expected traffic loads. Chapter 2 presents the findings from the literature review.

To identify factors important for load zoning, researchers evaluated the effects of design and materials related factors on predicted pavement response and performance. Nonlinear elastic and elasto-plastic pavement models were used to evaluate the change in the Mohr-Coulomb yield function and the predicted plastic strain, with changes in the values of the factor considered. Predicted pavement response from the nonlinear model were also used with existing performance models to evaluate the sensitivity of predicted service life to the factors considered. Chapter 3 presents the findings from the sensitivity analysis.

As part of the ongoing development of a permanent deformation model, researchers also conducted repeated load-permanent deformation tests on a number of base and subgrade materials. Laboratory tests were conducted at various stress conditions on molded specimens prepared at three different moisture levels. Chapter 4 presents findings from the repeated load-permanent deformation tests.

CHAPTER 2
LITERATURE REVIEW ON LOAD-ZONING PROCEDURES

In order to obtain a more comprehensive understanding of problems and needs, a survey of all TxDOT Districts was performed to establish the state of the practice of load-zoning in Texas. In addition, a review of load-zoning practices in other agencies was conducted. The following presents a review of the current practice.

THE STATE OF THE PRACTICE OF LOAD-ZONING IN TEXAS

Load Restrictions in Texas

Most of the load-zoned pavements in Texas are posted with a gross vehicle weight (GVW) restriction of 260 kN. Currently more than 22 percent (28,175 km) of the 123,513 centerline kilometers of highways on the state-maintained system are posted or load-zoned. These pavements are primarily low-volume farm-to-market roads that do not have enough structural adequacy for the non-restricted use of overloaded trucks.

Maximum legal weights are the same as Federal law except for tridem axles where a limit of 187 kN is used. Tire pressure is limited to 1.05 kN per centimeter of tire width and no wheel load may exceed 35.6 kN. For vehicles carrying agricultural products, axle loads up to 12 percent higher than the legal axle weight limit are allowed without a permit. In addition, vehicles under the permit may operate within a 5 percent tolerance of legal gross vehicle weights.

From a survey of load-zoning practice in Texas, load restrictions are posted based on Falling Weight Deflectometer (FWD) data and local experience. Texas triaxial tests are also used to check subgrade soil strength and adequacy of pavement structure. Backcalculated moduli from FWD data are used in an elastic layered analysis to predict pavement response under an 80 kN single axle load. The predicted pavement response is then used with existing performance models to predict the service life of the given pavement based on fatigue cracking and rutting. Predicted service life is then checked against the expected equivalent

80 kN single axle load applications to evaluate the need for load restrictions. Finally, engineering judgment plays a key role in determining whether to post load restrictions or not.

In the 1980s, the Texas Transportation Institute (TTI) developed the LOADRATE program in an attempt to analyze load-zoned pavements (Chua et al. 1987). Using deflection basins from FWD and the ILLI-PAVE finite element program, nonlinear elastic properties of the base and subgrade are back-calculated, and then the residual deformation of pavements is determined. From the results of LOADRATE, the expected life of the pavement and allowable axle loads for low-volume roads are calculated on the basis of a specified rut depth.

Yapa and Lytton (1988) performed another study connected with predicting permanent deformation of low-volume roads. A three-dimensional analysis program, where a multi-layered flexible pavement is represented by assemblies of the Mechano-lattice element, was used to predict rut depth development in a given pavement. The required parameters are the thickness of the pavement layers, and the resilient moduli of the base and the subgrade layers. Of these, the resilient modulus can be estimated using FWD testing or in the laboratory. Then the rut depth for different pavements can be predicted using the Mechano-Lattice program, which uses a multidimensional polynomial interpolation technique. Finally, the service life based on rut depth of a given pavement can be estimated.

The LOADRATE program was compared with the Texas triaxial class method by Jackson and Murphy (1992). Their study showed that the allowable wheel loads from LOADRATE were not as sensitive to changes in pavement thickness as the wheel loads determined from the Texas triaxial class method. In addition, the results from LOADRATE indicated that load-zoning was not required for most of the pavements tested. Based on the results, the authors recommended further review and evaluation of LOADRATE before it is implemented in Texas.

Survey of TxDOT Districts

Table 1 shows a summary of the total amount of posted roads in each district as provided by the Pavements Section of the Design Division of TxDOT. Many of the districts in the state are removing the 260 kN restriction from FM roads as these roads are

Table 1. Load-Zoned Roads per District.

District	Length, km	Percent of Total
(1) Paris	2494	7.26%
(2) Fort Worth	1963	5.71%
(3) Wichita Falls	2413	7.02%
(4) Amarillo	1337	3.89%
(5) Lubbock	0	0
(6) Odessa	0	0
(7) San Angelo	249	0.72%
(8) Abilene	1152	3.35%
(9) Waco	9097	26.47%
(10) Tyler	2500	7.28%
(11) Lufkin	924	2.69%
(12) Houston	688	2.00%
(13) Yoakum	1867	5.43%
(14) Austin	1058	3.08%
(15) San Antonio	1370	3.99%
(16) Corpus Christi	1810	5.27%
(17) Bryan	1029	2.99%
(18) Dallas	1592	4.63%
(19) Atlanta	0	0
(20) Beaumont	807	2.35%
(21) Pharr	1080	3.14%
(22) Laredo	540	1.57%
(23) Brownwood	227	0.66%
(24) El Paso	92	0.27%
(25) Childress	75	0.22%

rehabilitated. Pavement engineers were contacted in each district to identify current methods/procedures for posting (or removing load limits on) a road. Appendix A provides a summary of district responses. In general, researchers found that those districts which are actively changing load-zone requirements work with FWD data, visual evaluations and triaxial classifications. Pavement analyses regarding load-zone requirements are performed by the Pavements Section of TxDOT's Design Division. Most of the load-zone changes are done after a pavement is rehabilitated. On rehabilitation projects on FM roads, every effort is made to design and construct the pavement so that the 260 kN load restriction can be removed. The following is a summary of information related to load-zoning practices provided by Mr. Michael Murphy of the Pavements Section.

Factors Considered for Posting or Removing Load Limits on a Roadway

Traffic:

- 80 kN ESALS (10 year and 20 year projections; 10 year typically used for analysis).
- ADT (average daily traffic at present and future).
- Traffic directional distribution.
- ATHWLD (average of the ten heaviest wheel loads).
- Percentage of tandem axles.
- Current or future planned commercial activities which generate high truck volumes. [An on-site investigation of local land use is desirable. The traffic projections from the Transportation Planning and Program (TPP) Division do not reflect the presence of businesses or other activities which generate heavy truck traffic. However, due to time and travel constraints, an on-site investigation is not common.]

Pavement Typical Section and Subgrade Conditions:

- Layer thicknesses.
- Material type(s).

- Presence of stabilized or bound layers, especially lime-, asphalt- or cement-treated.
- Presence of old pavement structures which may underlie the load-zoned pavement in some areas. For example, old 9-6-9 concrete pavements may underlie portions of a load-zoned pavement.
- Depth to rigid layer or bedrock.
- Subgrade type(s) (typically refers to Soil Conservation Service [SCS] soil surveys).
- Local geology (typically refers to geologic maps, and/or Texas roadside geology).
- Pavement age.
- Lane and shoulder widths (if a shoulder is present).

Monitoring Data:

- PMIS or project level, visual pavement condition including distress type, extent, and severity.
- FWD deflection data (four load levels: 26.7, 35.5, 44.4, 66.7 kN). Typically, deflections measured at a load level of 44.4 kN are used for the analysis.
- Core data, if available, to verify thicknesses.
- Back-calculated layer moduli.
- Modular ratios (greater than 4:1 or 6:1 is typically cause for further investigation).
- Texas triaxial classification of the subgrade.
- Estimated cohesiometer values for bound layers; used in Texas triaxial methodology to account for allowable reductions in layer thickness; chart in Materials and Tests manual typically used to determine cohesiometer value.
- Local climatic conditions (east Texas = high rainfall, for example).

***Pavement Response Data*:**

- Deflection bowl parameters including Surface Curvature Index (SCI), and magnitudes of sensor 1 and sensor 7 displacements.
- Horizontal tensile strain at the bottom of the AC layer.
- Vertical compressive strain at the top of the subgrade.

Other Factors:

- Will load posting restrict local business activities?
- Are feasible, alternate routes available which can carry legal loads?
- Is the load posting to be permanent or temporary (60 days or less)?
- Are other pavements in the area that have similar structures load posted?
- If the roadway is currently load posted, is a local company requesting the load posting to be lifted? Is the roadway currently programmed for rehabilitation or reconstruction ? If not, the requesting company will have to pay for rehabilitating the roadways so that load restrictions can be lifted.

Data Collection

- Falling Weight Deflectometer (FWD) Data: The District is requested to obtain FWD data using project level/load-zone criteria. This means that drop intervals are spaced at a maximum of 0.16 km, and at least 30 intervals per section are evaluated. A series of drop loads (26.6 kN, 40.0 kN, 53.5 kN, and 71.1 kN) is taken at each drop location. If the route is long (> 15 km), the test spacing may be increased so that the number of test sites is not excessive. The FWD operator is asked to reduce test spacing if unusual deflections are noted in a given area.
- Visual evaluations are performed by District personnel during FWD data collection. A summary of the pavement condition (sometimes with photographs) will be provided to the Pavements Section on Form 1084R (*Recommended Change in Road Load Zoning*).

- Pavement cores may be requested if the deflection data indicates unusually low or high deflections for the specified structure. If the FWD data is difficult to interpret, a field visit may be made by the District and Pavements Section staff.
- Triaxial testing is rarely performed. The District historical records or laboratory personnel experiences are typically relied on for triaxial classification.
- If construction plans are available and bridges are along the route, the available bridge foundation core log information are sometimes used to verify depth to rigid layer calculations made by the MODULUS program (Uzan et al. 1988).

Engineering Methodology Used to Post a Roadway

Typically, an analysis of the pavement structure is performed using backcalculated moduli and FWD deflection bowl parameters. The moduli and layer thicknesses are used in the BISAR layered elastic program to compute strains at selected points in the pavement structure based on a 44.5 kN single-wheel load. The Asphalt Institute rutting and fatigue models are then used to compute 80 kN ESALs to failure. The results are compared with the 10-year projected traffic (ESALs) to determine if the pavement structure is adequate. The results are then checked against the Texas triaxial classification methodology. The Texas triaxial method evaluates the structure to determine if an adequate thickness of better material is available to carry a design wheel load (44.5 kN). Engineering judgment is used to evaluate the results of the layered elastic and Texas triaxial analyses based on knowledge of local conditions, historical performance of similar pavements in the area and other factors.

Analysis Procedures Used

Modified triaxial procedures are used as a check against subgrade compressive failure. The average of the ten heaviest wheel loads (ATHWLD), a statistically generated variable provided by TPP, is used as the design load. It has nothing to do with actual traffic using the route. These loads are considerably heavier than traffic loads allowed on a load-zoned roadway. If the route is a typical thin structure, the more lenient 10-year performance period

is generally used, since these pavements would generally receive an overlay or other rehabilitation around this time frame.

FWD data are analyzed by using the remaining life and back-calculation routines in MODULUS. Generally a 10-year accumulation of ESALs is used in the remaining life analysis for thin pavement structures. Raw deflections and back-calculated layer moduli values provide a method for estimating layer strength (SCI, BCI, W7 deflections, E2/E4). The moduli values are also used as input in linear elastic programs like WESLEA.

WESLEA is used to generate tensile strain values at the bottom of the asphalt layer and compressive strains at the top of the subgrade. These values are then used as input into the Asphalt Institute's equations for predicting service life based on fatigue cracking and rutting criteria. Repetitions to failure are then compared against the estimated traffic (accumulated ESALs).

In one case, an analysis was made for a pavement having a thin asphalt overlying a 15 cm cement stabilized base. In this case, Westergaard formulas were used to predict the edge stress at the bottom of the stabilized layer which was compared to an assumed modulus of rupture (stress ratio). Repetitions to failure were estimated using a PCC fatigue model. Plots are typically made of the following factors:

- Layer moduli along the project length. Low, medium, and high moduli bands may be identified on the graph to help in interpreting outliers.
- SCI and W7 sensor readings. Low, medium, and high deflection bowl parameter bands may be identified on the graph to help in interpreting weak spots or outliers.
- Estimated 80 kN ESALs to failure plotted in relation to the 10 and 20 year design traffic.
- Modular ratios between surface and base, or base and subgrade may be plotted if unusual circumstances (high ratios) are noted.

Average moduli values are typically used unless engineering judgment dictates otherwise. An analysis may be performed using the average surface, base, or subgrade moduli value minus one standard deviation if the values are highly variable. Poisson's ratios are assumed as follows:

- AC Surface 0.35
- PCC Slab 0.15
- Flexible Base 0.30
- Cement Stabilized Base 0.20
- Lime Stabilized Base 0.20
- Lime Treated Subgrade 0.25-0.30
- Raw Subgrade 0.40

Pavement Types Typically Posted

Many of the pavement roadways which are currently posted have 100 mm or 150 mm flexible base layers with multiple surface treatments or seal coats. However, many other types of pavement structures are also posted. The rehabilitation or reconstruction of a load-zoned roadway may result in a new structure which requires load-zone evaluation. The new structure may include multiple layers with moderate or thick asphalt surface and asphalt stabilized base layers, stabilized, or chemically treated base layers and lime or cement treated subgrades. Table 2 is a list of roadways that have been analyzed during the past few years.

The length of a roadway may be as short as 1 km and as long as 30 km. The typical section along a load-zoned roadway can vary substantially in widths, layer thicknesses and material types; for example, refer to the sections associated with FM 907 (Pharr District), FM 1957 (San Antonio) and FM 1098 (Houston) in Table 2. Form 1084R contains a description of the typical section of a load-zoned road. This information includes lane and shoulder widths, layer types and thicknesses, and subgrade type or triaxial class. A typical section drawing is not usually provided unless requested, or unless a Flexible Pavement System (FPS) analysis has been performed as part of a rehabilitation or reconstruction project.

Table 2. Roadways Analyzed in the Last few Years For Load Zoning.

District	Roadway	Surface	Base	Subbase	Subgrade
Amarillo	FM 2250	1-CST	127 mm Flexible Base	-	Trx. Cl. 3.3
	FM 2373	38 mm ACP	305 mm Caliche/Sand gravel mix	-	Black Clay
	FM 2202	1-CST	203 mm Caliche Base	-	Sandy Loam
	FM 722	3-CST	152 mm Caliche Base	-	Sandy Loam
	FM 1412	1-CST	127 mm Flexible Base	-	Clay
	FM 809	2-CST + 3SC	152 mm Caliche Base	-	Sandy Loam
	FM 809	2-CST + 4SC	127 mm Caliche Base	-	Clayey Loam
	FM 924	1-CST	152 mm Flexible Base	-	Sandy Loam
	FM 296	1-CST + 4SC	127 mm Caliche Base	-	Clay
	FM 1259	2-CST	254 mm Flexible Base	-	Clay
	FM 290	2-CST	127 mm Flexible Base	-	Sandy Loam
Childress	FM 392	2-CST	279 mm Flexible Base	-	Sandy Loam
	FM 277	2-CST	279 mm Flexible Base	-	Sandy Loam
	FM 925	2-CST	152 mm Flexible Base	-	Sandy Loam
	FM 267	1-CST	152 mm Flexible Base	-	Sandy Loam
	FM 267	2-CST	203 mm Flexible Base	-	Sandy Loam
	FM 1919	2-CST	203 mm Flexible Base	-	Sandy Loam
	FM 98	1-CST	152 mm Flexible Base	-	
Corpus Christi	FM 1355	2-CST	305 mm Stabilized Caliche	-	Trx Cl. 4.9
	FM 1945	2-CST	457 mm Lime Treated Base (Caliche)	-	Trx Cl. 4.2
Dallas	FM 1722	2-CST	203 mm Flexible Base	-	Trx. Cl. 5.3
	FM 1722	64 mm ACP	203 mm (avg) Lime-Treated Salvaged Base	-	Trx. Cl. 5.3
	FM 148	2-CST	203 mm Flexible Base	-	Trx. Cl. 5.0
	FM 85	89 mm ACP	203 mm Flexible Base	-	Trx. Cl. 5.4
	FM 2786	1-CST	203 mm Flexible Base	-	Trx. Cl. 6.0
	FM 1171	76 mm ACP	203 mm Flexible Base	-	Trx. Cl. 6.0
El Paso	FM 260	32 mm ACP	203 mm Flexible Base	-	-
	FM 260	2-CST	203 mm Flexible Base	-	-
Houston	FM 1098	159-178 mm ACP	152 mm Iron Ore Base	-	Trx. Cl. 3.8
	FM 1098	108 mm ACP	203 mm Lime Treated Base	-	Trx. Cl. 3.8
	FM 359	76 mm ACP	305 mm Cement Stabilized Base	152 mm LTS	Trx. Cl. 5.9
	FM 1488	38 mm ACP	102 mm Asphalt Stabilized Base	152 mm Flex	Clay
	FM 1488	57 mm ACP	51-102 mm Asphalt Stabilized Base	152 mm Iron Ore	Clay
Paris	FM 269	2-CST	102 mm New Flexible Base	102 mm Old Base	Trx. Cl 3.4
Pharr	FM 493	38 mm ACP	102 - 152 mm Flexible Base	203 mm LTS	Trx. Cl. 4.8
	FM 907	38 mm ACP	165 mm Asphalt Stabilized Base	9-6-9 PCC	Trx. Cl. 5.0
	FM 907	38 mm ACP	254 mm Lime Treated Base	-	Trx. Cl. 5.0 Trx.
	FM 907	38 mm ACP	229 mm Flexible Base	-	Cl. 5.0
	FM 907	38 mm ACP	64 mm ASB + 203 mm Flex Base	-	Trx. Cl. 5.0
	FM 2348	89 mm ACP	152 mm Flexible Base	203 mm LTS	Trx. Cl. 6.4
	FM 490	76 mm ACP	152 mm Flexible Base	-	Trx. Cl. 4.5
	FM 490	38 mm ACP	102 mm Lime Treated Base (1%)	-	Trx. Cl. 4.5
San Angelo	US 87	114 mm ACP	305 mm Flexible Base	-	Clay
San Antonio	FM 1044	38 mm ACP	305 mm Flexible Base	-	Trx. Cl. 4.9
	FM 1937	32 mm ACP	254 mm Flexible Base	152 mm LTS	Trx. Cl. 4.6
	FM 1957	51 mm ACP	457 mm Flexible Base	-	Trx. Cl. 4.9
	FM 1957	51 mm ACP	254 mm Asphalt Stabilized Base	-	Trx. Cl. 4.7
	FM 1957	51 mm ACP	203 mm Asphalt Stabilized Base	-	Trx. Cl. 4.9
	FM 1957	32 mm ACP	254 mm Flexible Base	-	Trx. Cl. 4.6
Wichita Falls	FM 372	64 mm ACP	229 mm Flexible Base	152 mm LTS	-
Yoakum	FM 3131	2-CST	279 mm Lime Treated Base	-	Trx. Cl. 5.2
	US 87	25 mm ACP	305 mm Lime Treated Base	203 mm LTS	Trx. Cl. 5.5

Surface layers may vary from one or two Course Surface Treatments (CST) to several centimeters of asphalt concrete mix. It is common for a load-zoned pavement to have a two CST with up to five or more seal coats. The thicknesses of these surface treatments may easily exceed 75 to 100 mm; however, little structural capacity is typically assigned to these layers. For surface treatments, the moduli value has typically been fixed at 690 - 1,035 MPa for analysis purposes.

Base layers may also vary substantially in thickness and material types. From Table 2, note that base layers may include an old concrete pavement, low quality caliche, high quality crushed limestone, iron ore topsoil, asphalt stabilized base (ASB), or lime treated base (LTB). Subgrade soil types also vary substantially, but typically are weaker soils with triaxial classes above 4.5. Subgrades may be lime or cement treated and can vary in thickness from 150 to 200 mm typically.

Some older load-zoned roadways contain material types that are no longer used such as the following:

- 150 mm road bed treatment (It was a common practice in the 20's and 30's to mix fuel oil with subgrade material to form a treated subgrade prior to placement of the base).
- 150 mm sledge stone base. Some base or subbase layers were formed by breaking up large rocks with sledge hammers.

Vehicle Types which Typically Use Posted Roads

Since the passage of House Bill (HB) 2060, any type of vehicle may be found on a load-zoned roadway. School buses, farm equipment (including heavily loaded grain), or livestock trucks are common. In addition, heavy oil field equipment, 18-wheelers, and other trucks may be seen on load-zoned roadways. Some vehicles, for example, cement trucks, milk trucks, and grain haulers are permitted to carry higher than legal axle-load limits by state law. Some load-zoned pavements only carry local light traffic including cars, pick ups, and light delivery vehicles.

Traffic analyses are provided by the Transportation Planning and Program Division. These analyses are traffic projections based on data collected with Automatic Traffic Recorders (ATR) or Automatic Counter Recorders (pneumatic tube counters). A count on the actual road being analyzed may not be performed. Rather, the ATR and ACR data from roadways in the vicinity may have to suffice for the analysis. Traffic field surveys are not common, but may be done by the District or Pavements Section staff if warranted.

Load magnitudes vary significantly. The types of loads vary depending on the district. For example, in the Pharr District, it is common for load-zoned roadways to carry heavily laden farm trucks during certain seasons of the year. Other districts (for example, Wichita Falls) may have load-zoned pavements that periodically carry very heavy oil field equipment.

LOAD-ZONING PRACTICES IN OTHER HIGHWAY AGENCIES

U.S. Federal Law

Current U.S. Federal law specifies the following restrictions on vehicle weight and size (FHWA 1995).

- 89 kN for single axles.
- 151 kN for tandem axles.
- Application of Bridge Formula B for other axle groups up to 356 kN gross vehicle weight (GVW).

$$W = 500 \left[\frac{LN}{N-1} + 12N + 36 \right]$$

where

W = Overall gross weight on any group of two or more consecutive axles to the nearest 2.2 kN,

L = Distance in feet between the extreme of any group of two or more consecutive axles, and

N = Number of axles in the group under consideration.

- 2.59 m for vehicle width.
- 14.63 m (maximum length) for semitrailers.
- 8.53 m (maximum length) for trailers in a twin-trailer combination.

Pennsylvania

From the study by Fernando et al. (1987), a load limit procedure based on predicted pavement performance was developed for the Pennsylvania DOT. In this procedure, pavement life is predicted using deflection measurements from either the Road Rater or FWD. This study indicated that axle load limits for different axle configurations may be established based on the allowable load per tire determined from prediction of pavement service life for various load magnitudes. A performance model based on subgrade compressive strain is used to predict service life along with the deflection data collected on a given route. Load limits are established based on the service life required of a given pavement.

Minnesota

For spring-thaw load restrictions, deflection tests are used to indicate when the spring posting period should end in Minnesota (Allen and Bullock 1987). The removal of posted load limits is considered three weeks after peak deflections are measured. However, the tests are not used to determine when spring axle load limits should be posted. No information is provided by the authors concerning this.

Indiana Study

The current procedure for permitting overloaded trucks is based on the federal bridge gross weight formula. The loads determined from the bridge formula are subject to the following limits:

- Maximum gross vehicle weight - 356 kN.
- Maximum single axle group weight - 89 kN.

- Maximum tandem axle group weight - 151 kN.
- Maximum wheel weight - 1.4 kN/cm of tire width measured between the flanges of the rim.

Two consecutive sets of tandem axles that may carry a gross load of 151 kN per tandem are excluded from the above formula provided that the center-to-center distance between the first and last axles is 11 m or more. When truck loads are greater than the weights allowed by the formula, overloaded trucks with an overweight permit are allowed subject to the following load restrictions:

- Maximum gross vehicle weight - 480 kN.
- Maximum single axle group weight - 124 kN.
- Maximum tandem axle group weight - 213 kN.
- Maximum axle group weight - 227 kN.
- Maximum wheel weight - 1.4 kN/cm of tire width measured between the flanges of the rim.

For heavy duty highways, the following load restrictions are used on special weight permits. An example of a heavy duty highway is a 64-km long corridor built especially for passage of heavy trucks from Chicago to the Michigan border. Moffett and Whitford (1995) do not give any information about the pavement structure of this heavy duty highway.

- Maximum gross vehicle weight - 596 kN.
- Maximum single axle group weight - 80 kN.
- Maximum tandem axle group weight - 284 kN.
- Maximum wheel weight - 1.4 kN/cm of tire width measured between the flanges of the rim.
- Axle spacing not less than 1.07 m between each axle in an axle combination and not less than 2.44 m between each axle group.

According to the current permit regulation, the axle configurations of trucks whose gross vehicle weight (GVW) is between 356 kN and 480 kN are not constrained.

Procedures Developed from Study by Purdue University (Zaghloul et al. 1994)

A three dimensional, dynamic finite element program (3D-DFEM) was developed to analyze pavements. The required material properties in this program are:

- Asphalt concrete (viscoelastic material):
  - Instantaneous shear modulus: determined at a loading time of 0.1 second representative of a vehicle traveling at 64 kph.
  - Long-term shear modulus: determined at a loading time of 1.0 second representative of a vehicle traveling at 2.4 kph.
- Base and subbase (granular material)
  - Drucker-Prager model parameters
- Subgrade soils (cohesive material)
  - Cam-Clay model parameters

The 3D-DFEM program was used to develop load equivalency factors (LEF) based on permanent deformation of pavement layers. A comparison of LEFs for flexible pavements and for single axles did not show a good match with other procedures such as CANROAD, FATIGUE, VESYS 5-R, and VESYS 5-C. While the study showed good agreement with AASHTO LEFs, it is not clear from the paper whether the LEFs compared are based on the same criteria. The AASHTO LEFs are based on the concept of serviceability while the LEFs developed by the author are based on total permanent deformation.

The study also found that the rate of increase in maximum surface deflection with LEFs increase significantly when the LEF is greater than 35. Therefore, when the LEF of any axle group exceeds 35, the permit is not approved. Other criteria used in permitting overweight trucks are:

- if the stress due to any axle group exceeds the yield stress, the truck is not permitted to use the highway under consideration and
- if the accumulated LEF for the truck, which is the sum of the LEFs for the truck axle groups, exceeds a given percent of the average daily truck traffic, no permit is given to use the highway.

Seasonal Load Restrictions

In cold climates, a thin pavement over frost susceptible subgrade could lose over 50 percent of the summer strength, and a gravel road would lose much more (Isotalo 1996). From the literature, road damage due to spring-thaw has a huge impact on the cost of road repair and the overall economy of a given locality.

In the U.S., 19 states have seasonal load restrictions that in most cases are enforced during the spring and, on few occasions, during periods of winter thawing. However, there are few procedures for seasonal load posting. Therefore, posted load limits for spring-thaw conditions are determined primarily on the basis of experience and judgment of the local highway agency.

Even though devices such as the Falling Weight Deflectometer (FWD) can be used to evaluate pavement structural adequacy, their operation is considered too expensive for the purpose of evaluating load restrictions on low-volume roads. Only a few agencies apply these methodologies (Mahoney et al. 1990).

Washington DOT

The determination of load restrictions is based on the agency's experience and the interpretation of surface deflection measurements such as FWD. A study conducted in Washington reveals that a 50 percent load reduction will prevent damage from heavy loads during the spring-thaw period. It also found that the timing and duration of load restrictions are important factors in minimizing pavement damage during spring thaw.

Guidelines for Load Restrictions in Washington:

1) Where to apply load restrictions

The Washington study indicates that pavements with spring thaw surface deflections that are 45 to 50 percent greater than summer surface deflections are good candidates for seasonal load restrictions. Site condition and various other factors are considered in determining whether to post load restrictions or not:

- surface deflection data for summer and spring thaw condition,
- pavement surface thickness,
- moisture condition,
- subgrade soil, and
- local experience.

2) The magnitude of load restriction

Based on elastic layer pavement analysis, the following table shows the effectsof load restrictions (Mahoney et al. 1987). From a practical viewpoint, approximately 50 percent reduction of loads can reduce damage on pavements due to loss in strength attributed to spring-thaw, as shown in Table 3.

Table 3. The Benefits of Using Load Restrictions (Mahoney et al. 1987).

Load reduction (%)	Pavement life increase (%)
20	62
30	78
40	88
50	95

3) When to apply load restrictions

A Thawing Index (TI) is used to determine the timing of load restrictions on the basis of air temperature data from local weather stations or measured data on

specific pavement sections. TI is an index value based on a -1.7 ^{0}C datum of air temperature as given by the following equation:

$$TI = \Sigma \ (\ T \ + \ 1.7 \ )$$

where

TI	=	Accumulated thawing index (^{0}C-day),
T +1.7	=	Daily thawing index (^{0}C-day),
T	=	Average temperature $= 0.5\ (T_H + T_L)$ in ^{0}C,
T_H	=	Maximum daily temperature (^{0}C), and
T_L	=	Minimum daily temperature (^{0}C).

Using the sum of daily TI, the timing of load restrictions can be found. From a thermal analysis conducted by the finite element method, the timing for load restrictions was determined as shown in Table 4.

Table 4. Timing for Load Restrictions (Mahoney and Jackson 1990).

Pavement	A/C thickness	Base thickness	TI , Should level (^{0}C-day)	TI, Must level (^{0}C-day)
Thin	5 cm or less	15 cm or less	5.6	22.2
Thick	Greater than 5 cm	Greater than 15 cm	13.9	27.8

For thin pavements, the <u>should</u> load restriction is applied when the accumulated TI is equal to 5.6 ^{0}C-days and the <u>must</u> load restriction is applied when the accumulated TI is equal to 22.2^{0}C-days. Table 5 gives example data.

4) Duration of load restrictions

The duration of load restriction can be determined using the relationship between Thawing Index (TI) and Freezing Index (FI). The freezing index is the accumulated daily freezing degree days from the start of freezing and is computed as

Table 5. Example Freeze and Thaw Data (Mahoney and Jackson 1990).

Average Daily Temperature (^{0}C)	Daily Freezing Index (^{0}C-days)	Sum of Daily Freezing Index (^{0}C-days)	Daily Thawing Index (^{0}C-days)	Sum of Daily Thawing Index (^{0}C-days)
-3.9	-	264	-	-
-1.7	2	266	0	0
-1.1	1	267	0.6	0.6
-1.1	1	268	0.6	1.2
0.6	0	268	1.1	3.3
-1.1	-1	267	0.6	3.9
0.0	0	267	1.7	5.6
1.7	-2	265	3.4	9.0

follows.

$$FI = \Sigma\ (-T)$$

where

FI = Accumulated freezing index (^{0}C-day),

- T = Daily freezing index (^{0}C-day)

When the average daily air temperatures go over - 1.7 ^{0}C for several days, the end of the freezing period is determined based on the agency's judgment and local temperature variations. The freezing index is then calculated. The time at which load restrictions can be lifted is predicted approximately by estimating TI from the following regression equations:

$$TI = 4.15 + 0.26\ (FI)$$

or

$$Approximate\ TI \approx 0.3\ (FI)$$

The day on which load restrictions can be lifted is the time when the calculated TI from the regression equations is equal to the observed TI. Table 6 gives an example.

Table 6. Example Freeze and Thaw Data (Mahoney et al. 1987).

Average Daily Temperature (°C)	Daily Freezing Index (°C-days)	Sum of Daily Freezing Index (°C-days)	Daily Thawing Index (°C-days)	Sum of Daily Thawing Index (°C-days)
-14.4	14	717		
-13.3	13	730		
-10.0	10	740		
-5.6	6	746		
3.3			5	5
6.1			8	13
4.4			6	19
2.2			4	23
2.8			4	27
~			~	~
~			~	~
6.7			8	163
10.0			12	175
10.0			12	187
10.0			12	199
11.1			13	212

From this table, the accumulated thawing and freezing index is calculated from the following equation:

$$TI = 4.15 + 0.26\ (746) = 198.$$

Thus, the local agency would consider lifting the load restrictions on the day when the accumulated TI equals 199 (^{0}C - days).

Finland Practice

Low-volume roads in Finland have traffic volumes less than 1,500 vehicles per day. Gross vehicle weight restrictions are as follows (Isotalo 1996).

- For agricultural tractors - 35.6 kN.
- For empty trucks - 71.2 kN.
- For normal buses and tandem axle trucks - 106.8 kN

Basically, heavy timber and earth-moving transports are not allowed. However, temporary permits can be issued by the road agency. Finnish experience indicates that surface deflections measured using the Benkelman beam under a five-ton double wheel axle can be used to determine the need for load restrictions. For this purpose, Benkelman beam deflections are checked against allowable surface deflections that are related to the type of road as shown in Table 7. However, no information is provided regarding what load limits are used when the allowable surface deflection is exceeded.

Table 7. Threshold Values for Weight Restrictions in Finland (Isotalo 1996).

Type of road	Allowable surface deflection (mm)
Asphalt pavement	1.20 - 1.40
Surface dressed roads	1.60
Secondary gravel roads	1.80
Tertiary gravel roads	2.00

Canadian Practice

Of the 825,743 km of roads in Canada, 65 percent are classified as low-volume roads (Rogers et al. 1995). In Ontario, 74 percent of roads are classified as low volume roads, which have annual average daily traffic (AADT) less than 2000. Load limits are generally based on the Transportation Association of Canada (TAC) recommendations (Nix et al. 1992). Axle weight limits and gross vehicle weight and size restrictions are shown in Tables 8 and 9. The province of Ontario has design guidelines for low-volume roads (Rogers et al. 1996). Granular bases are required to have permeabilities between 10^{-4} and 10^{-3} cm/sec. If the permeability is less than 10^{-4} cm/sec, base failure can occur. The percentage passing the 75 μm sieve size is required to be no more than 8 percent for base materials. Due to this permeability concern, mica has a certain specification in the 75μm sieve fraction. A limit of 10 percent mica content has to be achieved. Permeability also can be reduced by the breakdown of aggregate material. In the spring, coarse aggregate particles are broken down to sand-sized particles due to the abrasion or impact of vehicle loadings. Consequently, Ontario changed the specification for granular aggregate base in 1994. The Micro-Duval test was adopted replacing the LA abrasion and impact test, and petrographic examination requirement. The Micro-Deval test is conducted as follows:

- Two liters of water and a 1.5 kg test sample of 19 to 9.5 mm aggregate are poured into a 5 L steel jar containing 5 kg of 9.5 mm steel balls and
- The jar is turned at 100 rpm for 2 hours, and the amount of aggregate breakdown is measured by sieving the sample over a 1.18 mm sieve.

The aggregate breakdown from the Micro-Deval test should be no more than 25 percent for granular base materials and no more than 30 percent for granular subbase materials.

Table 8. Axle Weight Limits in Canada and the U.S. (Nix et al. 1992).

	Single (tonnes)	Tandem (tonnes)	Tridem (tonnes)
TAC	9.1	17	24
Ontario	10	19.1	28.6
Quebec	10	20	30
U.S. (Federal)	9.1	15.4	19.1

Table 9. Gross Vehicle Weight and Size Restrictions in Canada and the U.S. (Nix et al. 1992).

	Max. GVW (tonnes)	Max. Base Length (m)	Tonnes / m
TAC	39.5	10.4	3.8
Ontario	47	11.75	4
Quebec	45.5	11.1	4.1
U.S. (Federal)	36.3	15.5	2.34

Base length: the distance from the first to the last axle

U.K. and E.C. Practices on Load Limits

The European Community (E.C.), including the United Kingdom (U.K.), have standards for vehicle weights and dimensions. Limits on vehicle height are from 4.0 m for E.C. and 4.25 m for U.K.. Vehicle widths up to 2.6 m are allowed in E.C. (Nix et al. 1992). Tables 10 and 11 show axle weight limits and gross vehicle weight.

Table 10. Axle Weight Limits in the E.C. and the U.K. (Nix et al. 1992).

	Single (tonnes)	Tandem (tonnes)	Tridem (tonnes)
E.C.	10	20	24
U.K.	8.2	15.5	18

Table 11. Gross Vehicle Weight and Size Restrictions in the E.C. and the U.K. (Nix et al.1992).

	Max. GVW (tonnes)	Max. Base Length (m)	Tonnes / m
E.C.	44	14.33	3.07
U.K.	39	13.5	2.89

Base length: the distance from the first to the last axle

South African Study

A study from South Africa indicated that 9 tons is the optimum limit of single axle loads (Vantonder et al. 1992). The AASHTO relationship based on an exponent of 4.0 to 4.5 was used. Costs and benefits of road maintenance were considered with changes in axle load. The study recommended effective dual (18.0 tonnes) and tridem (21.0 tonnes) axle load limits. Table 12 shows current load limits.

Table 12. Axle Load Limits in South Africa (Vantonder et al. 1992).

Axle Type	Two wheel axle (tonnes)	Four wheel axle (tonnes)
Single	7.7	8.2
Tandem	15.4	16.4
Tridem	21	21

Maximum combination length = 22.0 m

In South Africa, low-volume roads have 400 or less vehicles per day. South Africa has developed guidelines for structural design of low-volume roads using the Dynamic Cone Penetrometer (DCP) by Zyl et al. (1996). Recommendations for DCP testing are given below:

- Five DCP tests per kilometer conducted on the outer and inner wheel paths of both lanes and on the road centerline for two-lane highways.

- Additional DCP testing at each significant location (e.g. failed areas).
- At least eight DCP tests for each uniform section.
- Additionally, two soil samples per kilometer are taken to the laboratory for tests of soaked CBR, index properties, and in-situ moisture content.
- The minimum length of test section is 0.1 km, and section lengths of 1.0 km are preferred.

The other study by Wolff (1996) discusses the development of S-N curves for low-volume roads based on permanent deformation of granular base layers. Different S-N curves depending on various levels of allowable permanent strain were developed using Heavy Vehicle Simulator (HVS) data. The bulk stress (θ) at the center of the granular layer is calculated for a given loading. The service life is determined from HVS data relating the development of permanent strain with load repetitions. By use of the S-N curves, a catalog of pavements with granular bases and asphalt surfacing for low-volume roads was compiled. Designs that will satisfy different service life requirements using a number of different base and subgrade materials are provided.

Permit Fee and Enforcement

NCHRP Study (1987)

The study indicates that 10 to 25 percent of truck operations are overloaded. In addition, there is no uniform practice in pavement design, permit issuance, and enforcement between the states. Current issuance of permit fees is not based on an evaluation of the pavement damage due to overloaded vehicles. Many states are of the opinion that heavy vehicle electronic licence plates (HELP) can be used for implementing the weight-distance fee structure with weigh-in-motion (WIM) devices.

Indiana Study

A permit fee for overloaded trucks is required to have the overweight permit. The fees assessed are as follows:

- For overweight vehicles, there is a $20 base fee plus a mileage charge of $0.22/km for vehicles with GVWs up to 480 kN, and $0.40/km for vehicles with GVWs between 480 kN and 667 kN.
- For overweight and oversized vehicles, there is a $20 base fee plus a mileage charge of $0.22/km for vehicles with GVWs up to 480 kN or the oversize permit fee of $30, whichever is greater.
- For loads greater than 667 kN, there is a $0.63/km fee.

For transporting heavy vehicles or loads, or other heavy objects which exceed the legal limits and dimensions, the permittee should pay only the greater of the two fees, and the permitting office shall issue a single oversized-overweight permit.

A permit fee study by Purdue University (Moffett and Whitford 1995) suggested that the current single-trip permit fee is better than other alternatives, such as the annual permit fee, in terms of revenue neutrality. In an attempt to improve and simplify the current fee system in Indiana, the following changes were recommended:

- For loads less than 356 kN and for any single axle weight exceeding 89 kN and a tandem axle of 151 kN, there is a $0.21/km fee.
- Trucks under above conditions may purchase a 90 day permit for $200 per truck traveling over specified routes.

In addition, the following were recommended to improve the current administrative system:

- A route map that shows the allowable weight and size restrictions for various routes.
- Permits that are valid for 24 hours from the time of issuance instead of permits expiring at midnight.
- Voice response system or computer permitting system to handle questions that are most frequently asked in an automated fashion.

- Allow multiple permits to be included in a single application (bundle of permits).

Tables 13 through 20 present a survey of current fee schedules and load zoning practices from this study. The tables provide a concise summary of current practices.

Australian Study

In Australia, two kinds of Weigh-In-Motion (WIM) systems (low and high speed) are available depending on speed of vehicle (Koniditsiotis 1995). There are also five high speed WIM systems depending on sensors such as the bending plate, the capacitance pad, the capacitance strip, the load cell, and the strain gauge. Of these, CULWAY, based on strain gauge sensor type, is most widely used in practice due to low cost of installation and management. The principle is that the weight is recorded by measuring the bending strain due to axle loads.

Information on Load Restrictions from Web Sites

Using the World Wide Web (WWW) in the Internet system is another way for state transportation agencies to disseminate information and data about load restrictions. Currently, several road agencies have WWW information about load restrictions. Among the Web sites visited, the Florida DOT provides the most information. The information available on load-zoning and permit schedules from DOT Web sites are presented in Table 21. Table 22 shows the Intenet addresses of the DOT Web sites.

Table 13. Annual Overweight Permit Fees for Those States Who Base Their Fees on Vehicle Weight and Distance Traveled (Moffett and Whitford 1995).

State	Fee
Idaho	$1.3 / km / 8.9 kN excess weight and $40 flat fee / year (all collected quarterly)
Montana	$3.5 / 40km / 22.25 kN excess weight over 356 kN and $200 flat fee / year
Ohio	Switching from a flat fee to a ton km rate

Table 14. Annual Overweight Permit Fees for Those States Who Charge Flat Fee Independent of Vehicle Configuration, Distance Traveled, and Commodity Shipped (Moffett and Whitford 1995).

State	Fee
Alabama	$100 / year
Arizona	$640 / year if load specific, $1,500 if blanket
California	$90 / year
Colorado	$400 / year
Florida	$500 / year
Georgia	$100 / year
Massachusetts	$300 / year
Nevada	$50 / year
New Hampshire	$100 / year
New York	$360 / year
North Carolina	$50 / year
Ohio	$25 / quarter
Rhode Island	$100 / year / Trailer
Tennessee	$500 / year for vehicles GVW up to 534.1 kN $1,000 / year for vehicles GVW over 534.1 kN
Virginia	$60 / two years

Table 15. Annual Overweight Permit Fees for Those States Who Base Fees on Vehicle Configuration (Moffett and Whitford 1995).

State	Fee
Alaska	$40 to $720
Connecticut	$7 to 4.5 kN / year
Kentucky	$60 to $160 / year
Minnesota	$200 to $800 / year
Pennsylvania	$25 to $300 / year
Rhode Island	$50 to 4.5 kN / year (out-of-state power units)

Table 16. Maximum Weight That Each State Will Issue an Annual Overweight Permit (Moffett and Whitford 1995).

State	Maximum Weight
Alabama	667.6 kN
Alaska	125 % of legal weight
Arizona	1,112.6 kN
California	Numerous permits available
Colorado	890.1 kN
Connecticut	890.1 kN
Florida	676.5 kN
Georgia	445 kN
Idaho	890.1 kN
Minnesota	645.3 kN
Montana	22.3 kN total excess axle weight
New York	516.3 kN
North Carolina	543 kN
Pennsylvania	Limited to quarrying operations moving up to 0.8 km along a highway and related trucks crossing a highway
Virginia	400.6 kN

Table 17. States Who Issue a Blanket Annual Overweight Permit with an Accompanying Official Route Map that Must Always be Attached to the Permit (Moffett and Whitford 1995).

State	Notes
California	Travel is allowed anywhere except weak bridges that are identified on a map.
Florida	Must stay on official map routes.
Idaho	Color-coded map with four weight-level categories.
Kentucky	Travel is allowed on any state-maintained roads within the county the permit was issued for, and any neighboring counties. Multiple annual overweight permits to allow travel in other counties may be purchased.
Minnesota	Vehicles that are less than 3.81 m in width and 2.6 m in axle width may travel anywhere on the official map after first consulting a weekly construction map is mailed by the Minnesota DOT to all holders of annual overweight permits.

Table 18. States Who Issue a Blanket Annual Overweight Permit Without Any Type of Accompanying Official Route Map (Moffett and Whitford 1995).

State	Notes
Alabama	Only if movement weighs 408.7 kN or less.
Arizona	Only at the $1,500 / year permit cost level.
Montana	Available routes are posted at weight stations.
New York	Blanket is restricted to routes within various air-km radii from trip origin.
Rhode Island	No maps are issued because it is a small state and therefore no special map is needed. Special route exceptions are published in local newspaper.

Table 19. States Who Issue Annual Overweight Permits that Restrict Movements to Either Specific Loads or Specific Routes (Moffett and Whitford 1995).

State	Notes
Arizona	Only at the $640 / year permit cost level.
Kentucky	For steel carriers only, they may travel on specific routes within a 56.3 km radius from their base of operations.
Massachusetts	Only issued for construction equipment, boat haulers, and self-propelled cranes.
Minnesota	Permits are only issued for movements of construction commodities.
New Hampshire	Only issued for construction industry movements on pre-approved routes.
New York	Various load-specific and route-specific permits.
North Carolina	Depending on vehicle configuration, may travel from one to ten company-requested routes that are submitted for pre-approval when applying for an annual overweight permit.
Ohio	Annual overweight permits are both load-specific and route-specific.
Pennsylvania	Limited to quarrying operations up to 0.8 km along a highway and related overweight vehicles that need to cross a highway from one side of a quarry to another side of a quarry.

Table 20. States Who Issue Annual Overweight Permits and Still Require a Company to Call-in or a Specific Route Authorization for Each Trip (Moffett and Whitford 1995).

State	Notes
Alabama	If movement weighs greater than 445 kN.
Minnesota	If movement is greater than 4.3 m in width, greater than 4.3m in height, and greater than 25.9 m in overall length.

Table 21. Summary of Load-Zoning Information from DOT Web Sites.

State	AK	BC	CA	FL	LA	MD	MN	OH	OR
Glossary of load-zoning				●					
Load limits on roads & bridges				●				●	
Payment of penalties and fees			●	●		●	●		●
Maximum size and weight limit			●	●		●			●
Weight tables				●					●
Bridge formula tables				●		●			
Special load limits			●	●					●
Axle weight limitations				●					
Types of permits			●	●		●	●		
Enforcement		●		●	●	●			
Route information	●	●				●		●	
Seasonal load restrictions	●	●							
Permit exemptions			●						●

Notes: AK = Alaska, BC = British Columbia (Canada), CA = California, FL = Florida, LA = Louisiana, MD = Maryland, MN = Minnesota, OH = Ohio, and OR = Oregon

Table 22. Summary of Internet Addresses of the DOT Web Sites.

State	Address
Alaska	http://www.dot.state.ak.us/external/state_wide/mno/mno_h.html
British Columbia (Canada)	http://www.bchighways.com/cgi-bin/weigh.pl
California	http://www.dot.ca.gov/hq/traffops/trksnwim/TrkManul.htm
Florida	http://www.dot.state.fl.us/trucking/index.htm
Louisiana	http://www.dotd.state.la.us/highway/permit.html
Maryland	http://www.inform.umd.edu:8080/UMS+State/MD_Resources/MDOT/trucking/trucking.htm#ex
Minnesota	http://www.dot.state.mn.us/guidebook/omotrpr.html
Ohio	http://www.dot.state.oh.us/dist2/i75proj/loadlims.htm
Oregon	http://www.odot.state.or.us/motor/hweb/od/od1.htm

SUMMARY

The literature review showed that, in many highway agencies worldwide, authority is given to impose restrictions on the size and weight of vehicles if it is determined that, without such restrictions, excessive damage may occur to a given route. Throughout the world, low-volume roads make up the greater part of most road networks. Because of economic considerations, many of these roads are simply not designed to carry heavy truck traffic. Consequently, load restrictions are necessary to avoid premature failures due to load applications not considered in the original design. In addition, seasonal variations necessitate load restrictions in many highway jurisdictions, particularly during spring thaw when the supporting pavement layers are weak and load carrying capacity is reduced.

The practice of load zoning varies between road authorities. From the review presented in this chapter, there is a range in procedures used. Many of the guidelines in place were developed from years of experience and typically rely on deflection measurements to establish the need for load restrictions and the magnitudes of load limits. In many agencies, these determinations are based on empirical correlations between pavement deflections and

pavement life. A number of states, like Indiana, Pennsylvania, and Washington have formal methodologies that are based on analyses of pavement response under loading to evaluate load restrictions appropriate for a given route. South Africa has a procedure which uses a performance model developed from accelerated load test data to predict the development of permanent deformation with load repetitions. This model has been used in South Africa for the structural design of low-volume roads.

Load limit postings also vary between highway agencies, from seasonal to year round, and from the simple use of gross vehicle weight limits to the combined specification of gross vehicle and axle load limits. While there are many agencies that post load limits on the basis of allowable axle weights, there are a number of agencies that implement uniform load limits on the basis of gross vehicle weights. Texas is an example. While efforts have been made recently to establish load limits on the basis of axle weights, most load-zoned roads in Texas are still posted with a gross vehicle weight limit of 260 kN, which corresponds to the legal load limit at the time these roads were designed and built. Since the load from a vehicle is transmitted to the pavement through its axles, determining load limits on the basis of axle weight is a more correct approach. With the current procedure of uniform GVW posting, a vehicle may be within the specified load limit but still be damaging because of high axle loads. Conversely, the gross vehicle weight may be above the posted limit, but still cause less deterioration if the vehicle load is distributed through the axles in such a way that the induced pavement stresses are minimized. Thus, axle weight restrictions may actually encourage the development and use of alternative vehicle configurations that will allow users to transport goods more efficiently while at the same time minimizing the damage done to the pavement. Consequently, this study seeks to develop a procedure for posting load limits in terms of axle load and axle configuration.

CHAPTER 3
SENSITIVITY ANALYSIS OF PREDICTED PAVEMENT RESPONSE AND PERFORMANCE

BACKGROUND

A sensitivity analysis was conducted to identify the factors that have a significant influence in the development of permanent deformation and fatigue cracking in flexible pavements. In this way, researchers identified the factors that are important in evaluating the need for load restrictions. For this purpose, two different types of pavement structure were assumed. In one case, a thin pavement comprising of a 25-mm surface layer and a 150-mm granular base was used (Figure 2). In another, the predicted pavement response and performance of a thick pavement (Figure 3) was evaluated.

Researchers used an incremental nonlinear elasto-plastic finite element program to establish the sensitivity of predicted pavement response and performance to changes in material parameters for the two pavement structures shown in Figures 2 and 3. The formulation of this axisymmetric finite element program is presented in Appendix B of this interim report. To model the pavement response under the standard 80 kN single axle load, researchers assumed a 40 kN single wheel load in the finite element analysis. A tire pressure of 690 kPa acting on a circular tire footprint of 136-mm radius was used. Figure 4 shows the finite element mesh used in the analysis. This axisymmetric representation of the pavement consisted of 90 elements and 309 nodes. For the boundary conditions, the sides of the finite element mesh were restrained in the horizontal direction, while the bottom of the mesh was restrained in both the vertical and horizontal directions to represent the rigid layer.

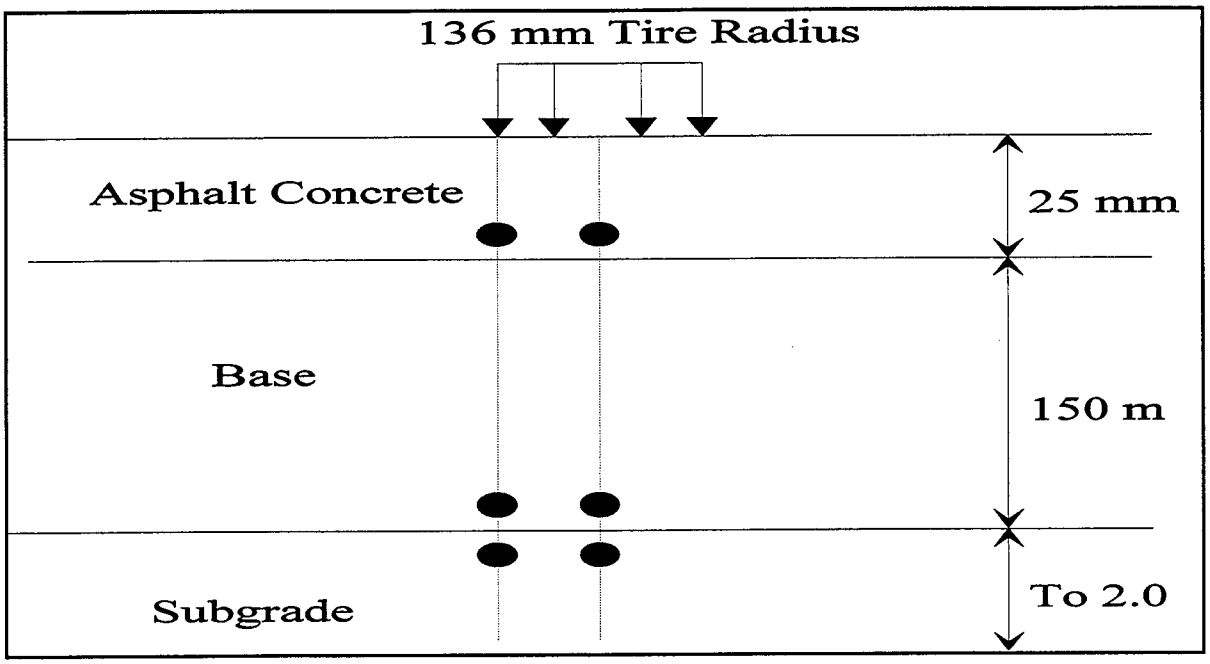

Figure 2. Thin Pavement Structure and Evaluation Points for Sensitivity Analysis.

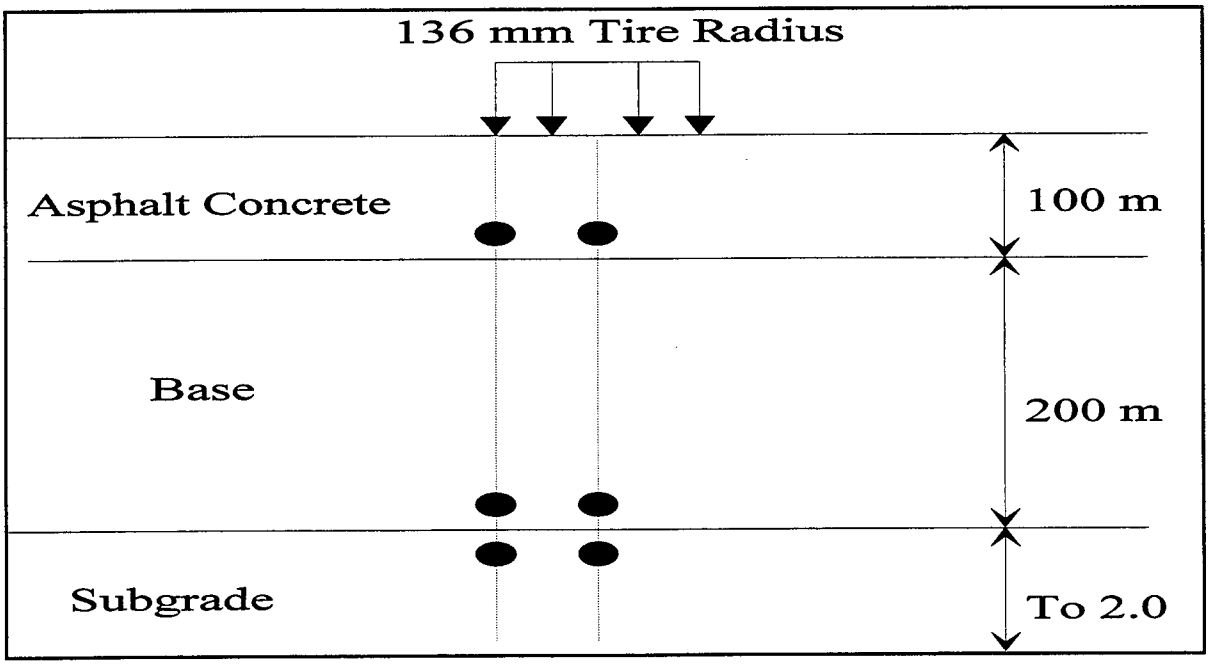

Figure 3. Thick Pavement Structure and Evaluation Points for Sensitivity Analysis.

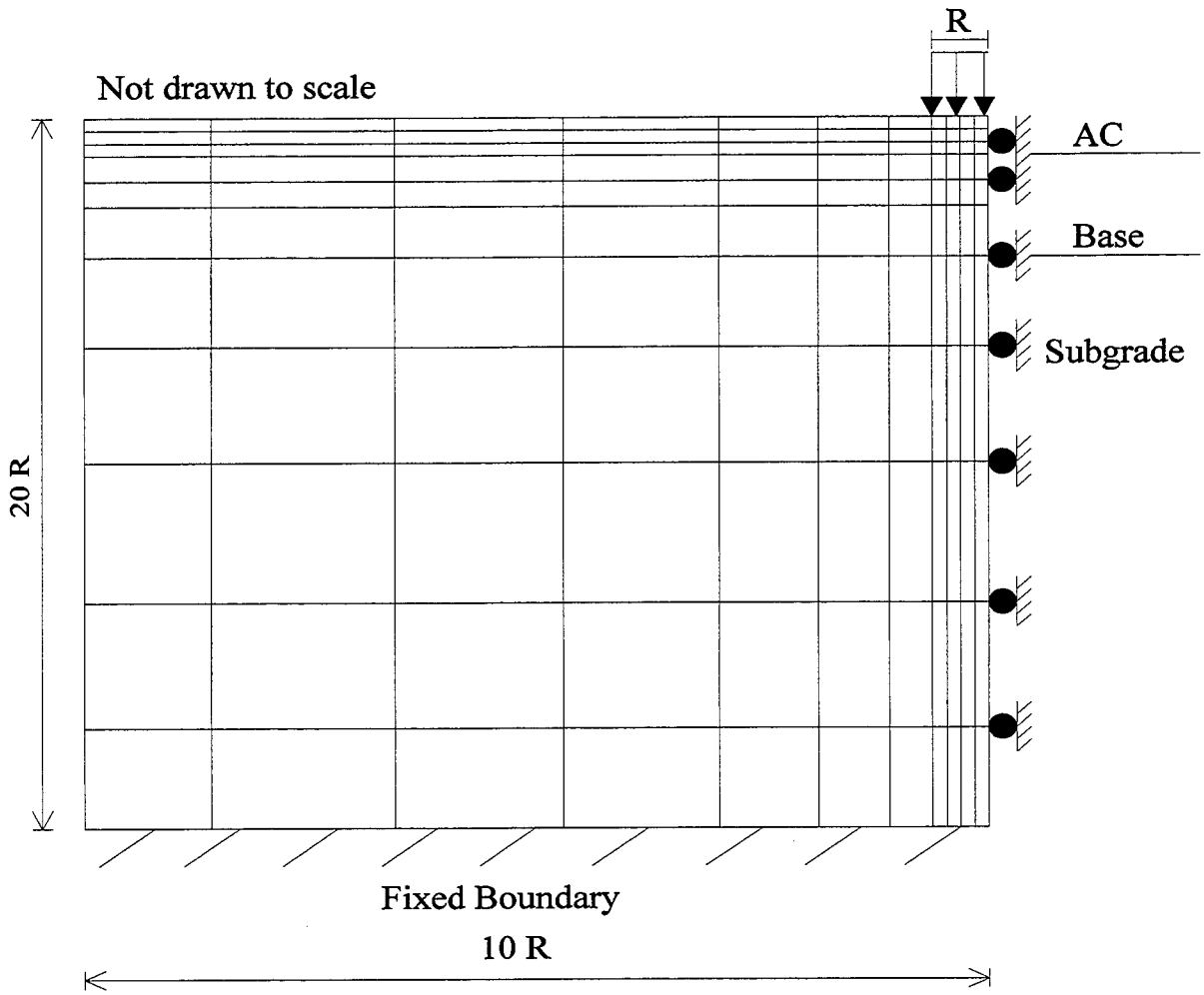

Figure 4. Finite Element Mesh for Pavement Structure.

The material parameters considered in the sensitivity analysis were the Mohr-Coulomb strength parameters defined by the cohesion and angle of internal friction of each pavement layer, and the parameters, k_1 to k_3, of the Universal Soil Model that govern the stress-dependency of the resilient modulus of each layer. This model is given by the relation:

$$E_r = k_1 \, Atm \left(\frac{\theta}{Atm} \right)^{k_2} \left(\frac{\tau_{oct}}{Atm} \right)^{k_3}$$

where

E_r	=	resilient modulus.
Atm	=	atmospheric pressure (100 kPa).
θ	=	first stress invariant = $\sigma_1 + \sigma_2 + \sigma_3$.
σ_i	=	principal stresses.
τ_{oct}	=	octahedral shear stress.

The coefficients, k_1, k_2, and k_3, are determined from resilient modulus tests. Since the calculated stresses are normalized with respect to the atmospheric pressure, these coefficients are dimensionless. From results of the study conducted by Jooste and Fernando (1995), the coefficient, k_1, was found to have the most influence on the predicted resilient modulus. In general, the higher the k_1, the higher the predicted resilient modulus. This is illustrated in Figure 5, which shows predicted resilient moduli for a granular base material at three different values of k_1. The data shown were calculated assuming a pavement with a 100-mm thick asphalt concrete surface layer and a 200-mm thick granular base layer. Values of 0.6 and -0.3 were assumed for the parameters, k_2 and k_3, respectively, for the base layer.

For a given curve, it is observed that the resilient modulus increases with increasing wheel load, illustrating the hardening effect of increasing confinement on the predicted resilient modulus. This hardening effect is associated with the k_2 term,

$$k_2 \; term = \left(\frac{\theta}{Atm} \right)^{k_2}$$

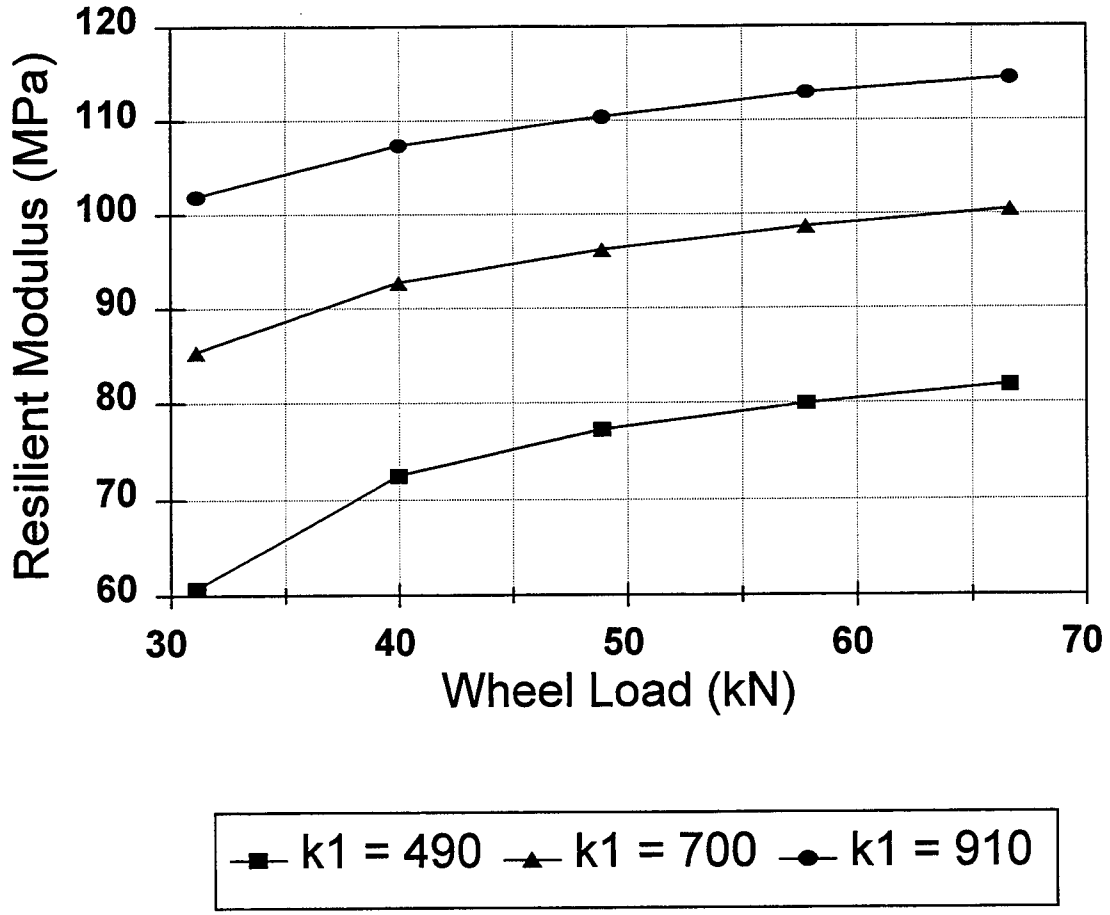

Figure 5. Variation in Resilient Modulus With Parameter, k_1 (Jooste and Fernando, 1995).

As the wheel load increases, the confining pressures also increase resulting in higher predicted values for the resilient modulus. The octahedral shear stress also increases with increasing wheel load, which will tend to decrease the resilient modulus. However, for the pavement and range of wheel loads considered in Figure 5, the increase in confinement with higher wheel loads more than compensates for the softening effect of the octahedral shear stress. Thus, the resilient modulus is predicted to increase with higher wheel loads in the figure shown. However, the opposite trend may be obtained for other pavements (such as thin pavements), where the softening effect of the octahedral shear stress may be more pronounced. The hardening effect of higher confinement and the softening effect of higher octahedral shear stress can be discerned from Figure 6. The k_3 term in the figure is

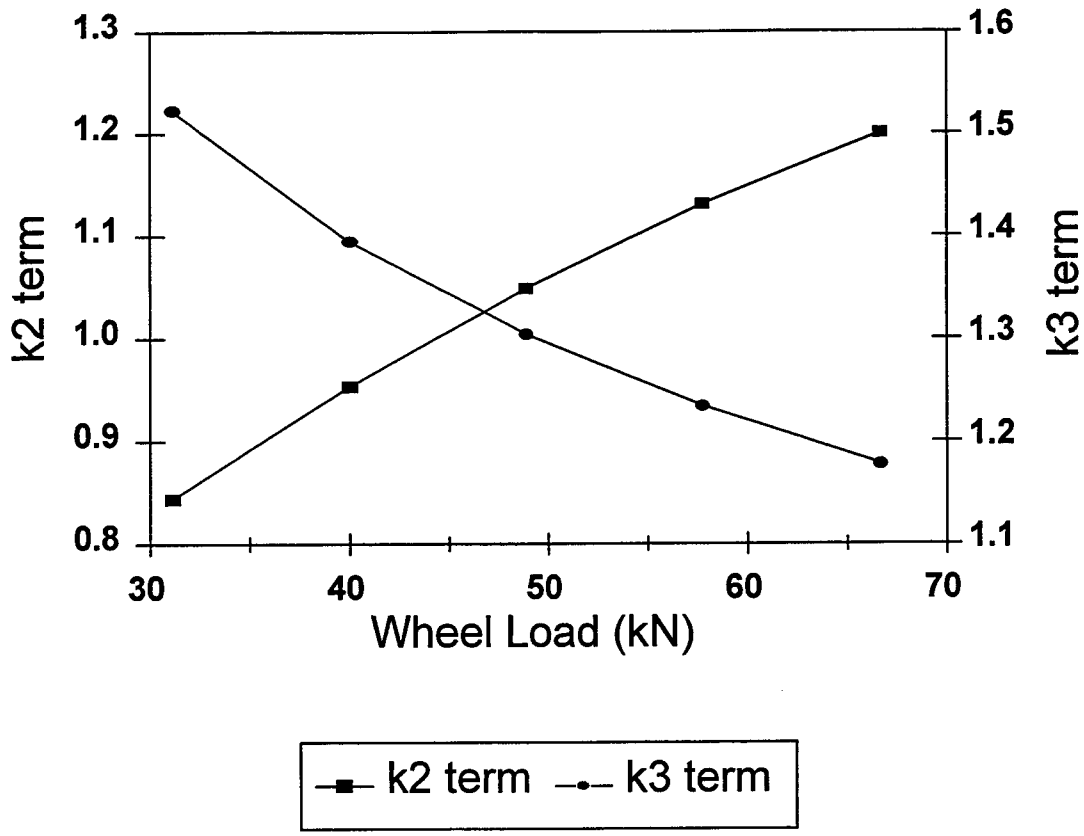

Figure 6. Illustration of the Hardening Effect Due to θ and the Softening Effect Due to τ_{oct} (Jooste and Fernando, 1995).

equal to,

$$k_3 \ term = \left(\frac{\tau_{oct}}{Atm} \right)^{k_3}$$

As the wheel load increases, the k_2 term increases because of higher confinement. However, the octahedral shear stress also increases so that the k_3 term diminishes with higher wheel loads. Consequently, while the effect of the higher k_1 is generally to increase the predicted resilient modulus, the effects of k_2 and k_3 depend on the interactions between these coefficients, the applied loads, and the pavement geometry. The tendency of a material to stiffen with increasing confinement, θ, is related to k_2. However, this tendency is counteracted by the softening effect under increasing shear, as controlled by the coefficient,

k_3. The greater the tendency of a material to stiffen under increasing confinement, the higher the effect of k_2. Similarly, the greater the tendency of a material to soften under shear, the higher the effect of k_3. The effects of these coefficients on the resilient modulus are also affected by the applied loads and pavement geometry due to the effects of these latter factors on the induced stresses. These effects are illustrated in Figures 7 and 8. Figure 7 shows that the magnitudes of the predicted stress invariants, θ, and octahedral shear stress, τ_{oct}, increase as the applied load increases for a given pavement structure. While the increase in the magnitude of θ will result in an increase in the k_2 term, the increase in τ_{oct} will diminish the k_3 term thus counteracting the effect of higher confinement on the predicted resilient modulus. Figure 8 shows the effects of pavement geometry on the induced stresses for the case where the base thickness is varied while the applied load and other variables are kept constant. As expected, the magnitudes of θ and τ_{oct} decrease as the base thickness increases. The coefficients, k_1, k_2, and k_3, are also used in evaluating the stress-dependency of the Poisson's ratio based on the relationship developed by Uzan (see equation in Appendix B).

In the sensitivity analysis, each of the k_1 to k_3 parameters was varied one at a time from its assumed base value, while the other parameters were held at their corresponding base values. The change in the predicted pavement response due to a change in a given parameter was evaluated using the finite element program. Tables 23 and 24 show the base values assumed in the sensitivity analysis for the stress-dependent and Mohr-Coulomb strength parameters, respectively. Each parameter was varied ±30 percent from its base value except for the surface layer, k_3, and the subgrade, k_2, which were fixed at zero. The predicted pavement response at each of the evaluation positions shown in Figures 2 and 3 was then evaluated. Specifically, the induced stresses at the edge and center of the 40 kN wheel load were evaluated at three different depths corresponding to the bottom of the surface and base layers, and the top of the subgrade. Figure 9 illustrates the stresses predicted from finite element analyses. These stresses were used to determine the Mohr-Coulomb yield function values at the evaluation positions. In addition, the predicted plastic strain under loading was also determined at each location. For the pavement structures considered, no plastic strains

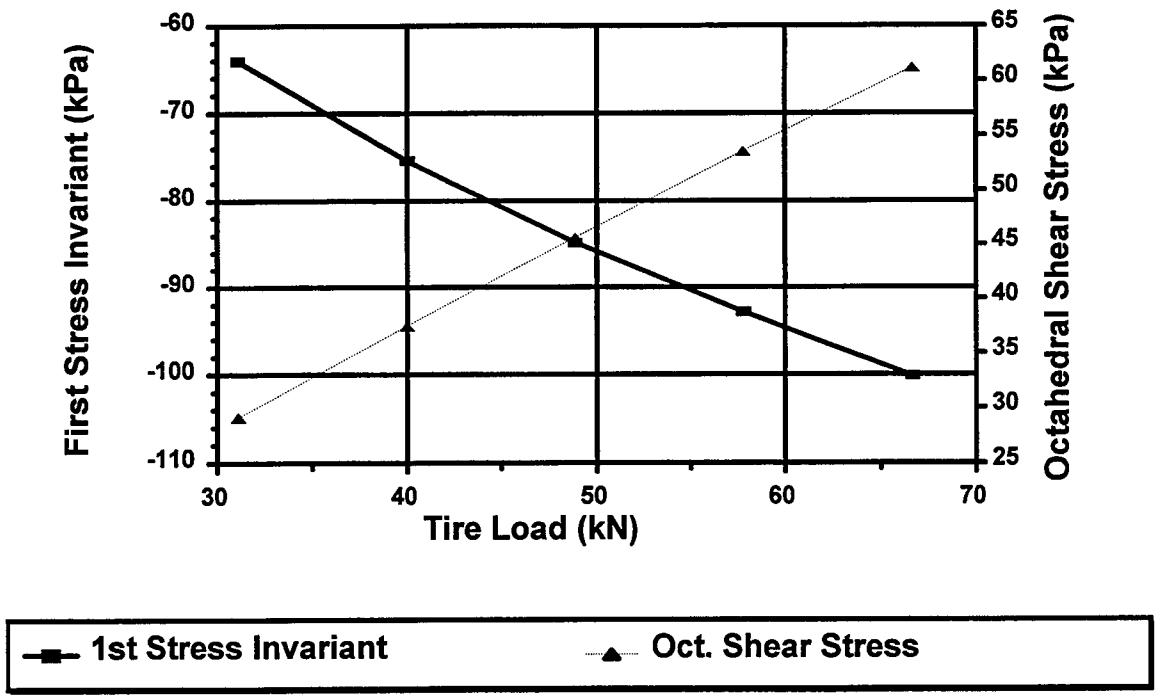

Figure 7. Illustration of the Effect of Load on θ and τ_{oct}.

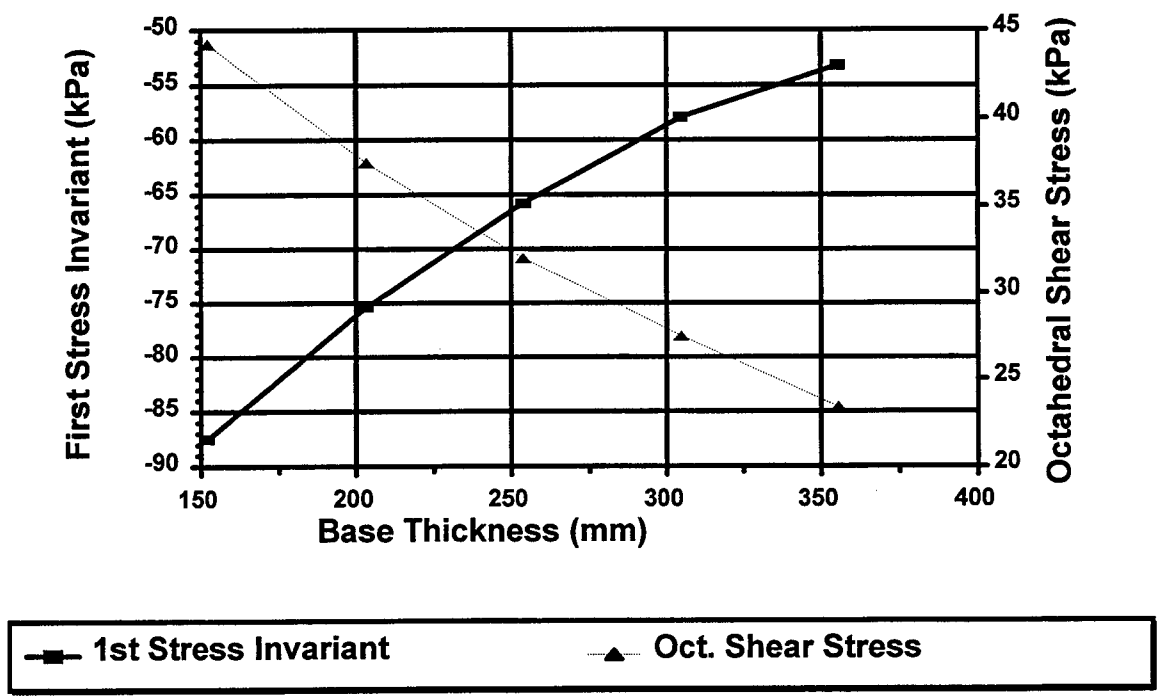

Figure 8. Illustration of the Effect of Base Thickness on θ and τ_{oct}.

Table 23. Base Levels of Resilient Parameters Used in Sensitivity Analysis.

Layer	k_1	k_2	k_3
Asphalt Concrete	50,000.0	0.1	0.0
Base	700.0	0.6	- 0.3
Subgrade	400.0	0.0	- 0.3

Table 24. Base Levels of Strength Parameters Used in Sensitivity Analysis.

Layer	Cohesion (kPa)	Friction Angle (degrees)
Asphalt Concrete	1720.0	0
Base	68.9	50
Subgrade	89.6	30

(i.e., no yielding) were predicted for the thick pavement. Consequently, the sensitivity of the predicted plastic strain to the k_1, k_2, and k_3 parameters, and to the cohesion and friction angle was established using the results for the thin pavement. For the thick pavement, the computed Mohr-Coulomb yield function values were used to evaluate the influence of these material parameters.

In addition to the predicted pavement response under loading, researchers used the predicted pavement performance to establish the importance of the factors considered in the sensitivity analysis. For this purpose, the Asphalt Institute models for fatigue cracking and rutting were used to predict service life for the different pavements included in the analysis. For rutting, service life is predicted using the relation:

$$N_r = 1.365 \ x \ 10^{-9} \left(\frac{1}{\epsilon_z} \right)^{-4.477}$$

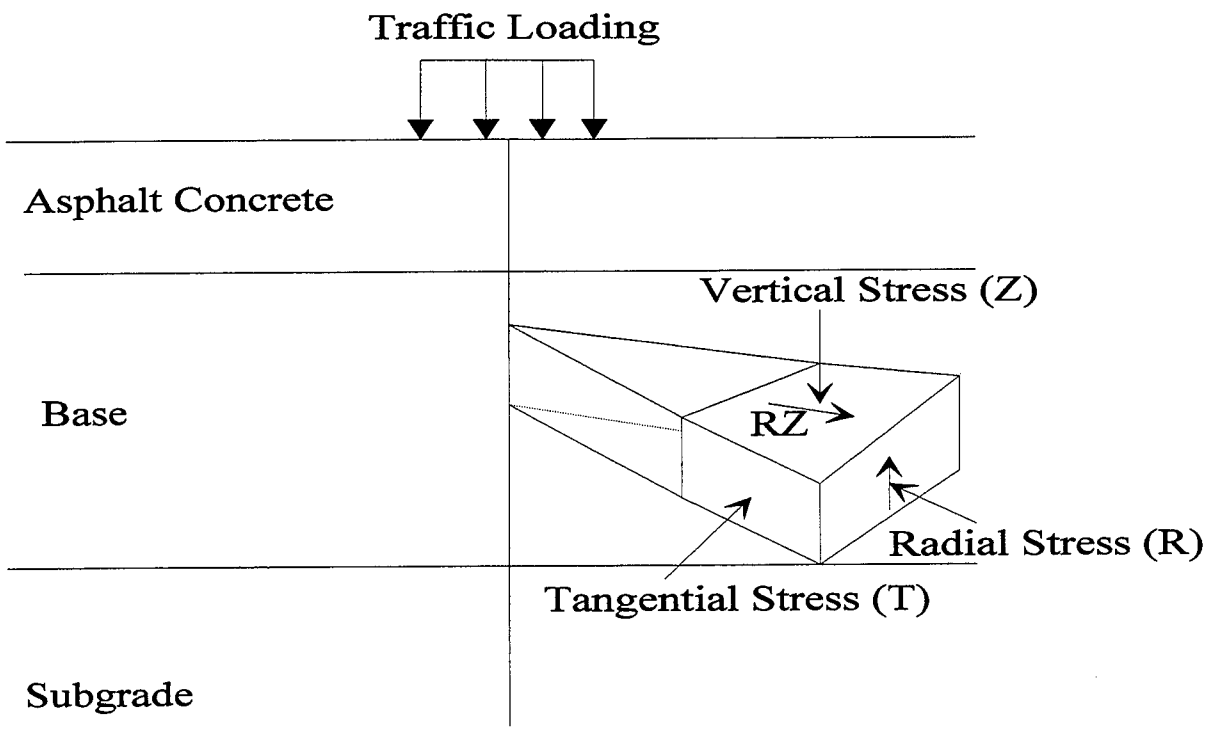

Figure 9. Component of Stresses Under Axisymmetric Loading.

where

N_r = allowable number of 80 kN equivalent single axle load (ESAL) applications prior to development of 13 mm ruts.

ϵ_z = predicted vertical compressive strain at the top of the subgrade.

For fatigue cracking, service life is predicted from the relation:

$$N_f = 0.079488 \left(\frac{1}{\epsilon_{ac}}\right)^{-3.29} \left(\frac{1}{E_{mix}}\right)^{-0.854}$$

where

N_f = allowable number of 80 kN ESALs based on fatigue cracking.

ϵ_{ac} = predicted tensile strain at the bottom of the asphalt surface layer.

E_{mix} = stiffness of the asphalt concrete mix in psi.

TxDOT presently uses the above equations to evaluate the need for load restrictions on a given highway. It is observed from the above equations that the higher the induced strains under loading, the shorter the predicted service life. These equations were developed by correlating the predicted pavement response under loading with observed pavement performance. Since pavement response is predicted based on layered elastic theory with no consideration of material yielding, the effects of cohesion and friction angle on the predicted service life were not evaluated. Thus, only the sensitivity of the predicted pavement performance to the stress-dependent material parameters was investigated. The following presents the findings from this analysis.

SENSITIVITY OF PREDICTED PLASTIC STRAIN

As mentioned previously, no yielding was predicted for the thick pavement considered in the sensitivity analysis. Consequently, the results herein are based on the predicted plastic strains from modeling of the post yield behavior of the thin pavement. Figures 10 to 14 show the results of the analysis. Plotted in these figures is the percent change in the predicted plastic strain due to a corresponding change in a given parameter. The higher the percent change in the predicted plastic strain, the higher the bar corresponding to that change and the more important a given parameter is. Since no yielding was predicted at the subgrade, the figures show the results based on the predicted plastic strains at the bottom of the asphalt surface and base layers. In all cases, the predicted plastic strains at the center of the wheel load were the most critical. The results shown in Figures 10 through 14 prompt the following observations:

1. The predicted plastic strain is most sensitive to the parameter, k_1. Figures 10, 12, and 14 show that the predicted plastic strain changes significantly whenever k_1 for a given layer is varied. Figure 10 shows that increasing the surface k_1 by 30 percent led to a higher predicted plastic strain at the bottom of the surface layer. This is due to the higher induced stresses resulting from a stiffer surface brought about by an increase in k_1. A stiffer material would show a higher

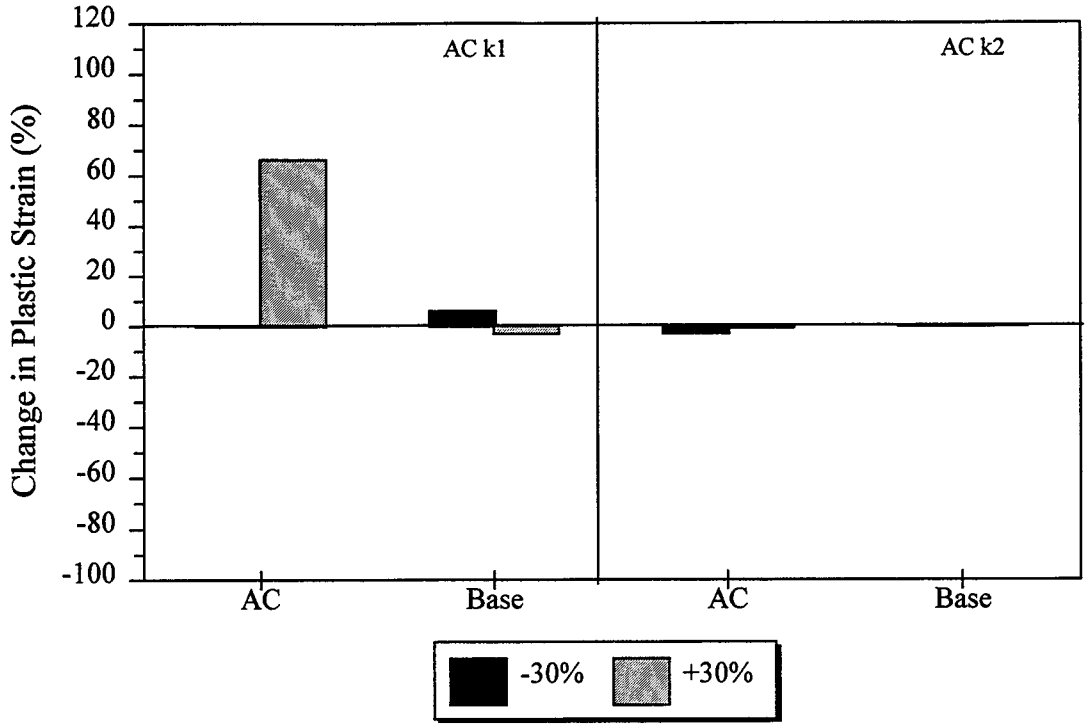

Figure 10. Sensitivity of the Plastic Strain to Changes in k1 and k2 Parameters of the Asphalt Concrete (Center of Load, Thin Pavement).

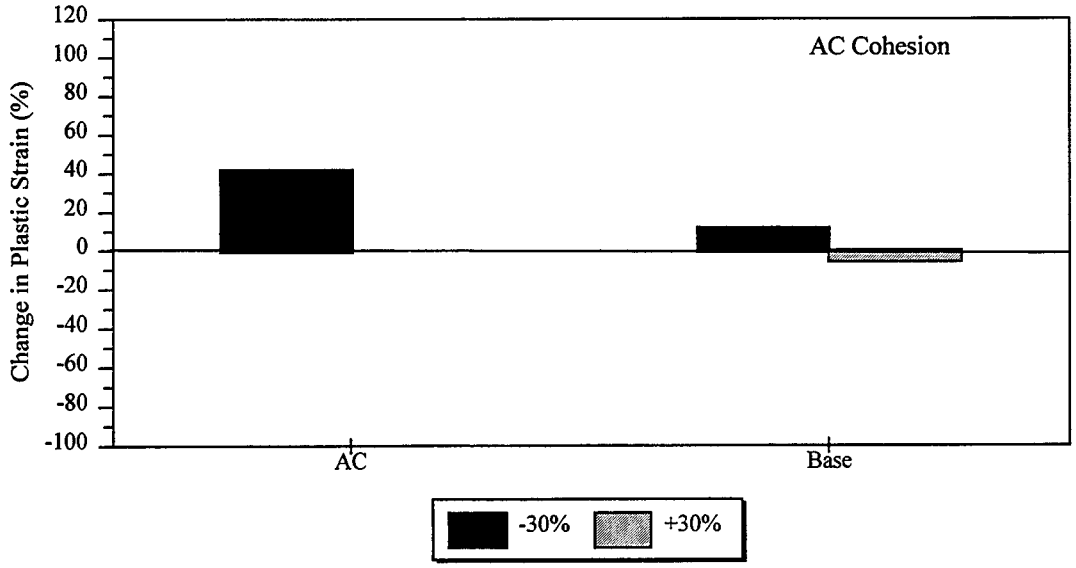

Figure 11. Sensitivity of the Plastic Strain to Changes in Cohesion of the Asphalt Concrete (Center of Load, Thin Pavement).

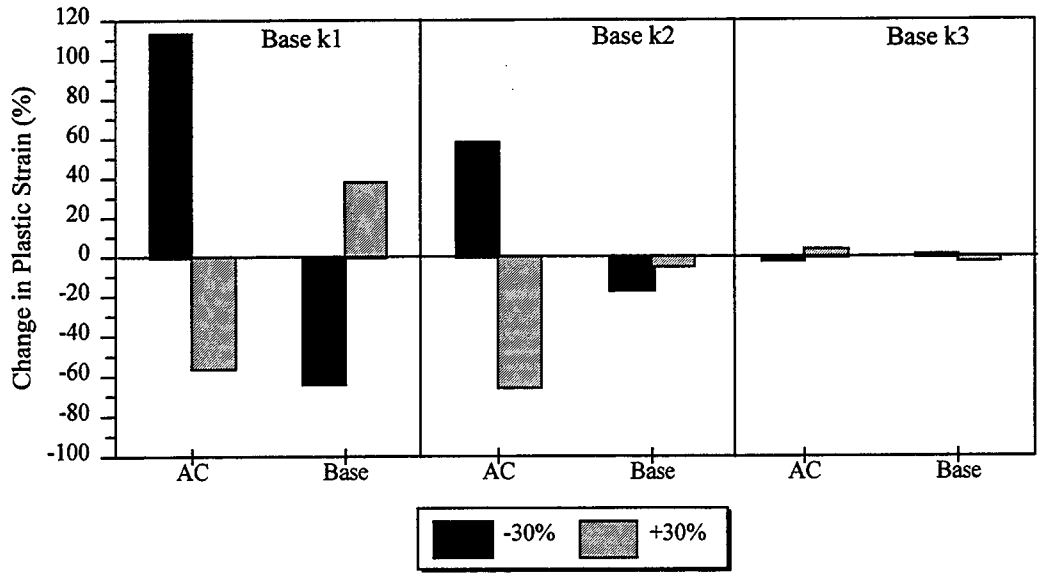

Figure 12. Sensitivity of the Plastic Strain to Changes in k1, k2, and k3 Parameters of the Base (Center of Load, Thin Pavement).

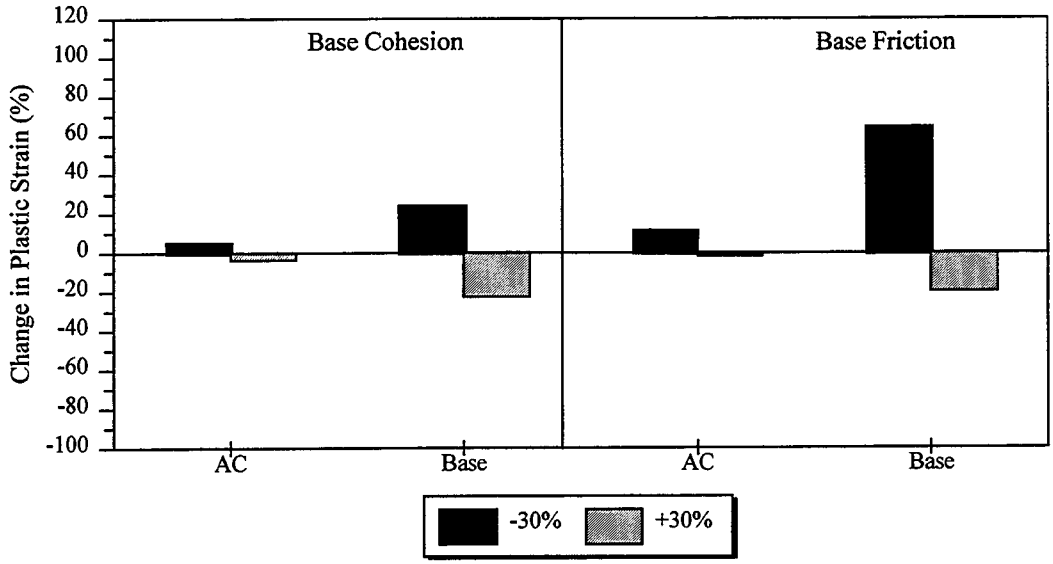

Figure 13. Sensitivity of the Plastic Strain to Changes in Cohesion and Angle of Friction of the Base (Center of Load, Thin Pavement).

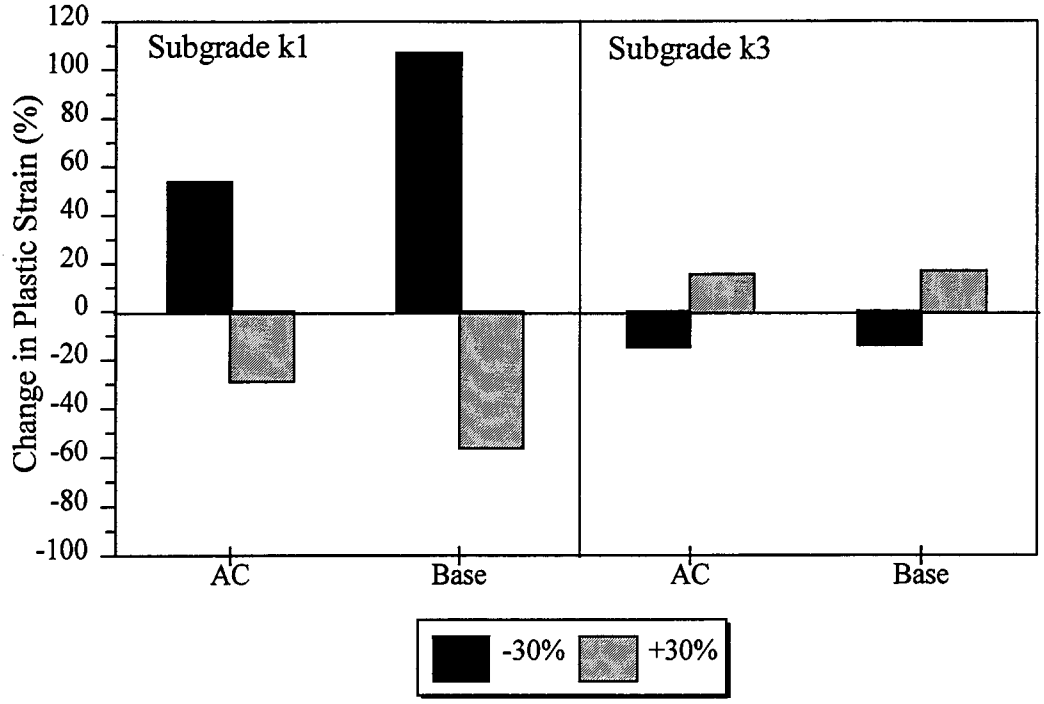

Figure 14. Sensitivity of the Plastic Strain to Changes in k1 and k3 Parameters of the Subgrade (Center of Load, Thin Pavement).

cohesion, which would counteract the effect of higher predicted stresses. However, since the parameters were varied only one at a time, this increase in cohesion with increase in k_1 was not considered in the sensitivity analysis. Thus, it is conceivable that the opposite effect may be observed in practice, depending on the relationships between stiffness, cohesion, and induced stresses for a given material.

2. The effect of varying the surface k_1 on the predicted plastic strain at the bottom of the base is relatively small compared to the corresponding effect on the predicted plastic strain at the bottom of the surface layer (Figure 10). It is observed that the higher the surface k_1, the lower the predicted plastic strain at the bottom of the base. This is due to the lower stresses predicted in the base because of the stiffer surface. Figure 10 also shows that the predicted plastic strain is not sensitive to changes in the surface k_2 for the pavement considered.

3. The cohesion of the surface layer has a significant effect on the predicted plastic strains as shown in Figure 11. The lower the cohesion, the higher the predicted plastic strain at the bottom of the surface. It is also observed that the predicted plastic strain at the bottom of the base increases when the surface cohesion is decreased by 30 percent. This reflects the redistribution of the stresses after initial yielding within the surface layer. Because of this, the base starts to carry more of the load, resulting in higher stresses at the bottom of the base and greater plastic strains.
4. The biggest change in the predicted plastic strain at the bottom of the asphalt layer occurred when the base k_1 was varied. Figure 12 shows that the predicted plastic strain in the asphalt layer increased by about a 110 percent when the base k_1 was reduced by 30 percent. This is due to the higher tensile stresses predicted in the surface layer as a result of a softer base providing diminished support to the overlying material. Figure 12 also shows that the predicted plastic strain at the bottom of the base increased when the base k_1 was raised by 30 percent. This effect was observed earlier in the asphalt layer when the surface k_1 was varied by +30 percent. Again, the observed effect is due to the higher induced tensile stresses at the bottom of the base due to the higher stiffness. Note, however, that the base cohesion was not varied at the same time that the base k_1 was increased.
5. The effect of base k_2 was most pronounced for the surface material. Figure 12 shows that the predicted plastic strain at the bottom of the surface increases by more than 50 percent when the base k_2 is reduced by 30 percent. The lower this parameter, the lower the base stiffness, leading to higher tensile stresses at the bottom of the surface and to higher predicted plastic strains at this same location. The effect of base k_2 is relatively less when the predicted plastic strain at the bottom of the base is considered. Note that when the base k_2 is reduced by 30 percent, the predicted plastic strain at the bottom of the base is also reduced owing to the decrease in the predicted tensile stresses as a result of a softer

material. Again, no corresponding change was made in the cohesion of the base when k_2 was reduced by 30 percent. Figure 12 also shows that the predicted plastic strains at the bottom of the asphalt and base layers are not sensitive to changes in the base k_3.

6. The effects of changes in the base cohesion and angle of internal friction are shown in Figure 13. It is observed that both parameters have a significant influence in the predicted plastic strains. The lower the values of the parameters, the higher the predicted plastic strains at the bottom of the base and surface layers. The angle of internal friction is observed to have a larger influence for the pavement considered.
7. Figure 14 shows that the subgrade k_1 significantly influences the predicted plastic strains in the asphalt and base layers. The lower the subgrade k_1, the higher the predicted plastic strains owing to the higher tensile stresses in the overlying materials because of a softer subgrade. The effect of subgrade k_3 is also significant but to a lesser extent compared to the effect of subgrade k_1. Note that the subgrade k_3 is negative. Since the predicted values for θ and τ_{oct} at the top of the subgrade are less than the atmospheric pressure, the stiffness of the subgrade decreases when the parameter, k_3, is increased by 30 percent. Thus, the predicted plastic strains at the bottom of the surface and base layers go up with increase in this parameter.

SENSITIVITY OF THE MOHR-COULOMB YIELD FUNCTION VALUE

Figures 15 through 17 illustrate the sensitivity of the Mohr-Coulomb yield function value to the material parameters considered in the analysis. The results shown are based on modeling the induced response under loading of the thick pavement illustrated in Figure 3. Mohr-Coulomb yield function value at the evaluation points shown in Figure 3. The Mohr-Coulomb yield function is given by the equation in Appendix B. The higher the yield function value, the greater the potential for pavement damage under loading. Based on the results shown in Figures 15 to 17, the following observations are made:

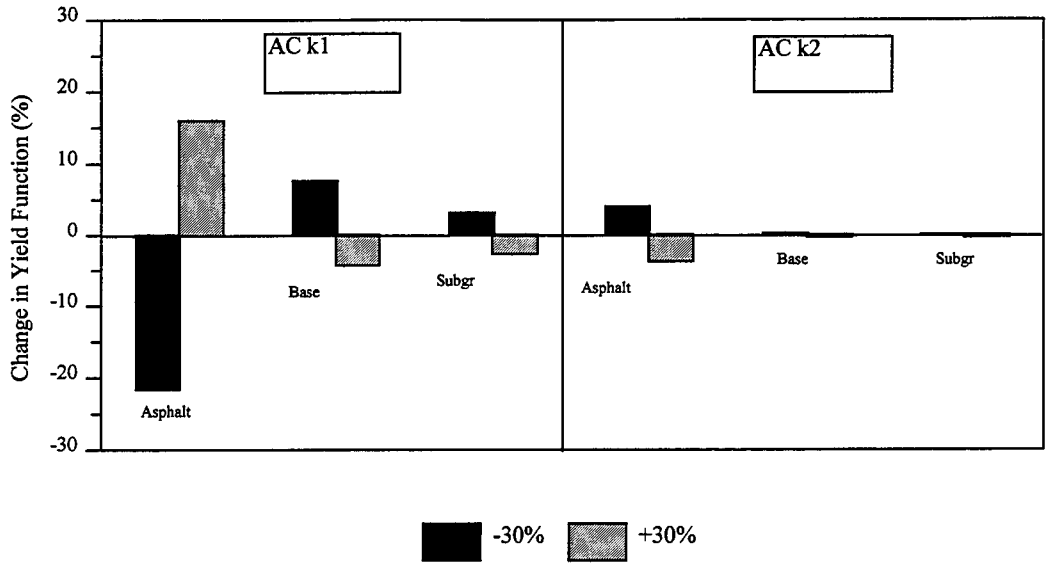

Figure 15. Sensitivity of the Yield Function to Changes in k1 and k2 Parameters of the Asphalt Concrete (Center of Load, Thick Pavement).

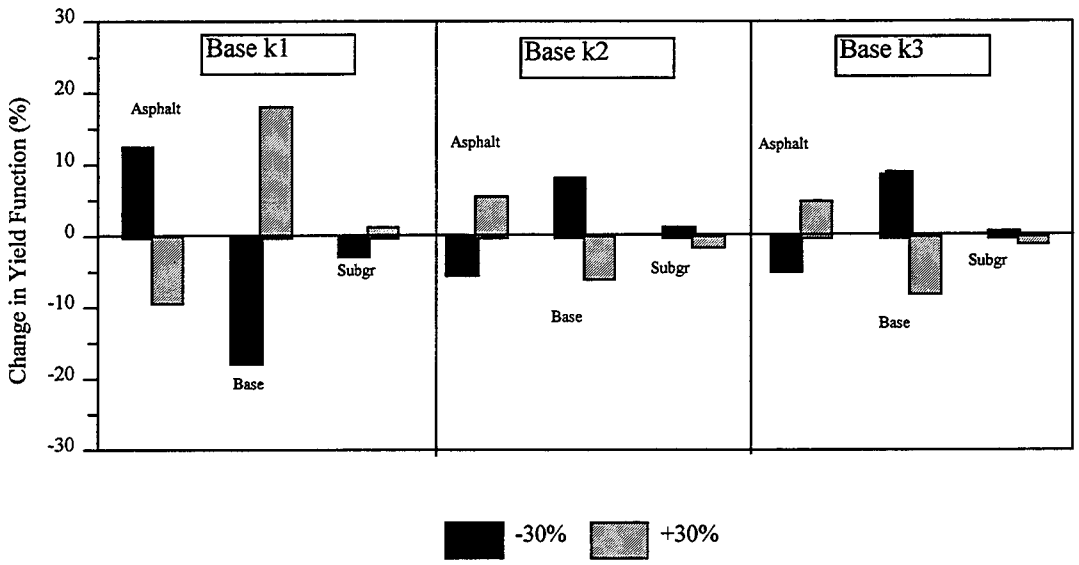

Figure 16. Sensitivity of the Yield Function to Changes in k1, k2, and k3 Parameters of the Base (Center of Load, Thick Pavement).

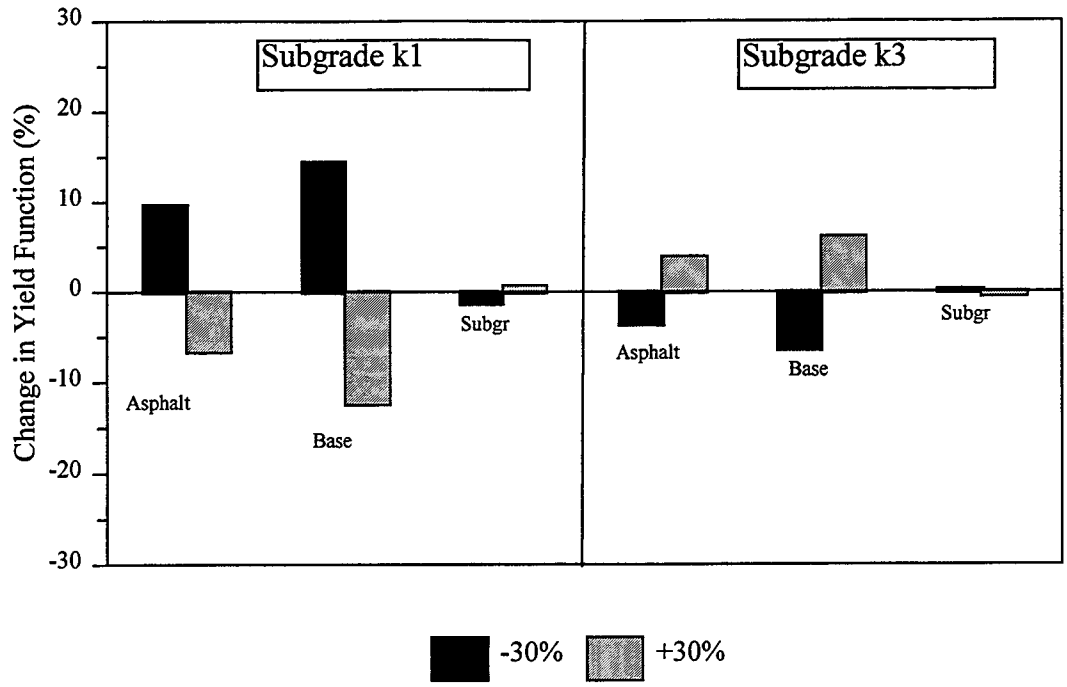

Figure 17. Sensitivity of the Yield Function to Changes in k1 and k3 Parameters of the Subgrade (Center of Load, Thick Pavement).

1. The biggest changes in the Mohr-Coulomb yield function value occurred when the parameter, k_1, of a given layer was varied. For the asphalt surface, an increase in k_1 led to a corresponding increase in the Mohr-Coulomb yield function indicating a higher potential for pavement damage under loading (Figure 15). This is due to the higher tensile stresses predicted at the bottom of the asphalt layer as the stiffness increases when k_1 is varied by +30 percent. Again, the cohesion was not varied with the change in k_1. For the base and the As mentioned earlier, no yielding was predicted for the thick pavement. Thus, the effects of changes in the material parameters were established based on the predicted changes in the subgrade, the predicted Mohr-Coulomb yield function values decreased with an increase in the surface k_1, reflecting the reduced stresses within these layers due to the stiffer surface. Figure 15 also shows that the effects of the surface k_2 parameter on the Mohr-Coulomb yield function

values at the bottom of the surface layer are relatively smaller compared to the effects of k_1. In addition, the effects of the surface k_2 parameter on the Mohr-Coulomb yield function values computed for the base and the subgrade are negligible.

2. Figure 16 shows that changes in the stress-dependent parameters of the base led to significant changes in the Mohr-Coulomb yield function values computed at the bottom of the asphalt and base layers. The effects of the base parameters on the yield function values computed at the top of the subgrade are minimal. Figure 16 shows that increasing the base k_1 led to a lower yield function value at the bottom of the surface layer, reflecting the reduction in the tensile stresses at this location due to the stronger support provided by the stiffer base. In general, the effects of the base parameters may be explained by the changes in the predicted base stiffness. For the pavement considered, increasing the base k_2 and k_3 parameters resulted in a lower base stiffness. Consequently, the Mohr-Coulomb yield function values computed for the surface went up with a +30 percent change in these parameters.
3. The benefit of a stiffer subgrade is illustrated in Figure 17 where it is observed that increasing the subgrade k_1 led to lower computed yield function values at the bottom of the surface and base layers. Since the predicted values for θ and τ_{oct} at the top of the subgrade are less than the atmospheric pressure, the stiffness of the subgrade decreases when the parameter, k_3, is increased by 30 percent. Thus, the computed yield function values at the bottom of the surface and base layers go up with a +30 percent change in this parameter. These effects mirror the results reported previously regarding the effects of subgrade k_3 on the predicted plastic strains.

SENSITIVITY OF PREDICTED SERVICE LIFE

Figures 18 through 29 illustrate the effects of the stress-dependent material parameters on the predicted service life based on rutting. The predicted service life is most

sensitive to changes in the k_1 parameter for both thin and thick pavements. Figures 18 to 23 show that the predicted service life based on rutting increases when this parameter is varied by +30 percent in the different layers. The figures also indicate that the thin pavement is influenced more by changes in the base and subgrade parameters than the thick pavement. The greatest change in the predicted service life occurred when the subgrade k_1 was varied by +30 percent for the thin pavement (see Figure 20). For the thick pavement, the biggest changes in the predicted service life occurred when the k_1 parameters for the surface and the subgrade were varied (Figures 21 and 23, respectively).

Figures 24 to 29 illustrate the effects of the stress-dependent material parameters on the predicted fatigue life. With respect to the thin pavement, the fatigue life is predicted to decrease with an increase in the surface k_1, as may be observed from Figure 24. Based on the Asphalt Institute fatigue equation, the predicted service life is inversely related to the stiffness of the asphalt concrete mix. The induced tensile strain will generally be less with a stiffer mix, which will tend to counteract the effect of the increased stiffness. However, differences in the predicted tensile strain associated with differences in asphalt concrete stiffness are relatively less for thin pavements compared to thick pavements. Thus, the effect of surface k_1 illustrated in Figure 24 is primarily attributed to the increase in stiffness associated with a +30 percent change in this parameter. For the thick pavement, the opposite effect is observed, as shown in Figure 27. In this case, the reduction in the induced tensile strain at the bottom of the asphalt with increase in stiffness was significant and controlled the predicted fatigue life.

The biggest changes in the predicted fatigue life for the thin pavement occurred when the base parameters were varied. Figure 25 indicates that increasing the support afforded by the base leads to a higher predicted fatigue life for thin pavements. For thick pavements, the predicted fatigue life is most sensitive to changes in the k_1 parameter for the asphalt concrete mix (Figure 27).

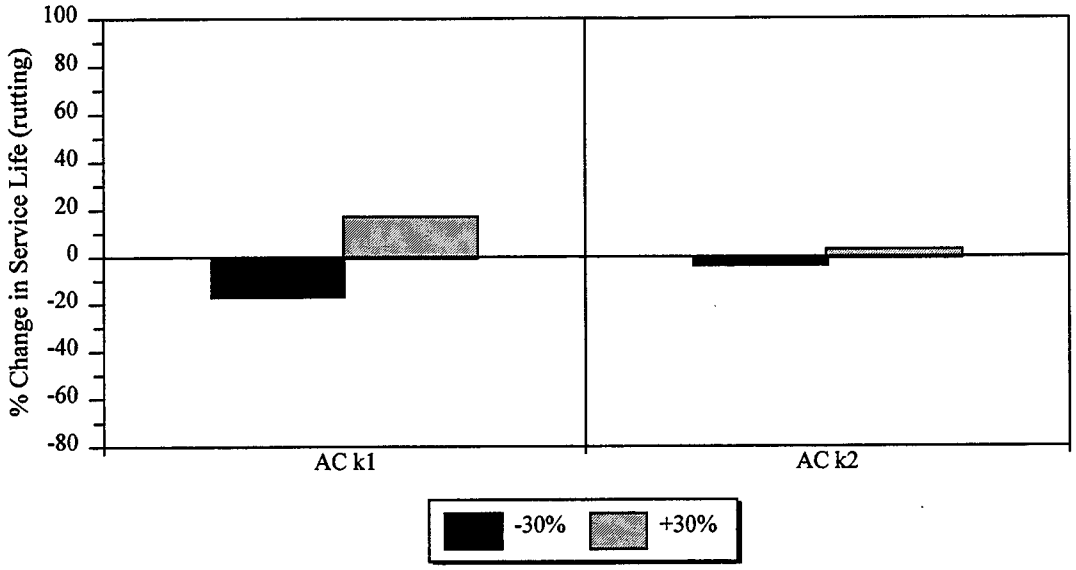

Figure 18. Sensitivity of the Service Life Based on Rutting to Changes in k1 and k2 Parameters of the Asphalt Concrete (Center of Load, Thin Pavement).

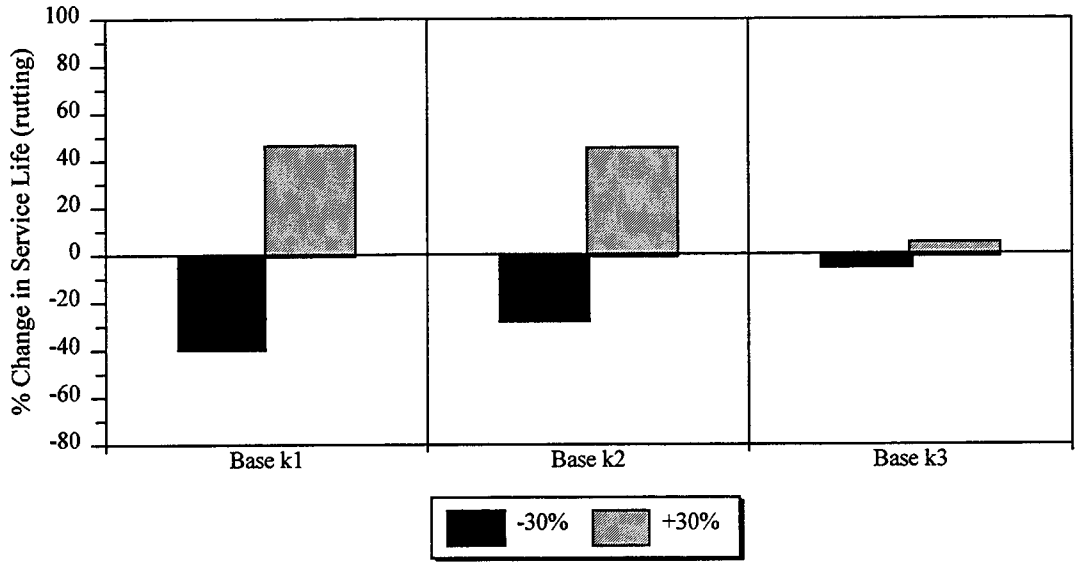

Figure 19. Sensitivity of the Service Life Based on Rutting to Changes in k1, k2, and k3 Parameters of the Base (Center of Load, Thin Pavement).

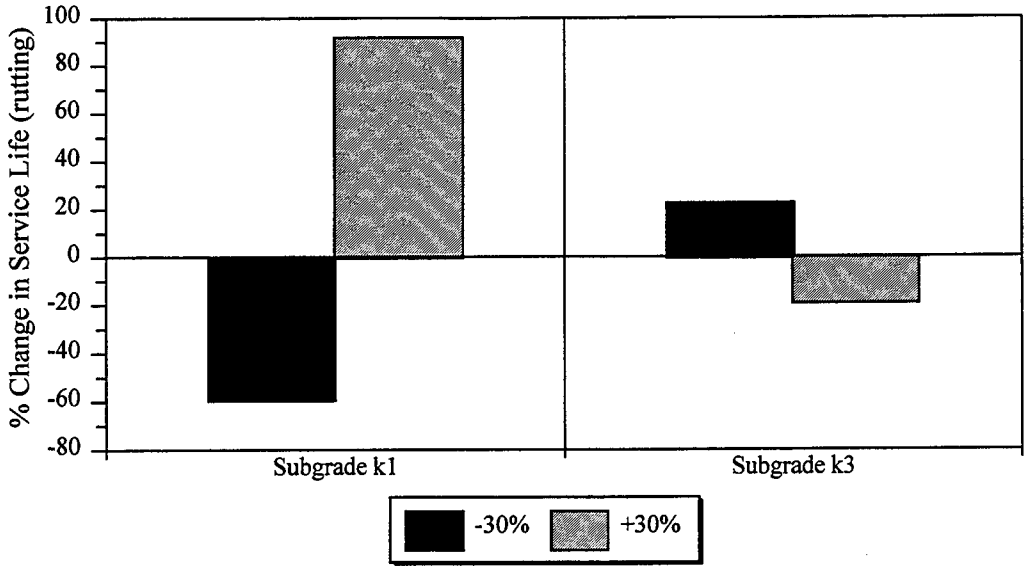

Figure 20. Sensitivity of the Service Life Based on Rutting to Changes in k1 and k3 Parameters of the Subgrade (Center of Load, Thin Pavement).

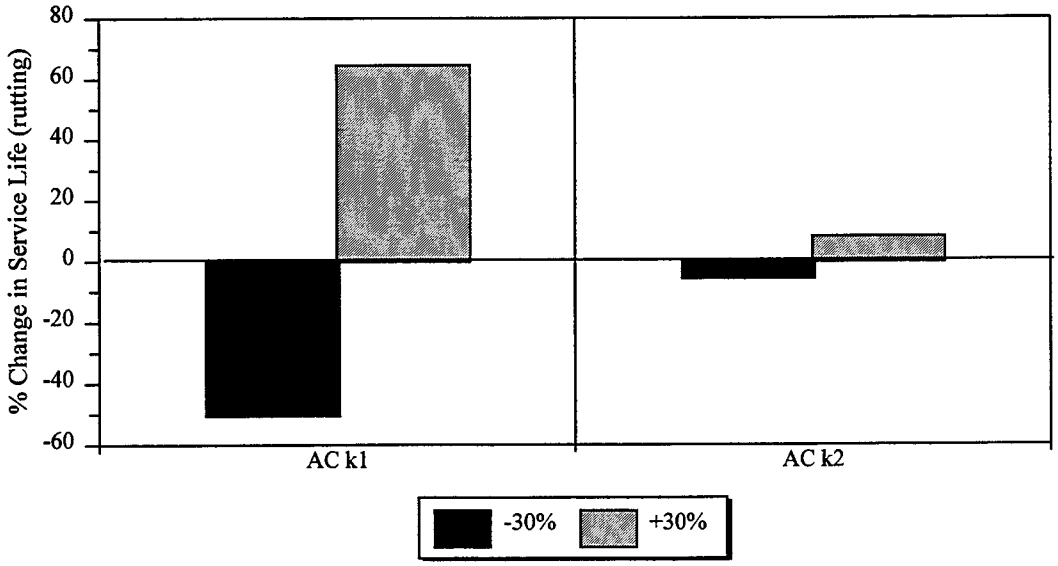

Figure 21. Sensitivity of the Service Life Based on Rutting to Changes in k1 and k2 Parameters of the Asphalt Concrete (Center of Load, Thick Pavement).

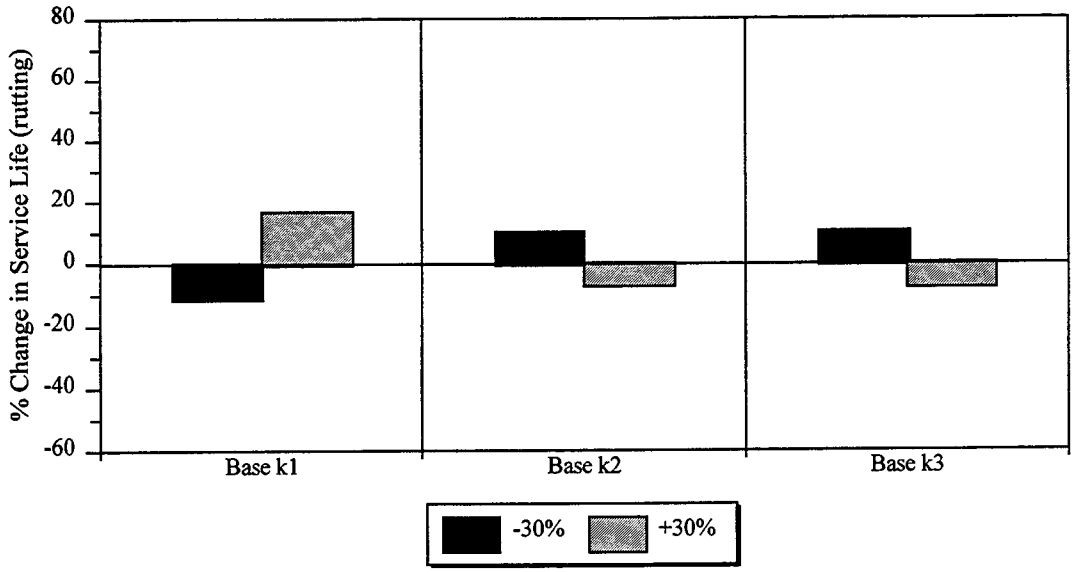

Figure 22. Sensitivity of the Service Life Based on Rutting to Changes in k1, k2, and k3 Parameters of the Base (Center of Load, Thick Pavement).

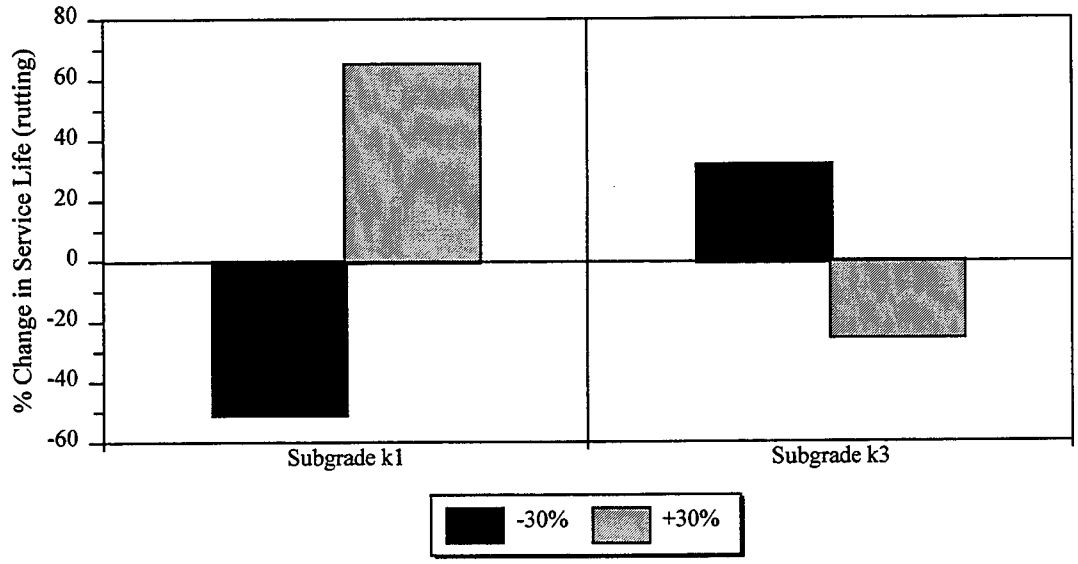

Figure 23. Sensitivity of the Service Life Based on Rutting to Changes in k1 and k3 Parameters of the Subgrade (Center of Load, Thick Pavement).

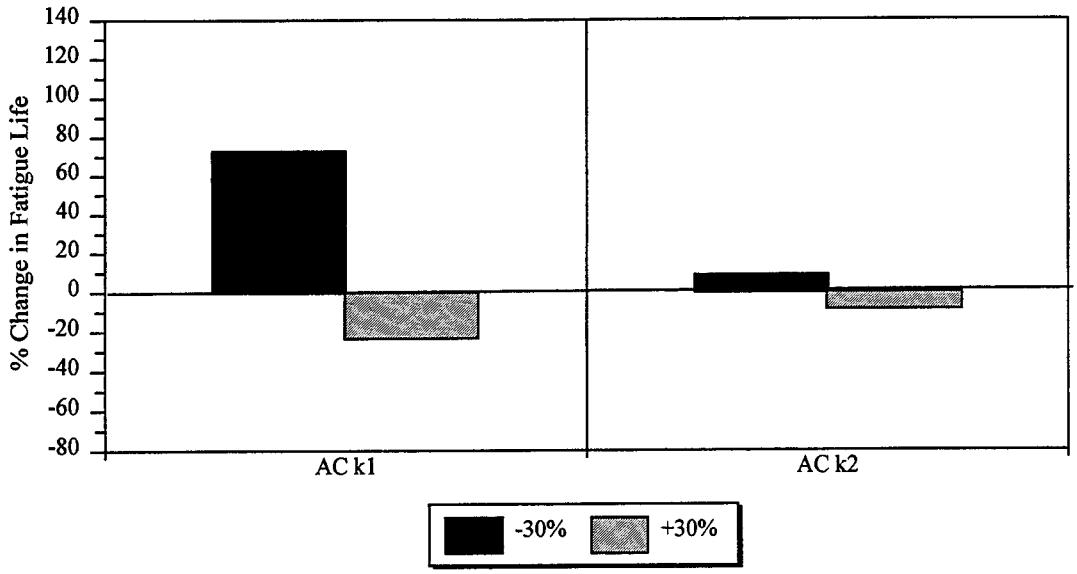

Figure 24. Sensitivity of the Fatigue Life to Changes in k1 and k2 Parameters of the Asphalt Concrete (Center of Load, Thin Pavement).

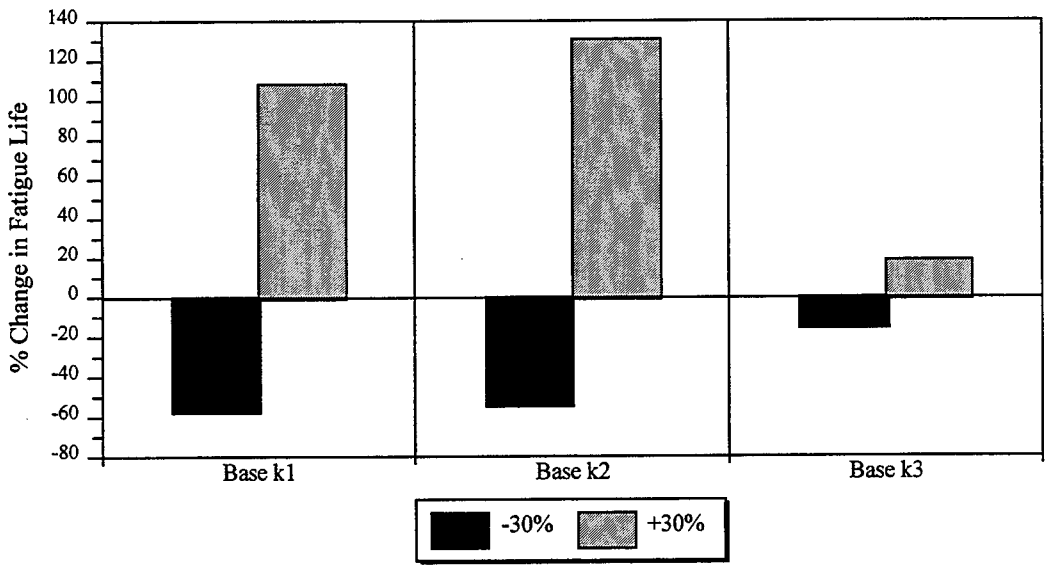

Figure 25. Sensitivity of the Fatigue Life to Changes in k1, k2, and k3 Parameters of the Base (Center of Load, Thin Pavement).

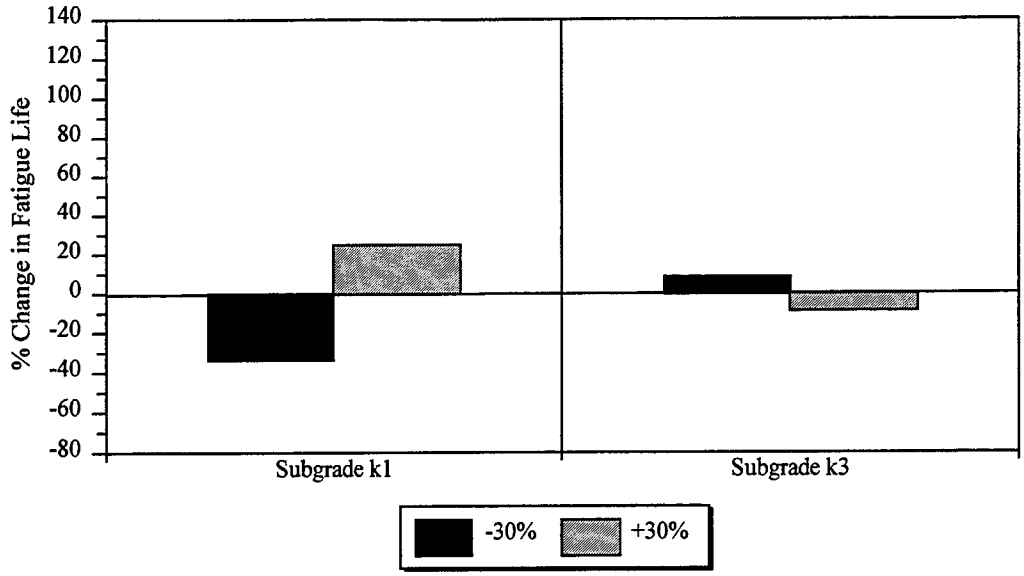

Figure 26. Sensitivity of the Fatigue Life to Changes in k1 and k3 Parameters of the Subgrade (Center of Load, Thin Pavement).

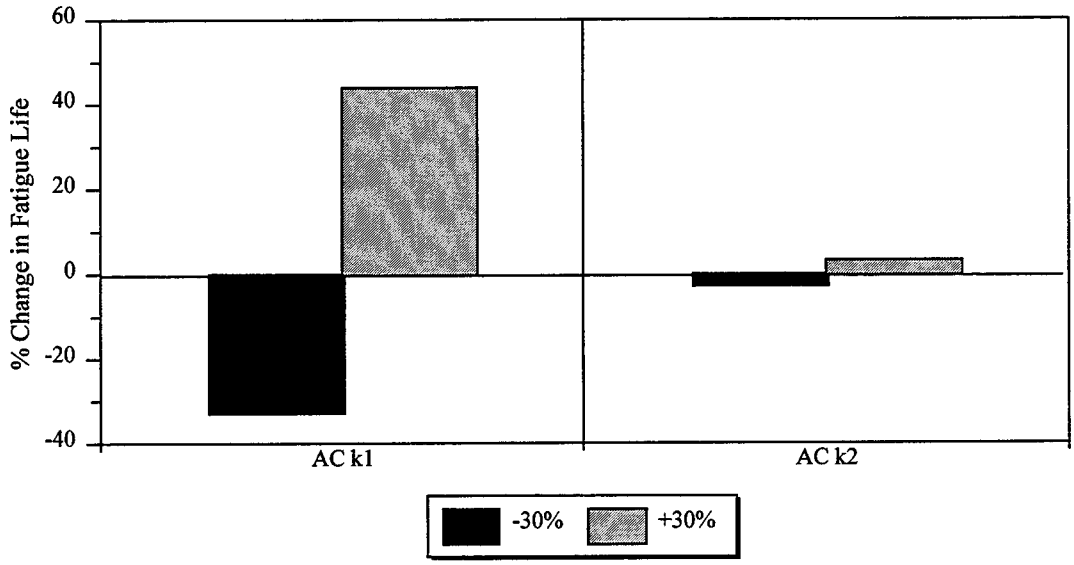

Figure 27. Sensitivity of the Fatigue Life to Changes in k1 and k2 Parameters of the Asphalt Concrete (Center of Load, Thick Pavement).

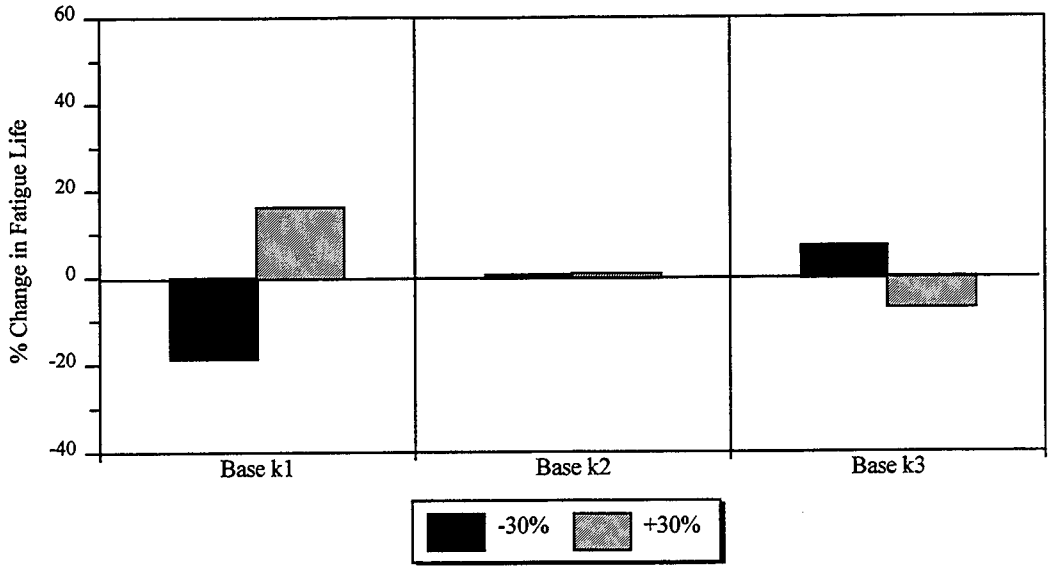

Figure 28. Sensitivity of the Fatigue Life to Changes in k1, k2, and k3 Parameters of the Base (Center of Load, Thick Pavement).

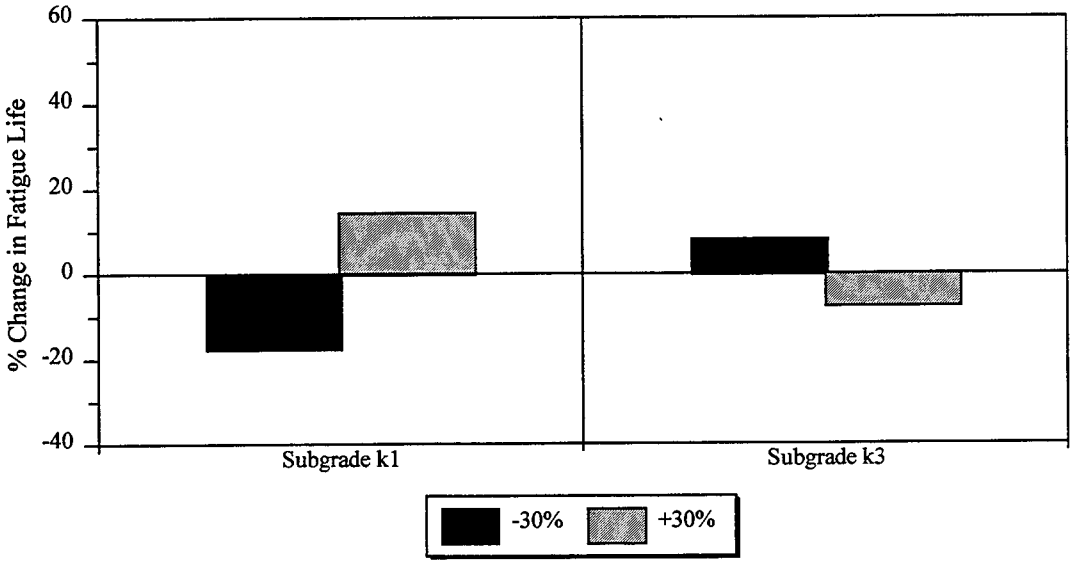

Figure 29. Sensitivity of the Fatigue Life to Changes in k1 and k3 Parameters of the Subgrade (Center of Load, Thick Pavement).

SUMMARY OF FINDINGS

The results from the sensitivity analysis consistently point to the importance of the k_1 parameter in the development of distress in flexible pavements. The effects of the k_2 and k_3 parameters, particularly for the base and subgrade are also significant, but to a lesser degree compared to the effects of k_1. Accurate estimates of these stress-dependent material parameters are important in predicting pavement response and performance for the purpose of evaluating the need for load restrictions.

The effects of the k_1 to k_3 parameters are primarily associated with the predicted layer stiffness. In general, increasing the value of k_1 results in a higher stiffness. The findings from the sensitivity analysis clearly show the importance of good base and subgrade support to pavement load carrying capacity. A good subgrade will mobilize the confining pressures in the base layer and reduce the bending of the upper layers under load. A strong base will reduce bending of the surface layer and reduce the stresses in the subgrade, which is particularly important for subgrade materials that exhibit stress-softening behavior.

Finally, the sensitivity analysis established the importance of the Mohr-Coulomb strength parameters in the development of plastic deformation under loading. Thus, accurate characterizations of the cohesion and angle of internal friction are necessary in evaluating the need for load restrictions. There is evidence from the study conducted by Glover and Fernando (1995) that cohesion is related to the stiffness of a given material. This relationship varies for different materials, and a need exists for a more detailed study to evaluate the relationships between cohesion and material stiffness. In this way, changes in cohesion with changes in layer stiffness may be estimated.

CHAPTER 4
EVALUATION OF PERMANENT DEFORMATION BEHAVIOR

When pavement materials are subjected to repetitive loading, both elastic and plastic strains are developed. Plastic strains are unrecoverable and manifest themselves in surface ruts, which represent the accumulated deformation in the underlying layers. For timely and cost-effective maintenance of pavements, the prediction of permanent deformation is very important. The development of distress with time or traffic is illustrated conceptually in Figure 30. For load-zoning purposes, permanent deformation properties are needed to predict the development of rutting under repeated traffic loads.

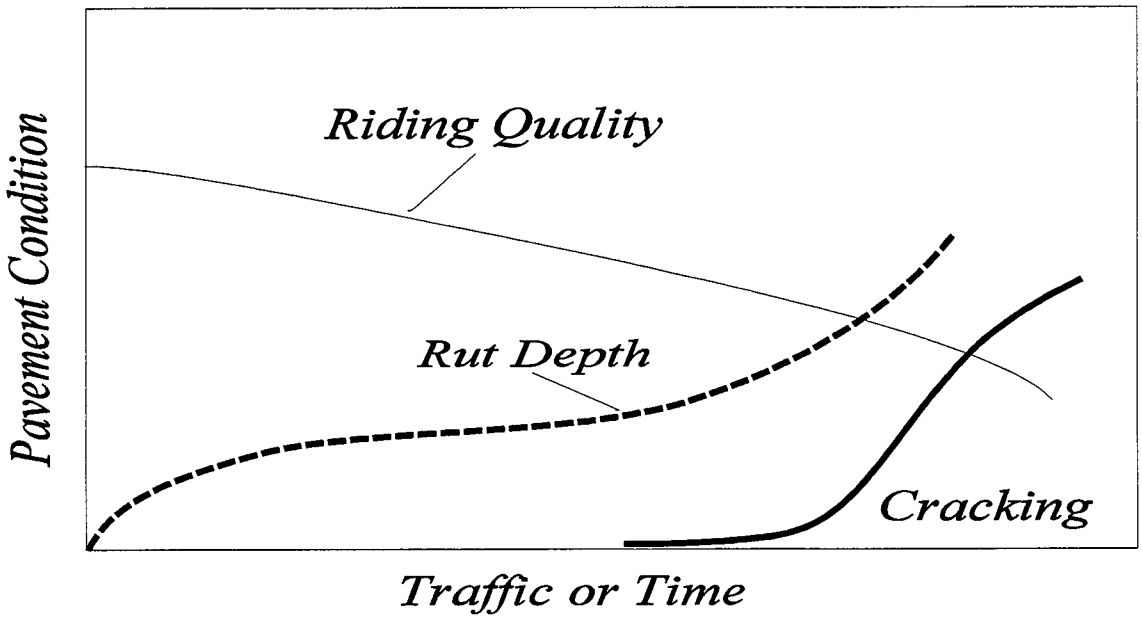

Figure 30. Conceptual Pavement Behavior Under Traffic (Redrawn from CSRA, 1985).

LABORATORY TESTS

In order to evaluate permanent deformation behavior under traffic loading, researchers conducted repeated-load permanent deformation tests in the laboratory on a number of base and subgrade materials at various moisture contents and stress conditions. Currently, there is no standard test procedure for determining the permanent deformation of unbound materials. For the laboratory tests conducted in this study, the VESYS procedure (Kenis 1978) was reviewed to establish the test plan for the repeated load-permanent deformation tests.

From the results of the sensitivity analysis of predicted plastic strain, the importance of a strong base and subgrade in minimizing the development of plastic strains was demonstrated. Considering that most load-zoned roadways in Texas are thin-surfaced pavements, the permanent deformation characterization of the base and subgrade will most likely control the predicted service life based on rutting. There are several factors that affect the permanent deformation of base and subgrade materials (Maree 1978):

- stress condition and number of stress applications,
- rate of stress application,
- compaction,
- grading,
- plasticity of fines,
- geological origin of materials,
- strength of materials,
- particle shape or form,
- surface texture,
- moisture, and
- temperature.

For this study, the factors investigated were the moisture content, stress state (confining pressure and deviatoric stress), and material type.

In general, the level of stress is one of the most important factors in the development of permanent deformation in pavements. Repetitive or cyclic loading may develop permanent deformation in unbound materials, including subgrade soils more rapidly than monotonic loading. Several studies found that the permanent axial strain increases with decreasing confining pressure, and increasing deviatoric stress (Shackel 1973 and Wood 1982). Barksdale (1972) has reported that the accumulated plastic strain of base materials increased with an increase in the deviatoric stress or with a reduction in the confining pressure. The effect of the deviatoric stress in the accumulation of plastic strains was also found to be more pronounced for clay soils than granular materials (Shackel 1973, Li and Selig 1996).

In addition, the accumulated permanent deformation is increased substantially with higher moisture contents primarily due to the loss of cohesion, particularly at moisture contents above optimum. There is also some interaction between the moisture content and the applied stress level. At high levels of deviatoric stress, an increase in moisture content will accumulate the development of permanent deformation more than at low levels of deviatoric stress.

For the tests conducted in this study, researchers used the Superpave Shear Tester (SST), originally developed for the Strategic Highway Research Program (SHRP), to characterize the permanent deformation behavior of three base materials and one subgrade material. The materials tested were crushed limestone, iron ore gravel, caliche, and clay. Axial and radial displacements were measured using linear variable differential transducers (LVDTs). This SHRP shear tester consists of 4 main parts: the testing apparatus, the test control unit and data acquisition, the environmental chamber, and the hydraulic system (McGennis et al. 1995). The testing chamber shown in Figure 31 is capable of providing confining pressure using compressed air. It also controls the test temperature. The testing apparatus has axial and horizontal actuators with accompanying LVDTs to measure the response of the specimen under repetitive loading. The equipment provides closed-loop feedback control using actuators.

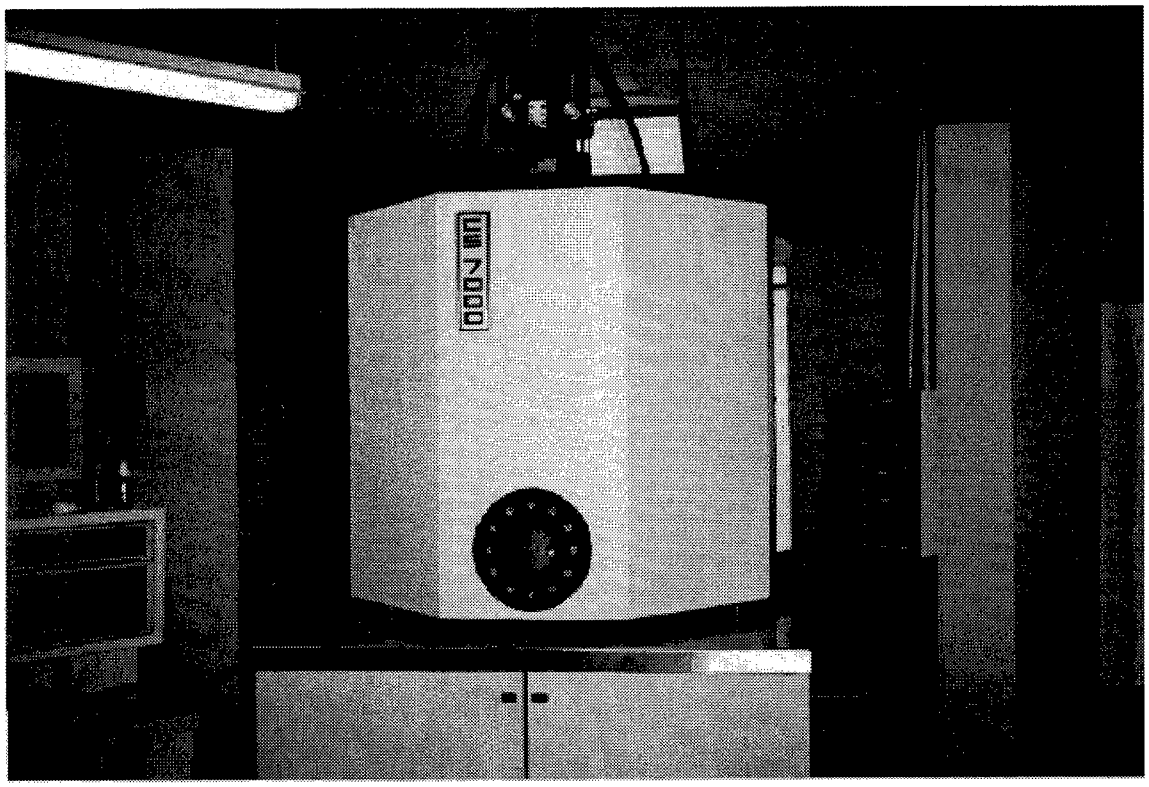

Figure 31. Environmental Control Chamber and Testing Apparatus of SST.

Tables 25 and 26 show the gradation and Atterberg limits of the materials tested (Titus-Glover and Fernando 1995). Test samples were prepared and compacted at various moisture conditions in accordance with test method Tex-113-E. Specimens were 152.4 mm in diameter and ranged in height from 229 to 259 mm. After molding, each sample was wrapped in plastic and stored in a temperature-controlled chamber until the test could be conducted.

A lubricated latex membrane was used around the sample as shown in Figure 32. Three axial LVDTs were then mounted 120 degrees apart around the specimen to measure the vertical displacement within the mid-height of the specimen. In addition, the radial displacement was measured at the middle of the specimen using a bracelet developed for this purpose. Figure 33 shows an instrumented sample. Confining pressure was applied using compressed air and was held at the specified level for the duration of the test.

Table 25. Gradation of Materials Tested (Percent Passing Under Sieve Size).

Sieve Size (mm)	Clay	Caliche	Limestone	Iron Ore Gravel
50.80	-	100.00	100.00	100.00
25.40	-	90.35	100.00	100.00
19.05	-	72.32	84.47	97.60
9.525	-	58.92	64.71	90.98
4.750	100.00	51.33	52.71	76.08
2.000	100.00	45.56	42.29	56.12
0.420	100.00	39.24	30.10	40.36
0.250	98.35	38.39	26.93	37.34
0.149	95.53	35.16	23.51	32.91
0.106	92.03	27.81	19.77	28.51
0.075	88.48	25.87	17.61	21.95

Table 26. Atterberg Limits of Materials Tested.

Material	Liquid Limit (%)	Plastic Limit (%)	Plasticity Index (%)
Clay	35.00	13.90	21.10
Caliche	33.26	18.37	14.69
Limestone	20.70	11.30	7.90
Iron Ore Gravel	18.35	16.63	1.72

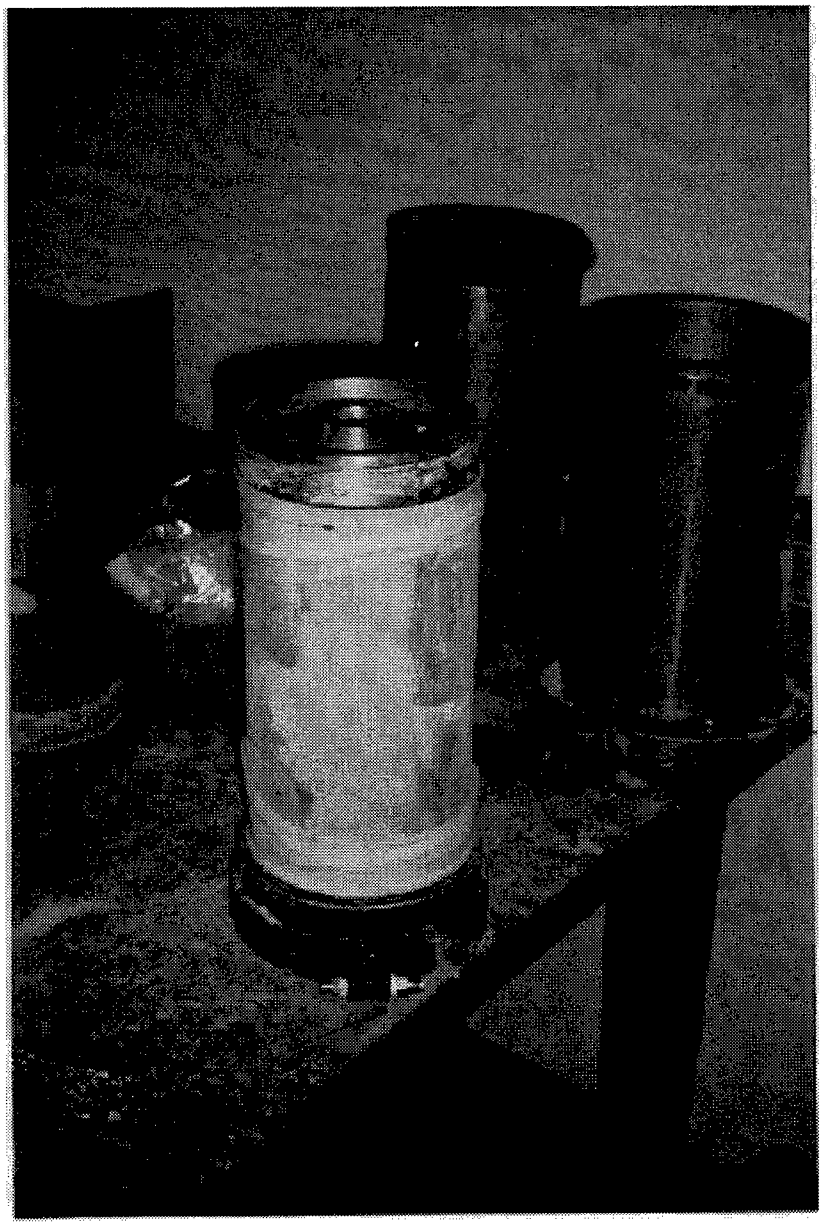

Figure 32. Test Specimen with Latex Membrane and Platens.

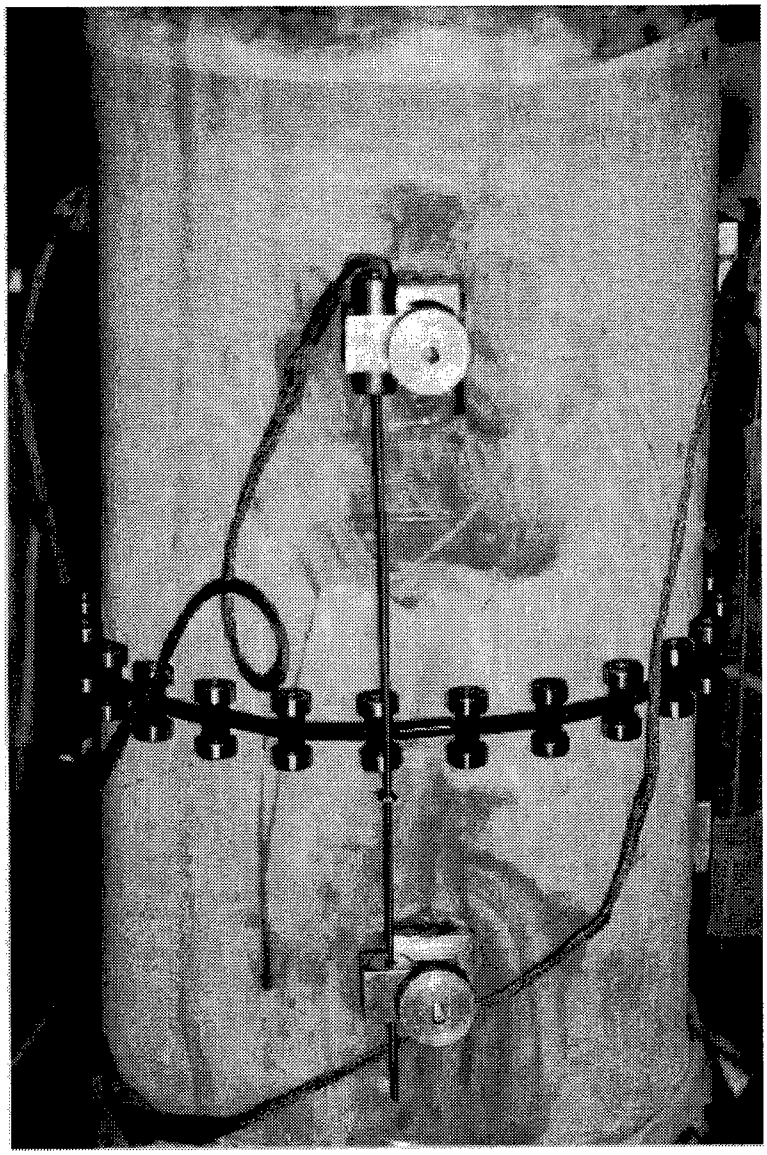

Figure 33. Vertical and Radial LVDTs on Sample.

After sample preparation and instrumentation, the specimen was tested under repetitive loading for up to 10,000 cycles or until the specimen failed, whichever came earlier. Each load cycle consisted of a 0.1 second loading time and a 0.9 second rest period. Initially, specimens were subjected to 200 cycles of preconditioning at vertical loads that were 10 percent of the deviatoric stress. After preconditioning, the full deviatoric stress was applied for up to 10,000 cycles or until failure, whichever came earlier. The accumulated vertical and radial deformations were recorded throughout the test. Figure 34 provides a conceptual illustration of the data from a repeated load-permanent deformation test.

For each material, tests were conducted at three moisture contents (Table 27), and at four stress states defined by four combinations of confining pressure and deviatoric stress (Table 28). Table 28 shows that the base materials were tested using one set of stress conditions, while the subgrade material (clay) was tested using a different set. The stress levels applied during the tests were established based on triaxial test data reported by Glover and Fernando (1995). Stress levels for the base are higher than those for the subgrade in consideration of the reduction in predicted stresses under loading with depth into the pavement.

For each test, the accumulated strain envelope illustrated in Figure 34 was determined. In addition, the full deformation data covering the loading and unloading portions of a given cycle were recorded for the 199th, 200th, and 201st load cycles to determine the resilient strain at the 200th repetition. This quantity is needed to characterize the parameters, α and μ, of the VESYS rutting model (Kenis 1978) given by the equation:

$$\epsilon_a = I\, N^S$$

where

ϵ_a	=	the accumulated strain at a given load cycle,
N	=	cumulative load cycles, and
I, s	=	model parameters.

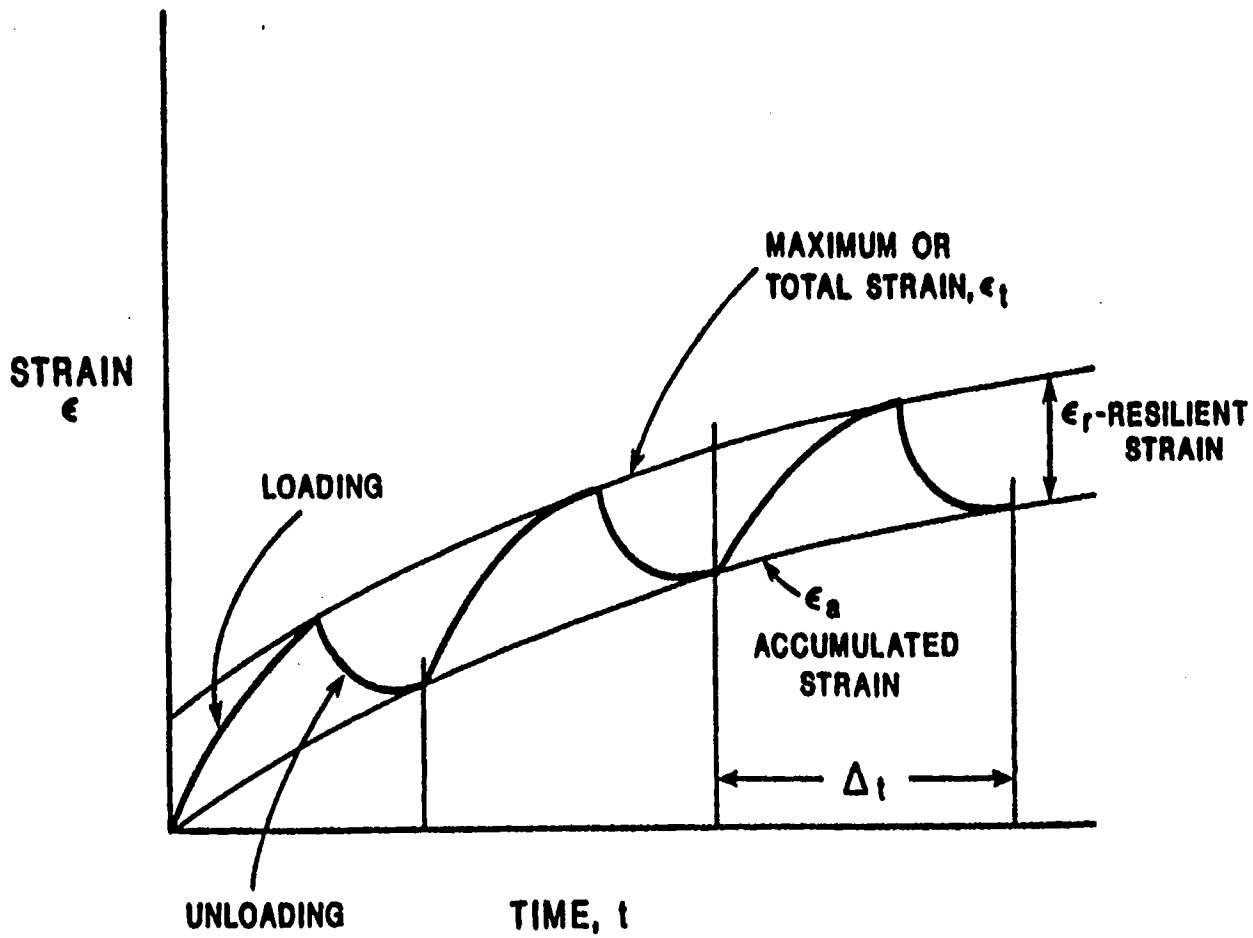

Figure 34. Conceptual Illustration of Test Results from Repeated Load- Permanent Deformation Testing (Hoyt et al. 1987).

Table 27. Moisture Content at Which Samples Were Prepared.

Level	Clay	Caliche	Limestone	Iron Ore Gravel
High	21.0 %	8.7 %	8.3 %	12.65 %
Optimum	19.0 %	6.7 %	7.3 %	10.65 %
Low	17.0 %	4.7 %	6.3 %	8.65 %

Table 28. The Level of Test Loads for Materials.

Material	Clay	Caliche	Limestone	Iron Ore Gravel
Confining pressure (kPa)	13.8 41.4	34.5 103.5	34.5 103.5	34.5 103.5
Deviatoric stress (kPa)	48.3 96.6	172.5 345.0	172.5 345.0	172.5 345.0

The above equation defines a linear relationship between the logarithm of the accumulated strain and the logarithm of the number of load cycles. The parameter, *I*, is the arithmetic value of the intercept and *s* is the slope of the logarithmic relationship. From these parameters, α and μ are calculated as follows:

$$\mu = \frac{I\,s}{\epsilon_r}$$

$$\alpha = 1 - s$$

where

ϵ_r = the resilient strain at the 200th load repetition.

The following discusses the effects of test variables on the observed permanent deformation behavior in the laboratory.

TEST RESULTS

The accumulated plastic strain was calculated from the test data as follows.

$$\epsilon_p = \frac{\sum h}{h_i}$$

where ϵ_p = the accumulated plastic strain,

$\sum h$ = the average of accumulated deformation from LVDTs for a given load cycle, and

h_i = the sample gage length.

Figures 35 through 46 show the accumulated plastic strains with number of load cycles. The results indicate that the accumulated plastic strains are nonlinear with load applications. Under repetitive loadings, plastic strains are accumulated and the accumulation of the plastic strain is directly dependent upon the number of load applications. Initially, the plastic strain increases rather rapidly. After some number of load applications, the rate of increase in plastic strain is then observed to diminish.

Figures 35 and 36 illustrate the effect of moisture content on the development of permanent strain for the clay samples tested. As observed from the figures, the measured accumulated strain increases with increase in moisture content. These results indicate the importance of moisture content in evaluating the load carrying capacity of pavements. Thus, the load-zoning procedure must allow the pavement engineer to consider the effects of moisture in the evaluation of permanent deformation, as the conditions warrant. This variable may vary not only seasonally but also with location along a given roadway.

Figures 37 and 38 illustrate the effect of confining pressure. As may be observed from these figures, the development of plastic strain is diminished by an increase in the

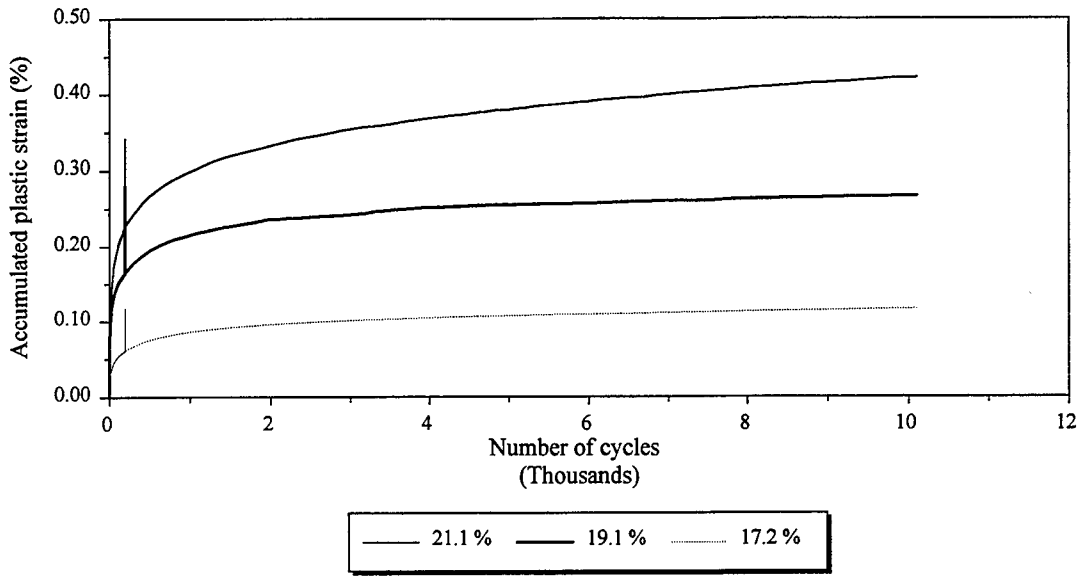

Figure 35. Effect of Moisture Content on Accumulated Plastic Strain in Clay (13.8 kPa Confining Pressure and 48.3 kPa Deviatoric Stress).

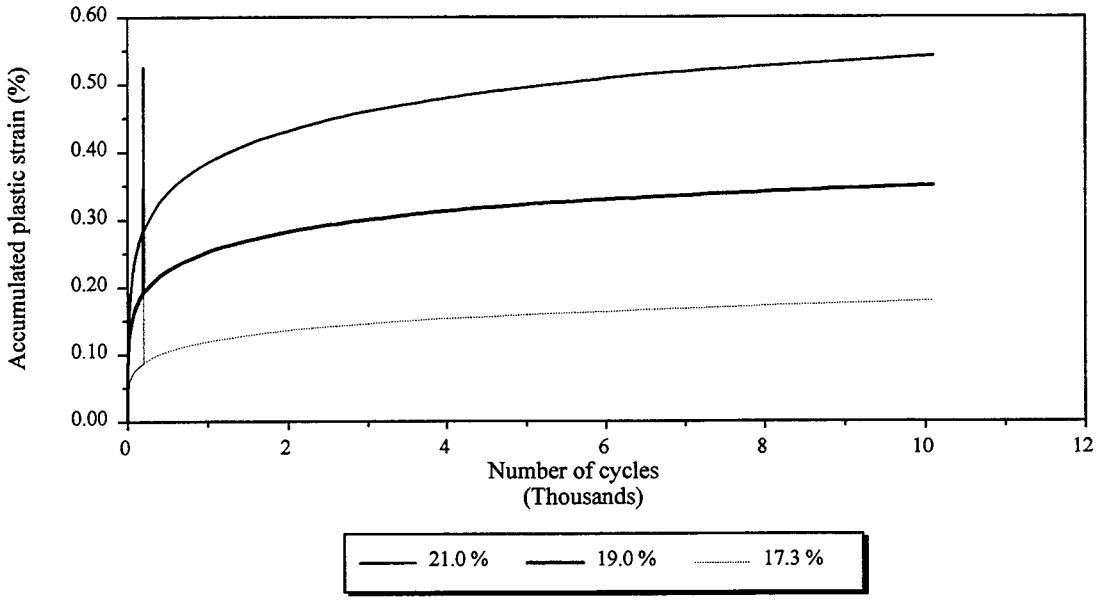

Figure 36. Effect of Moisture Content on Accumulated Plastic Strain in Clay (13.8 kPa Confining Pressure and 96.6 kPa Deviatoric Stress).

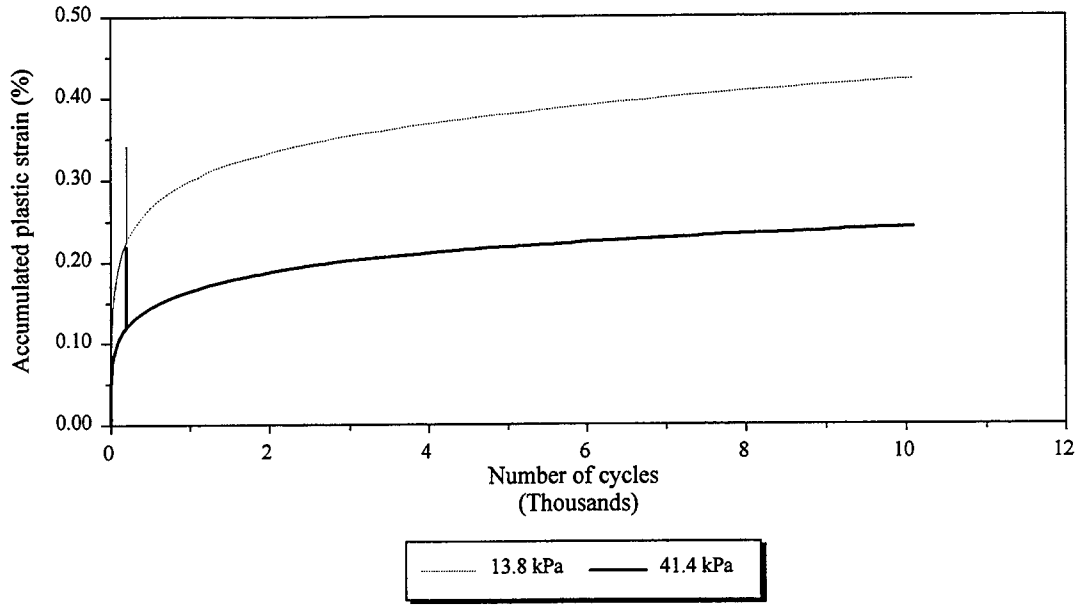

Figure 37. Effect of Confining Pressure on Accumulated Plastic Strain in Clay (48.3 kPa Deviatoric Stress and at Wet of Optimum Moisture Content).

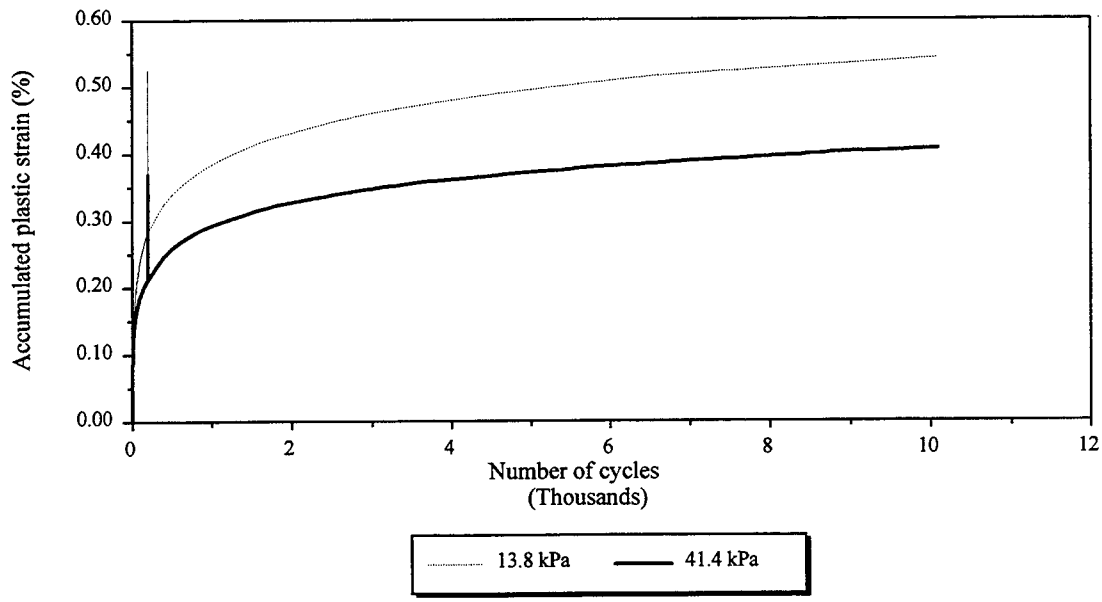

Figure 38. Effect of Confining Pressure on Accumulated Plastic Strain in Clay (96.6 kPa Deviatoric Stress and at Wet of Optimum Moisture Content).

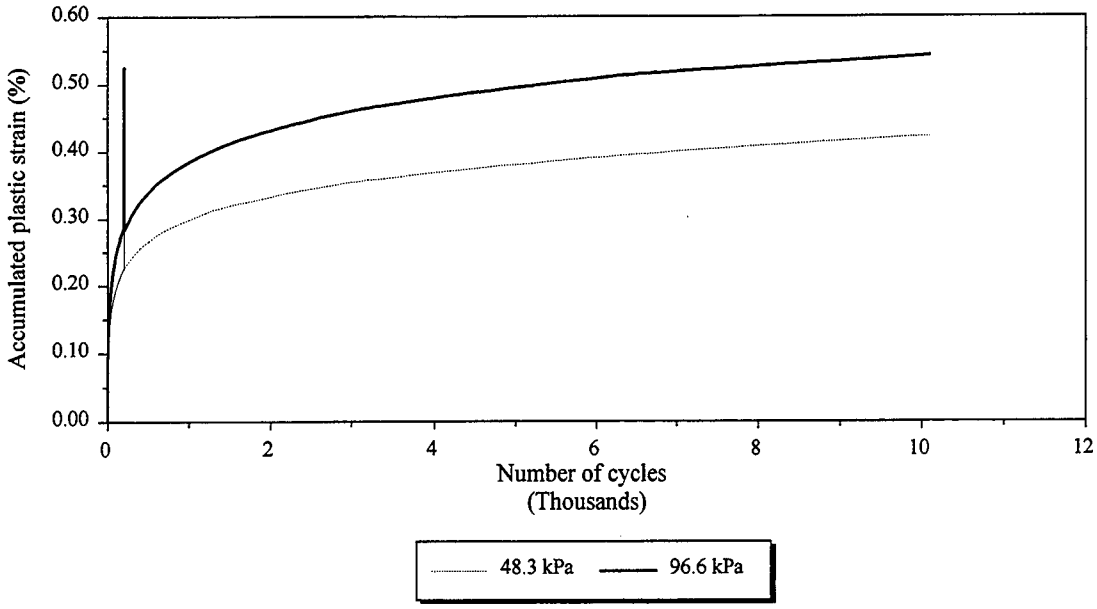

Figure 39. Effect of Deviatoric Stress on Accumulated Plastic Strain in Clay (13.8 kPa Confining Pressure and at Wet of Optimum Moisture Content).

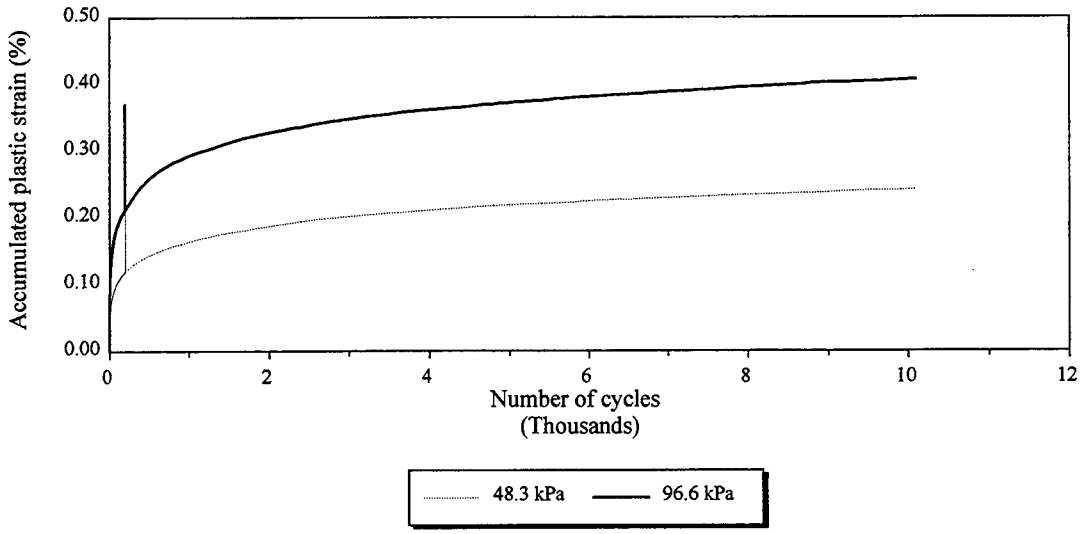

Figure 40. Effect of Deviatoric Stress on Accumulated Plastic Strain in Clay (41.4 kPa Confining Pressure and at Wet of Optimum Moisture Content).

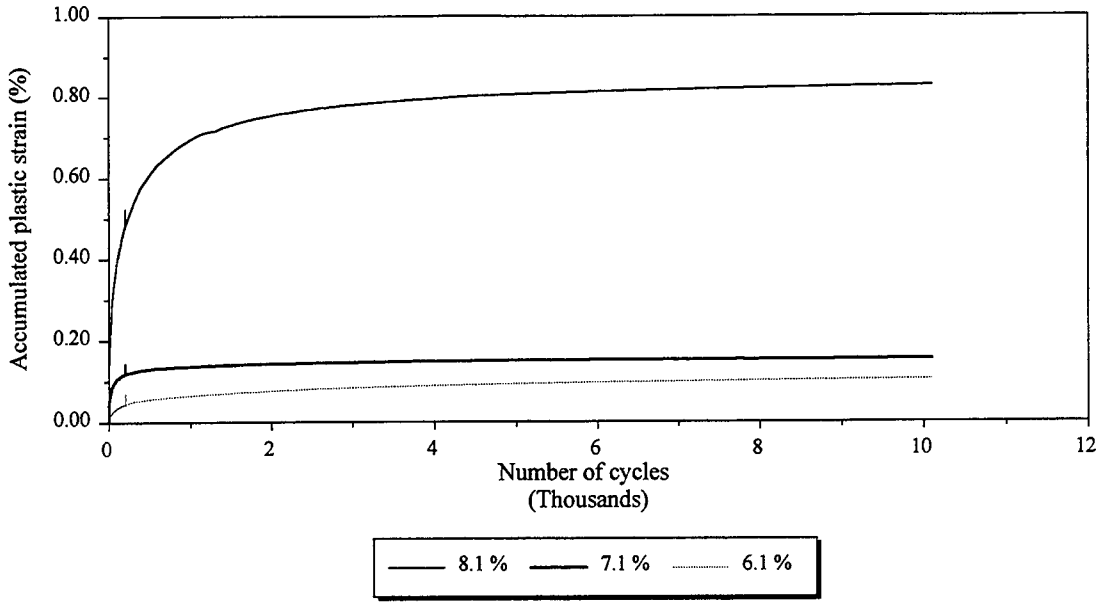

Figure 41. Effect of Moisture Content on Accumulated Plastic Strain in Limstone (34.5 kPa Confining Pressure and 172.5 kPa Deviatoric Stress).

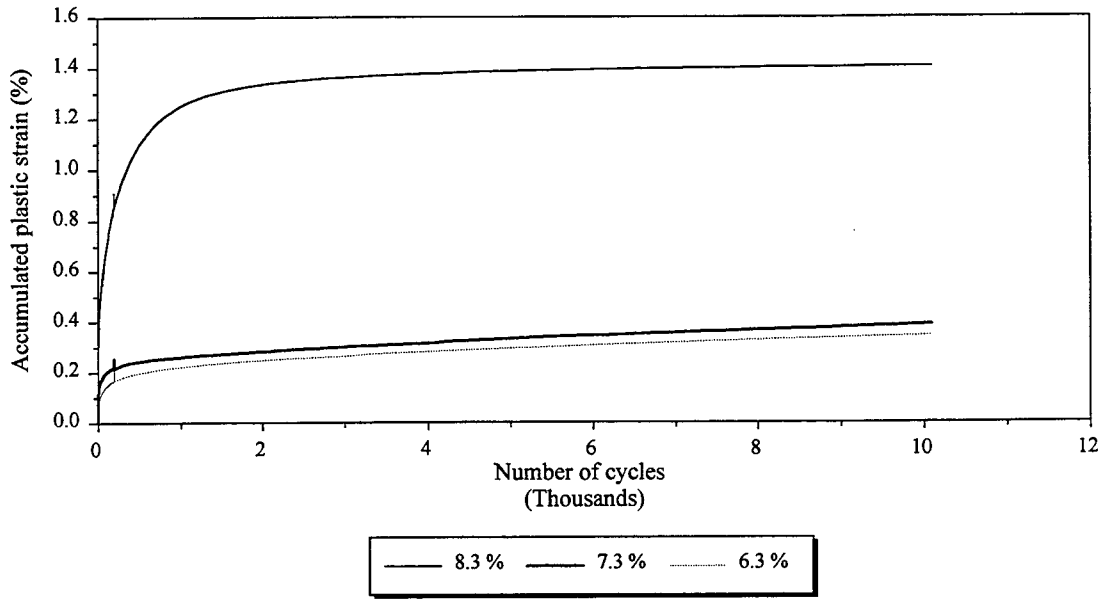

Figure 42. Effect of Moisture Content on Accumulated Plastic Strain in Limestone (103.5 kPa Confining Pressure and 345.0 kPa Deviatoric Stress).

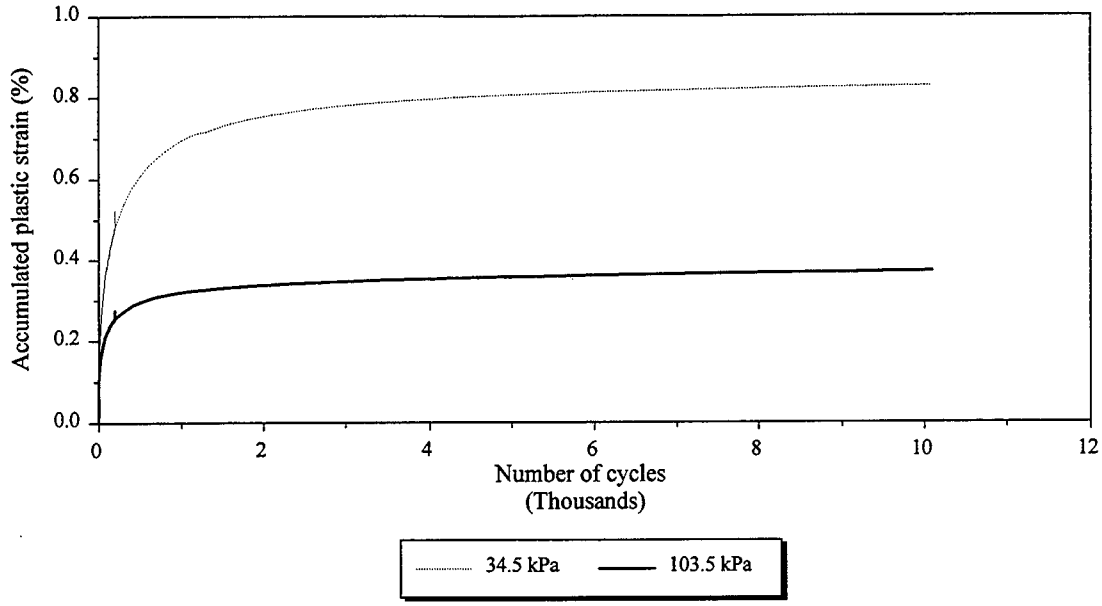

Figure 43. Effect of Confining Pressure on Accumulated Plastic Strain in Limestone (172.5 kPa Deviatoric Stress and at Wet of Optimum Moisture Content).

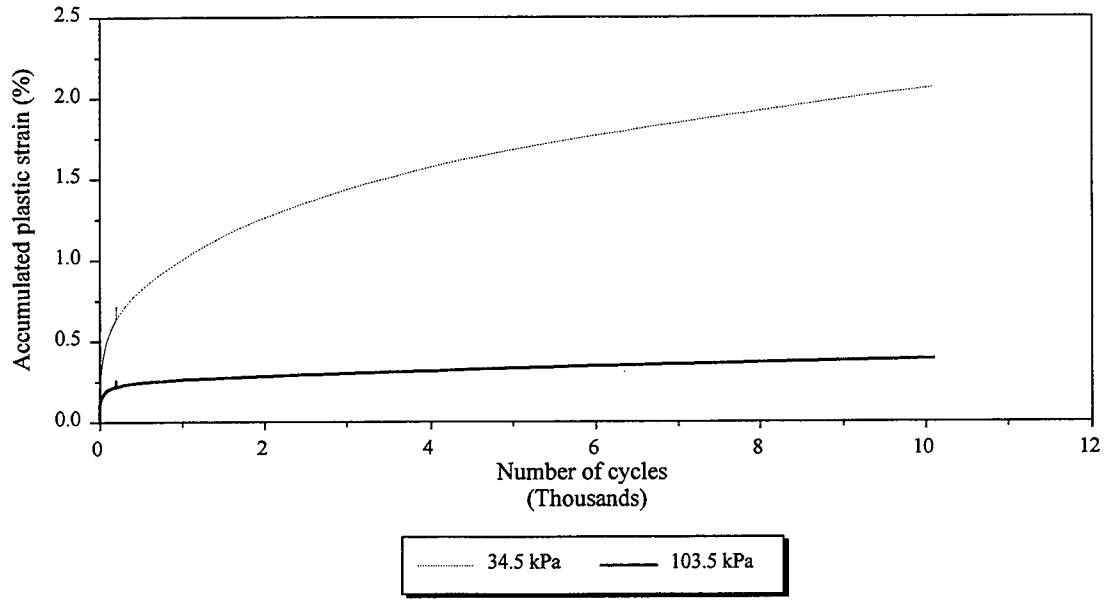

Figure 44. Effect of Confining Pressure on Accumulated Plastic Strain in Limestone (345.0 kPa Deviatoric Stress and at Optimum Moisture Content).

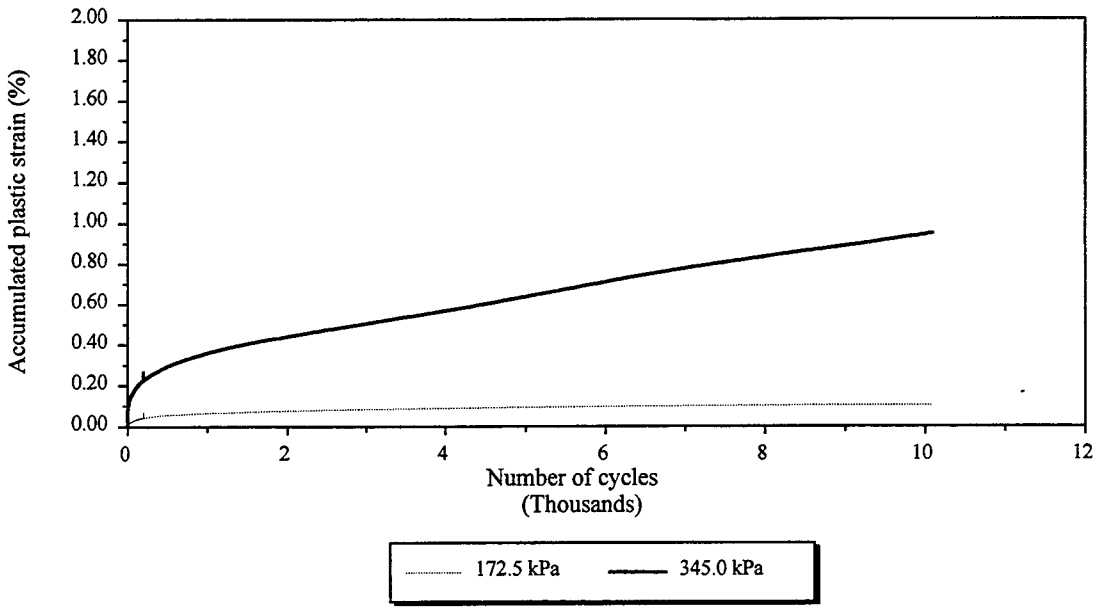

Figure 45. Effect of Deviatoric Stress on Accumulated Plastic Strain in Limestone (34.5 kPa Confining Pressure and at Dry of Optimum Moisture Content).

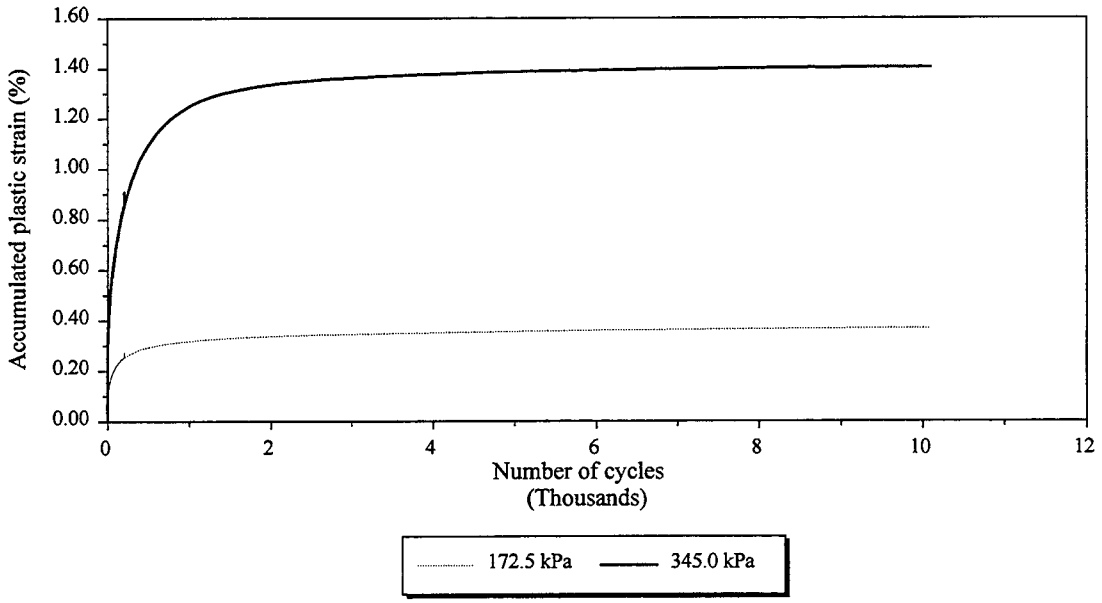

Figure 46. Effect of Deviatoric Stress on Accumulated Plastic Strain in Limestone (103.5 kPa Confining Pressure and at Wet of Optimum Moisture Content).

confining pressure. Figures 39 and 40 illustrate the effect of deviatoric stress level. As expected, the higher the deviatoric stress, the greater the measured accumulated strains. The figures also show that the effect of deviatoric stress is more pronounced at the lower confining pressure.

Figures 41 through 46 present test data for crushed limestone. A very pronounced increase in accumulated plastic strain is observed when the optimum moisture content varies from optimum to wet of optimum (Figures 41 and 42). This rapid increase in plastic strains could be due to a decrease in the cohesion of the material with an increase in the moisture content. This reduced cohesion may be attributed to lower suction in the crushed limestone at the wet condition. Based on a study by Sauer and Monismith (1968), the variation in plastic strain due to soil suction is very significant and the rate of increase in plastic strain is accelerated at lower suction values.

Figures 42 and 44 show the effect of confining pressure. The effect mirrors that shown previously for the clay material. The higher the confinement, the lower the accumulated plastic strain. Figures 45 and 46 illustrate the effect of deviatoric stress. There is an interaction between deviatoric stress and moisture level that is observed in these figures. Even if under higher confinement (Figure 46), the accumulated plastic strain for the same level of deviatoric stress may be more than the accumulated plastic strain measured at a lower confinement (Figure 45) due to the effect of moisture. This result again demonstrates the importance of moisture conditions in the development of pavement distress under repeated load applications. Appendix C graphically presents the results from all of the permanent deformation tests.

REFERENCES

1. Asphalt Institute (AI), *Thickness Design - Asphalt Pavements for Highways & Streets*, Manual Series No. 1., AI, Lexington, KY, 1991.

2. Barksdale, R.D., "Laboratory Evaluation of Rutting in Base Course Materials", *Proc. 3rd Int. Conf. on the Structural Design of Asphalt Pavements*, Vol. 1, Ann Arbor, MI, 1972, pp. 161-174.

3. Allen, H.S., and D.L. Bullock, "Evaluation of Deflection Data as Criteria for the Posting and Removal of Spring Load Limits," *Transportation Research Record*, No. 1106, Transportation Research Board, National Research Council, Washington, D.C., 1987, pp. 140-145.

4. Chen, W.F., and E. Mizuno, *Nonlinear Analysis in Soil Mechanics*, Developments in Geotechnical Engineering Vol. 53, Elsevier, New York, NY, 1990.

5. Chua, K.M., T. Scullion, and R.L. Lytton, "Structural Evaluation and Load Zoning of Low-Volume Roads: A Case Study," *Transportation Research Record*, No. 1106, Transportation Research Board, National Research Council, Washington, D.C., 1987, pp. 157-164.

6. Committee of State Road Authorities (CSRA), *TRH 4: Structural Design of Interurban and Rural Road Pavements,* CSRI, Pretoria, South Africa, 1985.

7. Crockford, W.W., *Weight Tolerance Permits*, Research Report 1323-2F, Texas Transportation Institute (TTI), College Station, TX, 1993.

8. Fernando, E.G., D.R. Luhr, and H.N. Saxena, "The Development of a Procedure for Analyzing Load Limits on Low-Volume Roads," *Transportation Research Record*, No. 1106, Transportation Research Board, National Research Council, Washington, D.C., 1987, pp. 145-156.

9. Federal Highway Administration (FHWA), *Synthesis of Truck Size and Weight Studies and Issues*, U.S. Department of Transportation, Washington, D.C., 1995.

10. Hoyt, D.M., R.L. Lytton, and F. L. Roberts, *Criteria for Asphalt-Rubber Concrete in Civil Airport Pavements: Vol. II - Evaluation of Asphalt-Rubber Concrete*, Report No. DOT/FAA/PM-86/39, II, Federal Aviation Administration, Department of Transportation, Washington, D.C., 1987.

11. Isotalo, J., "Seasonal Truck Load Restrictions: Mitigating Effects of Seasonal Road Strength Variations," *Proc. of the 6th International Conference on Low-Volume Roads*, Vol.1, Transportation Research Board, National Research Council, Washington, D.C., 1996, pp. 137-141.

12. Jackson, J. and M. Murphy, "Implementation of Falling Weight Deflectometer Load-Zoning Procedures in Texas," Transportation Research Record No. 1377, Transportation Research Board, National Research Council, Washington D.C., 1992, pp. 143-149.

13. Jooste, F.J. and E.G. Fernando, *Development of a Procedure for the Structural Evaluation of Superheavy Loads Routes*, Research Report 1335-3F, Texas Transportation Institute, College Station, TX, 1995.

14. Kenis, W.J., "Predictive Design Procedure, VESYS User's Manual: An Interim Design Method for Flexible Pavement Using the VESYS Structural Subsystem," Final Report No. FHWA-RD-77-154, Federal Highway Administration, Department of Transportation, Washington, D.C., 1978.

15. Koniditsiotis, C., "Australian Weigh-in-Motion Technology, " *Road and Transport Research*, Vol. 4, No. 2, 1995, Australia, pp. 114-120.

16. Liu, M., *Numerical Prediction of Pavement Distress with Geotechnical Constitutive Laws*, Ph.D. Dissertation. Texas A&M University, College Station, TX., 1993.

17. Li, D., and E. T. Selig, "Cumulative Plastic Deformation for Fine-Grained Subgrade Soils," *Journal of Geotechnical Engineering*, Vol. 122, No. 12, 1996, pp. 1006-1013.

18. Lytton, R.L., CVEN 616 Course Notes, Texas A&M Univ., College Station, TX, 1996.

19. Mahoney, J.P., and N.C. Jackson, "Guidelines on When to Apply and Remove Seasonal Load Restrictions: Development through Implementation," *Proceedings of the 3rd International Conference on Bearing Capacity of Roads and Airfields*, Trondheim, Norway, 1990.

20. Mahoney, J.P., M.S. Rutherford, and R.G. Hicks, "Guidelines for Spring Highway Use Restrictions," Research Report FHWA-TS-87-209, Federal Highway Administration, Department of Transportation, Washington, D.C., 1987.

21. Maree, J. H., *Design Parameters for Crushed Stone in Pavements*, MSc Thesis, University of Pretoria, Pretoria, South Africa, 1978.

22. McGinnis, R.B., R.M. Anderson, T.W. Kennedy, and M. Solaimanian, *Background of SUPERPAVE Asphalt Mixture Design & Analysis*, FHWA-SA-95-003, Asphalt Institute, Lexington, KY, 1995, pp. 119-128.

23. Moffett, D.P., and R.K. Whitford, *Development of Annual Permit Procedure for Overweight Trucks on Indiana Highways*, FHWA/IN/JHRP-95/5, Purdue University, West Lafayette, IN, 1995.

24. Nix, F.P., J.R. Billing, and A.M. Clayton, "Truck Weight and Dimension Regulations and Container Standards," *Proceedings of the 3rd International Symposium on Heavy Vehicle Weights and Dimensions*, Univ. of Cambridge, U.K., 1992, pp. 15-20.

25. Owen, D.R.J., and E. Hinton, *Finite Elements in Plasticity: Theory and Practice*, Pineridge Press, Swansea, U.K., 1980.

26. Powrie, W., *Soil Mechanics: Concepts and Applications*, E & FN Spon, London, U.K., 1997.

27. Rogers, C.A., et al., "Granular Base Failures in Low-Volume Roads in Ontario, Canada," Proc. of the 6th International Conference on Low-Volume Roads, Vol.2, Transportation Research Board, National Research Council, Washington, D.C., 1996, pp. 23-32.

28. Roschke, P., MEMA 647 Course Notes, Texas A&M Univ., College Station, TX, 1996.

29. Shackel, B., Repeated Loading of Soils: A Review, *Australian Road Research*, Vol. 5, No. 3, Kew, Victoria, pp. 22-49.

30. Sauer, E.K., and Monismith, C.L., "Influence of Soil Suction on Behavior of a Glacial Till Subjected to Repeated Loading," Record No. 215, Highway Research Board, 1968, Washington, D.C., pp. 8-23.

31. Shook, J.K., F.N. Finn, M.W. Witczak, and C.L. Monismith, "Thickness Design of Asphalt Pavements: The Asphalt Institute Methods," *Proc. 5th Int. Conf. on the Structural Design of Asphalt Pavements*, Vol. 1, Delft, The Netherlands, 1982, pp. 17-44.

32. Terrell, R.L., and C.A. Bell, *Effects of Permit and Illegal Overloads on Pavements*, NCHRP Synthesis of Highway Practice 131, Transportation Research Board, National Research Council, Washington, D.C., 1987.

33. Titus-Glover, L., and E.G. Fernando, *Evaluation of Pavement Base and Subgrade Material Properties and Test Procedures*, Research Report 1335-2, Texas Transportation Institute, College Station, TX, 1995.

34. Uzan, J., Granular Material Characterization, In Transportation Research Record 1022, Transportation Research Board, National Research Council, Washington, D.C., 1985, pp. 52-59.

35. Uzan, J., T. Scullion, C. Michalek, M. Paredes, and R.L. Lytton, *A Microcomputer Based Procedure for Backcalculating Layer Moduli from FWD Data*, Research Report 1123-1, Texas Transportation Institute, College Station, TX, 1988.

36. Uzan, J., "Resilient Characterization of Pavement Materials," *International Journal for Numerical and Analytical Methods in Geomechanics*, Vol. 16, 1992, Chichester, New York, pp. 435-459.

37. Vantonder, H.P., J.P. Hasluck, and D.J. Wium, "The South African Heavy Vehicle Load-Limit Study," *Proc. of the 3rd International Symposium on Heavy Vehicle Weights and Dimensions*, Univ. of Cambridge, U.K., 1992, pp. 413-417.

38. Wolff, H., et al., "Design Catalog for Low-Volume Roads Developed for South African Conditions," *Proc. of the 6th International Conference on Low Volume Roads*, Vol.2, Transportation Research Board, National Research Council, Washington, D.C.,1996, pp. 118-129.

39. Wood, D.M., "Laboratory Investigations of the Behavior of Soils under Cyclic Loading: A Review," *Soil Mechanics-Transient and Cyclic Loads*, G. N. Pance and O. C. Zienkiewicz, eds., John Wiley and Sons Inc., New York, NY, pp 513-582.

40. Yapa, K.A.S., and R.L. Lytton, *A Simplified Mechanistic Rut Depth Prediction Procedure for Low Volume Roads*, Research Report 473-1, Texas Transportation Institute, College Station, TX, 1988.

41. Zaghloul, S.M., et al., "Computerized Overload Permitting Procedure for Indiana," *Transportation Research Record*, No. 1448, Transportation Research Board, National Research Council, Washington, D.C., 1994, pp. 40-52.

42. Zyl, G.D., et al., "Guideline for Structural Design of Low Volume Rural Roads in Southern Africa," Proc. of the 6th International Conference on Low Volume Roads, Vol.2, Transportation Research Board, National Research Council, Washington, D.C., 1996, pp. 108-117.

APPENDIX A

SUMMARY OF TXDOT DISTRICT SURVEY RESPONSES

District	Factors Considered When Posting/Unposting a Road			Types of Roads Posted	Typical Base Materials for Posted Roads	Typical Vehicle Types	Typical Loads	Actual Truck Traffic Counts?	Truck Traffic Characterized?	District Personnel Interviewed	Other Comments
	Engr. Judgment or Formal Methodology	Specific Data Collected	Comments								
(1) Paris	Engineering judgment	Visual	Maintenance engineers makes decision on road postings.	Low Volume FM.	Crushed sandstone sometimes stabilized	Farm Equipment	Farm Equipment	No	No	Cliff CLottey (Pvmt Engr)	-
(2) Fort Worth	Combination.	No postings removed recently.	Done on a project by project basis, usually as a result of rehabilitation.	FM Roads	Crushed limestone.	Single unit, tractor-trailer	Concrete trucks, aggregate hauling vehicles	No	No	Andrew Wimsatt (Pavement Engr)	-
(3) Wichita Falls	Combination. We consider the pavement structure and its ability to withstand anticipated use.	Visual examination. FWD, cores, triaxial tests and traffic counts.	We perform a one-time battery of tests to determine appropriate posting. We repeat the tests if posting is seriously challenged. Analysis model used is FPS.	FM or State highways that usually have untreated subgrade, 6" flex base and thin overlay or surface treatment.	Untreated subgrade, 6" flex base, surface treatment.	Tractor trailers.	Oil field equipment, dairy trucks	Only from field surveys.	Perform field surveys to determine cause of distress. Frequency of trips is noted during field surveys.	Joe Anderson	All new FM roads are posted at 58420 unless specifically designed for heavier loads.
(4) Amarillo	Combination.	FWD Traffic	Roads are unposted as they are improved.	FM	4-6" Flexible Base (Caliche) 2 course surface treatment.	Tractor-trailers	Farm-related. In particular, feed-lots, pig farms.	Yes, project for 20 years.	Normally consider 18k ESALS and avg of 10 heaviest wheel loads. For some roads the traffic is easily characterized when it's servicing a particular industry such as a pig farm.	Ron Johnston	-
(5) Lubbock	-	-	-	-	-	-	-	-	-	Jack Tucker (Pavement Engineer)	Lubbock has no load-zoned pavements and are comfortable with this situation. Their pavements are adequately designed for the loads, they have no bridges, and they have a very low rainfall.
(6) Odessa	-	-	-	-	-	-	-	-	-	Jamshid Jahangiri (Pavement Engr)	No load-zoned pavements. Pavements are adequate, subgrades are good. Subgrade classification is typically 2 - 3.5. Base moduli are about 16,000 to 20,000 psi.

District	Factors Considered When Posting/Unposting a Road			Types of Roads Posted	Typical Base Materials for Posted Roads	Typical Vehicle Types	Typical Loads	Actual Truck Traffic Counts?	Truck Traffic Characterized?	District Personnel Interviewed	Other Comments
	Engr. Judgment or Formal Methodology	Specific Data Collected	Comments								
(7) San Angelo	Engineering judgement.	Also consider pavement structure, subgrade, ADT, types of loads using highway maintenance history.	Not Applicable.	Flexible base with multi-course surface treatments.	Caliche base, high PI (>30) subgrade.	Tractor-trailer.	Oil field.	No.	No.	Matt Carr (Pavement Engineer)	Texas Legislature has adopted rules which effectively do away with load-zoned roads. Therefore, the following responses are not based on what we do but what we would do to load-zone a road.
(8) Abilene	Engineering judgment based on design.	None.	Political/Commercial pressures influence postings (oil boom, gravel pits)	FM	5" pit run base with 2 course surface treatment.	Tractor-trailers and items they have.	Oil field, material pits, oil brought to power plants.	Yes, but not considered in postings.	Perform field surveys and monitor economic/industrial activities. More postings are removed because of political/commercial need and done arbitrarily or after reconstruction.	Douglas W. Eichorst (Pavement Engineer)	Most of our load posting came from the change from the 58420 to 80000 pound loading. Some roads have been removed from the load posting because of reconstruction or commercial/political pressures. The political/commercial load postings were done arbitrarily and many times without any engineering performed to determine load capacities.
(9) Waco	Combination.	None.	If pavement section gets upgraded, load posting is removed.	FM	6" base with surface treatment. Base material is a crushed limestone or bank run gravel (gravel sometimes stabilized). Heavy clay subgrades on east side and bedrock on west.	Mixed.	Crops, agricultural	NA	NA	Billy Pigg (Pavement Engineer)	In the mid to late 80s, the legislature provided a one-time opportunity to remove load zones on any pavement. Waco chose not to do that which is why there are so many miles of posted roads in Waco.
(10) Tyler	Combination.	-	No postings removed in recent years.	FM	6" iron ore base. Subgrade typically sand or clayey sand.	-	Logging , timber, agricultural	-	-	Dale Booth (Pavement Engr)	-
(11) Lufkin											
(12) Houston											

District	Factors Considered When Posting/Unposting a Road			Types of Roads Posted	Typical Base Materials for Posted Roads	Typical Vehicle Types	Typical Loads	Actual Truck Traffic Counts?	Truck Traffic Characterized?	District Personnel Interviewed	Other Comments
	Engr. Judgment or Formal Methodology	Specific Data Collected	Comments								
(13) Yoakum	Combination. Consult Joe Leidy in Pavement Design Division.	Perform FWD survey, FPS analysis, and Joe Leidy performs rest of analysis for removal of postings.	FM roads blanketed in the past to 58420 lb load limit. We take first available opportunity to prove road postings can be removed. Usually after rehabilitation.	FM	4-6" of flexible base (unstabilized subgrade) and 1-2" of HMAC. Subgrade materials clayey but not particularly a heavy or fat clay.	Tractor-trailer.	Oil field is main concern. In Wharton County concerned during the grain harvest of overloaded trucks.	No. Use predicted traffic for 20 year design.	-	Gerald Freytag (Pavement Engineer)	For rehabilitation of FM roads typically, we use the Modified Texas Triaxial Method New cross section will normally consist of at least 12 inches of base material. However, other economic considerations sometimes govern the pavement design and cross section may be less than what design calls for. If the pavement is improved (even though it may not meet the needed design criteria) we try to remove postings, if feasible.
(14) Austin	-	-	-	-	-	-	-	-	-	Chris Grose	No activity regarding load-postings or posting removals in recent years.
(15) San Antonio	Combination in cooperation with Pavement Design Division.	-	No postings removed in recent years.	FM	6" flexible LS base with 2-course surface treatment. Subgrade class 5.0 - 5.4 (southern areas) "New" designs in areas of expansive clays calling for 18" base with 1-2" AC.	Tractor-trailer, single unit	Ag. (East) Oil (South) Gravel pit hauling	-	-	Patrick Downey (Pavement Engr)	No activity regarding load-postings or posting removals in recent years.
(16) Corpus Christi	-	-	No postings removed in recent years.	FM	Base materials: caliche. Subgrade: plastic clay in some areas and sand near island.	Tractor-trailers, belly dumps	Oil and gas related, gravel trucks	-	-	John Hernandez	No activity regarding load-postings or posting removals in recent years.
(17) Bryan	Combination in cooperation with Pavement Design Division.	-	No postings removed in recent years.	FM	4-8 inches limestone base. Subgrade soils include sandy to high PI clays. Clays typically stabilized with lime.	Tractor-trailers.	Oil related.	-	-	Elias Rmeili (Pavement Engr)	No activity regarding load-postings or posting removals in recent years.

District	Factors Considered When Posting/Unposting a Road			Types of Roads Posted	Typical Base Materials for Posted Roads	Typical Vehicle Types	Typical Loads	Actual Truck Traffic Counts?	Truck Traffic Characterized?	District Personnel Interviewed	Other Comments
	Engr. Judgment or Formal Methodology	Specific Data Collected	Comments								
(18) Dallas	Combination in cooperation with Pavement Design Division.	-	No postings removed in recent years.	FM	6-12" of crushed limestone base. High PI subgrades.	Tractor-trailers, single unit.	Oil related and agricultural.	-	-	Joe Thompson (Pavement Engr)	Aware of one case recently where rail company paid to have pavement upgraded for hauling railcars.
(19) Atlanta	-	-	-	-	-	-	-	-	-	Tommy Ellison (Pavement Engr)	No load-zoned pavements.
(20) Beaumont	Combination. In cooperation with Pavement Design.	-	No postings removed in recent years.	FM	4-8" sand shale (sometimes lightly stabilized). Subgrade: silty clay.	Tractor-trailer, single unit.	Logging, petrochemical industry.	-	-	Susan Chu (Pavement Engr)	No activity regarding load-postings or posting removals in recent years.
(21) Pharr	Combination. In cooperation with Design Division	FWD Traffic Count	Postings removed as a result of rehabilitation and widening.	FM roads built in 1940s and 50s.	4-6" of caliche Flexbase with thin overlay or surface treatment. Sometimes a subgrade treatment.	Tractor-trailer.	Farm, oilfield, miscellaneous .	Yes, then predict for 20 years.	-	John Dela Garza (Pavement Engineer)	-
(22) Laredo	-	-	-	-	-	-	-	-	-	Roy Garcia (Pavement Engineer)	No load-zoned pavements.
(23) Brownwood	-	-	No postings removed in recent years.	FM roads.	4-8" crushed limestone base. Sandy subgrade.	Tractor-trailer, single unit.	Agricultural related.	-	-	Elias Rmeili	-
(24) El Paso											
(25) Childress	Combination. In cooperation with Pavement Design.	FWD, Visual survey.	-	FM	6" sand and gravel base with thin surface. Subgrade soils: eastern-higher PI clays, western - sandy soil.	Module trucks	Cotton, agricultural related.	-	-	Marty Smith (Pavement Engr)	-

APPENDIX B

FORMULATION OF FINITE ELEMENT MODEL

FORMULATION OF FINITE ELEMENT MODEL

Researchers developed an axisymmetric finite element program using elasto-plastic theory to model the pavement response under loading. The program is a modification of an elasto-plastic finite element program written by Owen and Hinton (1980), which provides a basis for modeling the development of permanent deformation in pavement layers. The modified program is based on the flow theory of plasticity and can account for the stress-dependency of the resilient modulus and Poisson's ratio. The non-linear analysis is made using an incremental loading and an iterative solution technique for each load increment. The stress-dependency of the resilient modulus is modeled using Uzan's Universal Soil Model (1985) that allows consideration of the stiffening effect due to confinement and the softening effect due to shear. The model also considers the dilation effects that occur when the principal stress ratio exceeds a certain value. For Poisson's ratio, a numerical solution using the backward difference method is used to solve the partial differential equation that governs the stress-dependency of this material property. This differential equation is given later in this appendix.

The finite element program uses an axisymmetric formulation and the isoparametric eight-node serendipity element. There are a number of advantages using the eight-node serendipity element (Roschke 1996):

- Boundary matches more closely,
- Fewer nodes, and
- More accuracy for stress interpolation because of quadratic nature.

Figure B1 shows the numbering of element nodes and Gaussian points. An element consists of eight nodes and nine Gaussian points. Figure B2 shows the flow diagram of the finite element (FE) program. This algorithm handles both stress-dependency and equilibrium criteria in an incremental scheme. The input to the program includes the pavement geometry,

boundary conditions, material properties, resilient parameters, and applied loading.

For non-linear analysis, an iterative procedure is used to achieve stress compatible moduli and Poisson's ratio for each load increment. The program also uses the tangential stiffness method for formulating the stress-strain relationship. However, the use of the tangential stiffness method can lead to errors when the stress-strain curve transitions from the linear elastic to the plastic region. The potential for error is reduced by applying the load in increments and using an iterative procedure (Powrie 1997).

The flow theory of plasticity is based on three main assumptions (Chen and Mizuno 1990):

- a yield criteria,
- a flow rule, and
- a hardening rule.

The yield criterion is a mathematical expression relating the state of stress to the onset of plastic deformation. Plastic behavior is evaluated in the FE program by irreversible straining, which is not time dependent and which can only be sustained once a certain level of stress has been reached. The plastic strains are predicted by elasto-plastic behavior of the material based upon the yield stress. The Mohr-Coulomb yield criterion is used to determine the yield point and to evaluate the potential for pavement damage.

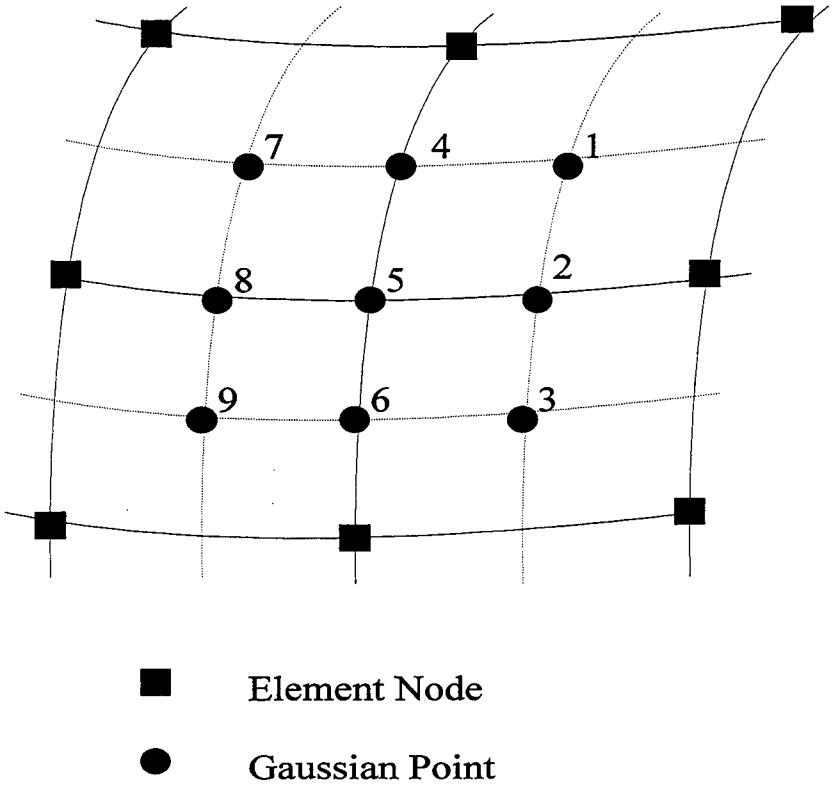

Figure B1. Gaussian Points in the Eight-Node Element.

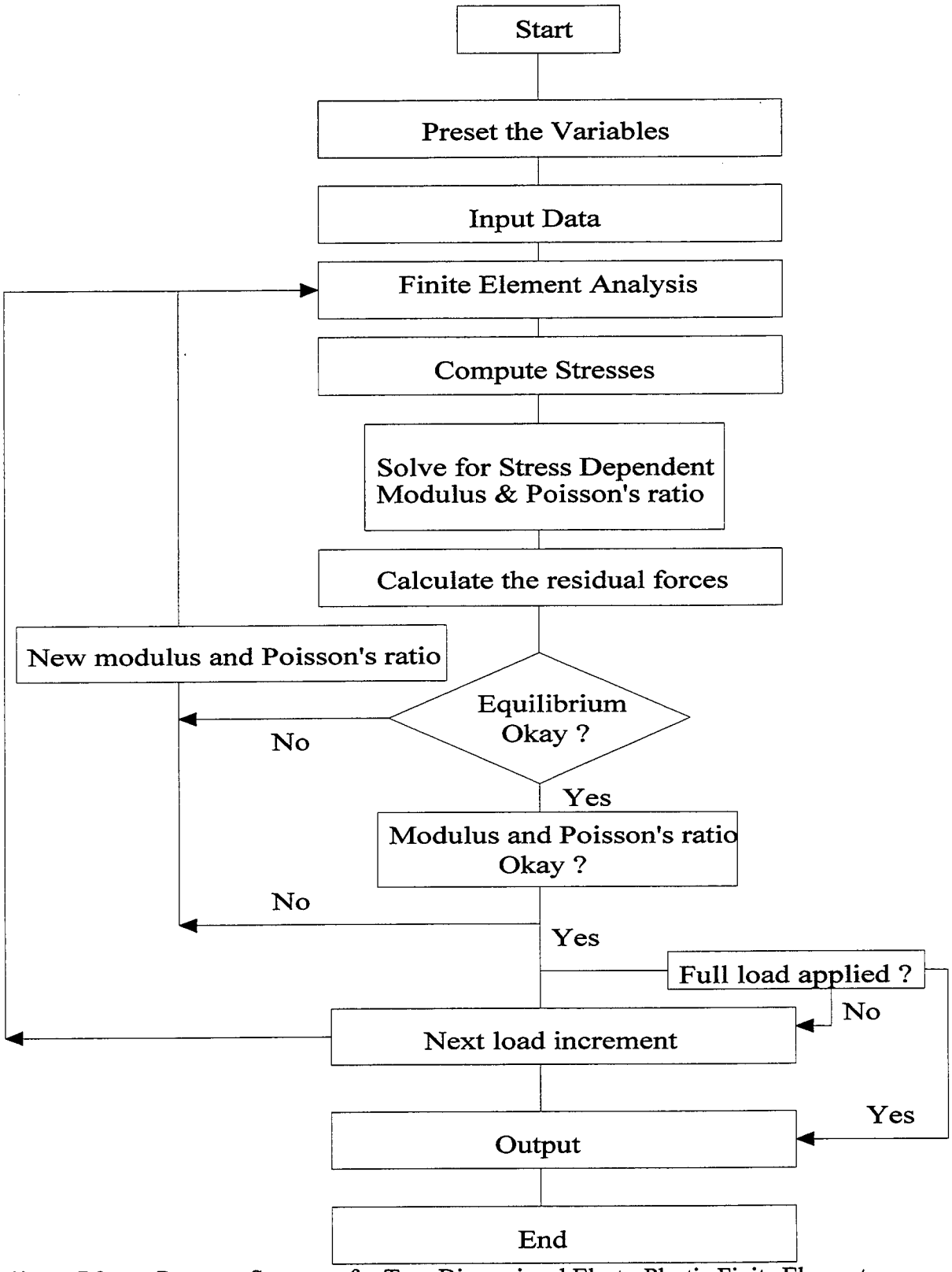

Figure B2. Program Structure for Two-Dimensional Elasto-Plastic Finite Element Analysis Using Stress Dependency.

The Mohr-Coulomb yield criterion in three dimensional stress space is related to first stress invariant, the second deviatoric stress invariant, and the lode angle as follows:

$$f = \frac{I_1}{3}\sin(\phi) + \sqrt{J_2}\sin\left(\Theta + \frac{\pi}{3}\right) + \frac{\sqrt{J_2}}{\sqrt{3}}\cos\left(\Theta + \frac{\pi}{3}\right)\sin(\phi) - c\cos(\phi) = 0$$

where

$$\theta = \frac{1}{3}\cos^{-1}\left[\frac{3\sqrt{3}}{2}\frac{J_3}{J_2^{3/2}}\right]$$

$$J_2 = \frac{1}{6}\left[(\sigma_1 - \sigma_2)^2 + (\sigma_2 - \sigma_3)^2 + (\sigma_3 - \sigma_1)^2\right] = \frac{1}{3}(I_1^2 - 3I_2)$$

$$I_1 = \sigma_1 + \sigma_2 + \sigma_3$$

f	=	the Mohr-Coulomb yield function,
θ	=	the lode angle,
I_1	=	the first stress invariant,
J_2	=	the second deviatoric stress invariant,
J_3	=	the third deviatoric stress invariant,
τ_{oct}	=	the octahedral shear stress,
σ_1	=	the major principal stress,
σ_2	=	the intermediate principal stress, and
σ_3	=	the minor principal stress.

Negative yield function values denote no yielding under the given stress state. After initial yielding, the material behavior will comprise of elastic and plastic components. The predicted strain is assumed to be divided into two parts as follows:

$$d\epsilon_{ij} = (d\epsilon_{ij})_e + (d\epsilon_{ij})_p$$

where

$d\epsilon_{ij}$	=	the total strain,
$(d\epsilon_{ij})_e$	=	the elastic strain, and
$(d\epsilon_{ij})_p$	=	the plastic strain.

Based on the classical theory of plasticity, the plastic strain increment is assumed to be proportional to the stress gradient of a quantity known as the plastic potential (Q). The relationship is as follows:

$$(d\epsilon_{ij})_p = d\lambda \frac{\partial Q}{\partial \sigma_{ij}}$$

The incremental plastic strain can be determined using the principle of equivalent plastic work. When the material reaches yielding, the level of stress can be converted into a uniaxial yield stress called an equivalent stress. Using this equivalent stress concept, the equivalent incremental plastic strain is determined as:.

$$d\epsilon_{eps} = \sqrt{\frac{2}{3}} (d\epsilon_{ij_p} d\epsilon_{ij_p})^{\frac{1}{2}}$$

In order to determine the limiting condition, a single load application is applied incrementally until failure. The identification of the limit load is taken as the step when the convergence criteria can no longer be met after yielding. In other words, if a significant number of elements have yielded (or permanently deformed) the tangential stiffness matrix

will be singular, and further steps can not be processed. Yielding implies local failure, and the yield surface becomes a failure criterion. Therefore, the limit loads (or collapse loads) can be taken as the loads at which the numerical process diverged for specified loads (Owen and Hinton 1980).

The stress-dependent moduli and Poisson's ratio are also determined by iterative procedures. For each load increment, these parameters are calculated iteratively until the specified convergence is accomplished. The Universal Soil Model (Uzan 1985) given below

$$E = k_1 Atm \left(\frac{\theta}{Atm}\right)^{k_2} \left(\frac{\tau_{oct}}{Atm}\right)^{k_3}$$

is used.

where

E	=	resilient modulus,
Atm	=	atmospheric pressure,
θ	=	first stress invariant (or bulk stress),
τ_{oct}	=	octahedral shear stress, and
k_1, k_2, k_3	=	material parameters.

The parameters, k_1, k_2, and k_3, are determined from resilient modulus tests. The first stress invariant or bulk stress term (k_2 term) considers the hardening effect that is associated with higher modulus, while the octahedral shear stress term (k_3 term) considers the softening effect. Both terms are expressed as follows:

$$k_2 \ term = \left(\frac{I_1}{Atm}\right)^{k_2}$$

and

$$k_3 \ term = \left(\frac{\tau_{oct}}{Atm} \right)^{k_3}$$

The predicted stresses are normalized with respect to the atmospheric pressure so that the k_1, k_2, and k_3 coefficients are dimensionless.

In general, the higher the k_1, the greater the predicted modulus. For the cases of k_2 and k_3, however, the results will not be dependent upon one term. As the wheel load increases, the k_2 term increases due to higher confinement. However, the k_3 term decreases with higher wheel loads due to an increase of the octahedral shear stress. The effects of these terms are greatly dependent upon the applied wheel loads and pavement geometry.

The parameters, k_1, k_2, and k_3, are also used for predicting the stress dependency of Poisson's ratio. Based on the above mentioned energy concepts, the relationship between Poisson's ratio and the stress state may be derived as follows:

$$\frac{2}{3}\frac{\partial \nu}{\partial J_2} + \frac{1}{I_1}\frac{\partial \nu}{\partial I_1} = \nu \left(\frac{2}{3}\frac{k_3'}{J_2} + \frac{k_2}{I_1^2} \right) + \left(-\frac{1}{3}\frac{k_3'}{J_2} + \frac{k_2}{I_1^2} \right)$$

where

ν	=	Poisson's ratio,
k_3'	=	$k_3/2$,
k_1, k_2, k_3	=	material parameters,
I_1	=	normalized first stress invariant, and
J_2	=	normalized second invariant of the deviatoric stress tensor.

A finite difference procedure is used to solve the above partial differential equation in the finite element program. The derivation of the relationship between Poisson's ratio and stress state is presented by Liu (1993).

The program has two convergence criteria. Equilibrium criterion is based on the residual force values. Convergence occurs if the norm of the residual forces becomes less than the specified tolerance times the norm of the total applied forces. Thus, equilibrium is satisfied when the applied loads and the nodal forces equivalent to the internal stress are balanced (Owen and Hinton 1980).

For the stress dependency criterion, the process is repeated until the difference in modulus calculated from following iteration and modulus calculated from the previous iteration is satisfied within a given tolerance. Convergence depends on the percentage difference between the new and previous values. In general, a 15 percent difference in the calculated moduli from the current and previous iteration is accepted. If large changes occur in the modulus, then the iteration is repeated until the change is no more than 15 percent. If the new modulus does not meet the convergence criterion, the modulus is recalculated. Upon convergence, a new load increment is applied. During the calculation of the new modulus and Poisson's ratio, a damping factor is applied to facilitate the convergence. At low stress levels the equation for resilient modulus may result in unreasonable modulus values. In order to prevent this, cutoff values for both the first stress invariant and octahedral shear stress are specified in the computer program.

APPENDIX C

PERMANENT DEFORMATION DATA

Table C1. Moisture Content and Measured Stress Level for Crushed Limestone and Clay.

Material	Specimen	Type	water content (%)	Confining pressure psi	Deviatoric stress psi	Deviatoric stress 199 th cycle psi	200 th cycle psi	201 st cycle psi
Crushed Limestone	LS05H25	A	8.10	5.00	25.00	24.65	24.66	24.66
	LS05H50	A	8.30	5.00	50.00	51.94	50.70	50.46
	LS05M25	A	7.10	5.00	25.00	22.19	22.16	22.16
	LS05M50	A	7.30	5.00	50.00	48.90	49.06	48.78
	LS05L25	B	6.10	5.00	25.00	27.20	27.27	27.12
	LS05L50	A	6.30	5.00	50.00	47.60	47.33	47.44
	LS15H25	A	8.30	15.00	25.00	23.69	23.46	23.42
	LS15H50	A	8.30	15.00	50.00	48.50	50.58	48.87
	LS15M25	B	7.20	15.00	25.00	26.17	25.76	25.84
	LS15M50	A	7.30	15.00	50.00	56.26	56.12	56.14
	LS15L25	B	6.30	15.00	25.00	23.13	23.06	22.85
	LS15L50	A	6.30	15.00	50.00	53.90	53.98	53.96
Fat Clay	CL02H07	B	21.10	2.00	7.00	6.53	6.69	6.70
	CL02H14	A	21.00	2.00	14.00	13.56	13.11	13.15
	CL02M07	B	19.10	2.00	7.00	7.49	7.58	7.52
	CL02M14	B	19.00	2.00	14.00	13.95	14.11	14.10
	CL02L07	B	17.20	2.00	7.00	6.63	6.70	6.73
	CL02L14	B	17.30	2.00	14.00	15.88	15.89	15.93
	CL06H07	B	21.20	6.00	7.00	7.13	7.27	7.28
	CL06H14	A	21.00	6.00	14.00	15.40	15.40	15.40
	CL06M07	A	19.00	6.00	7.00	6.53	6.56	6.58
	CL06M14	B	19.20	6.00	14.00	14.58	14.57	14.55
	CL06L07	A	17.00	6.00	7.00	6.80	6.83	6.84
	CL06L14	B	17.20	6.00	14.00	15.58	15.60	15.59

Table C2. Moisture Content and Measured Stress Level for Iron Ore Gravel and Caliche.

Material	Specimen	Type	water content (%)	Confining pressure psi	Deviatoric stress psi	Deviatoric stress 199 th cycle psi	200 th cycle psi	201 st cycle psi
Iron Ore Gravel	IR05H25	B	12.40	5.00	25.00	14.23	14.19	14.21
	IR05H50	B	12.50	5.00	50.00	13.04	13.08	13.07
	IR05M25	A	10.65	5.00	25.00	26.90	26.24	27.33
	IR05M50	A	10.65	5.00	50.00	53.50	48.89	48.95
	IR05L25	A	8.65	5.00	25.00	26.05	25.77	26.25
	IR05L50	B	8.20	5.00	50.00	51.43	51.43	51.50
	IR15H25	A	12.65	15.00	25.00	25.12	25.13	25.14
	IR15H50	A	12.65	15.00	50.00		FAIL AT 44 CYCLES	
	IR15M25	A	10.65	15.00	25.00	25.92	25.95	25.95
	IR15M50	A	10.65	15.00	50.00	51.52	46.16	46.16
	IR15L25	A	8.65	15.00	25.00	29.36	28.98	29.04
	IR15L50	A	8.65	15.00	50.00	53.37	53.46	53.43
Caliche	CA05H25	A	8.70	5.00	25.00	26.03	26.29	26.37
	CA05H50	N/A						
	CA05M25	A	6.70	5.00	25.00	24.62	24.96	24.71
	CA05M50	A	6.70	5.00	50.00	46.98	46.70	46.52
	CA05L25	A	4.70	5.00	25.00	22.72	22.60	22.51
	CA05L50	B	4.90	5.00	50.00	53.49	53.38	53.22
	CA15H25	A	8.70	15.00	25.00	26.04	26.33	26.35
	CA15H50	A	8.70	15.00	50.00	47.51	47.64	47.59
	CA15M25	B	6.90	15.00	25.00	22.77	22.85	22.85
	CA15M50	B	6.70	15.00	50.00	48.47	47.84	47.89
	CA15L25	A	4.70	15.00	25.00	27.78	27.62	27.69
	CA15L50	B	4.70	15.00	50.00	55.06	54.81	54.77

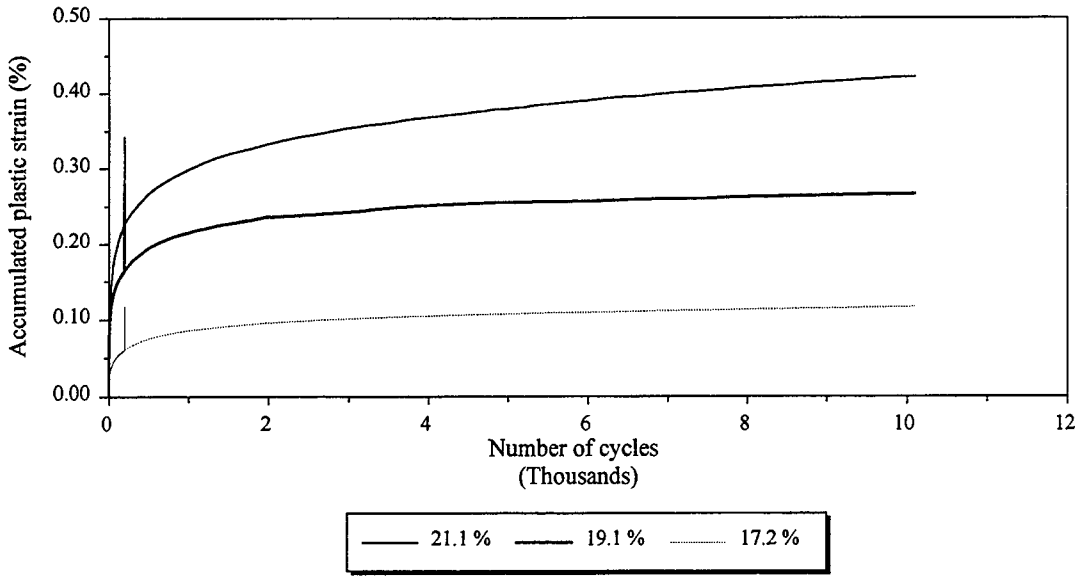

Figure C1. Influence of Moisture Content on Accumulated Plastic Strain in Clay (13.8 kPa Confining Pressure, 48.3 kPa Deviatoric Stress).

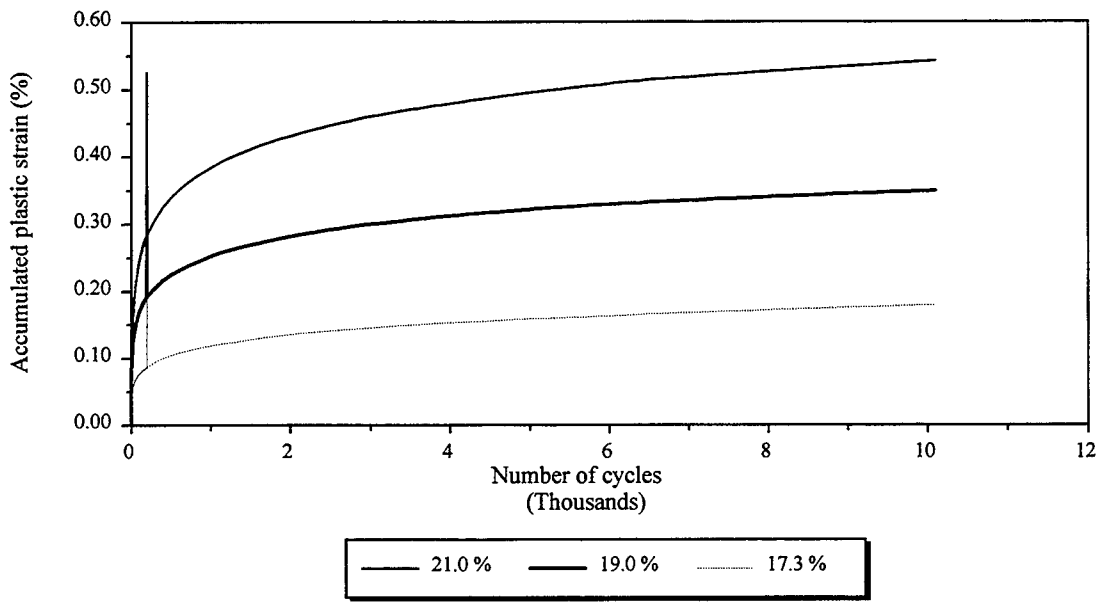

Figure C2. Influence of Moisture Content on Accumulated Plastic Strain in Clay (13.8 kPa Confining Pressure, 96.6 kPa Deviatoric Stress).

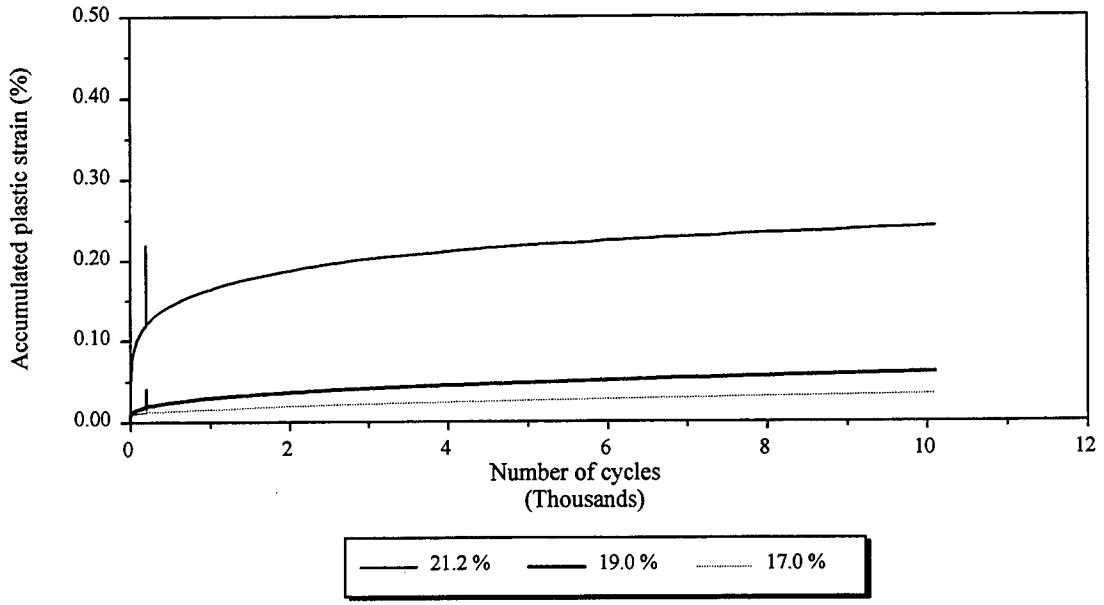

Figure C3. Influence of Moisture Content on Accumulated Plastic Strain in Clay (41.4 kPa Confining Pressure, 48.3 kPa Deviatoric Stress).

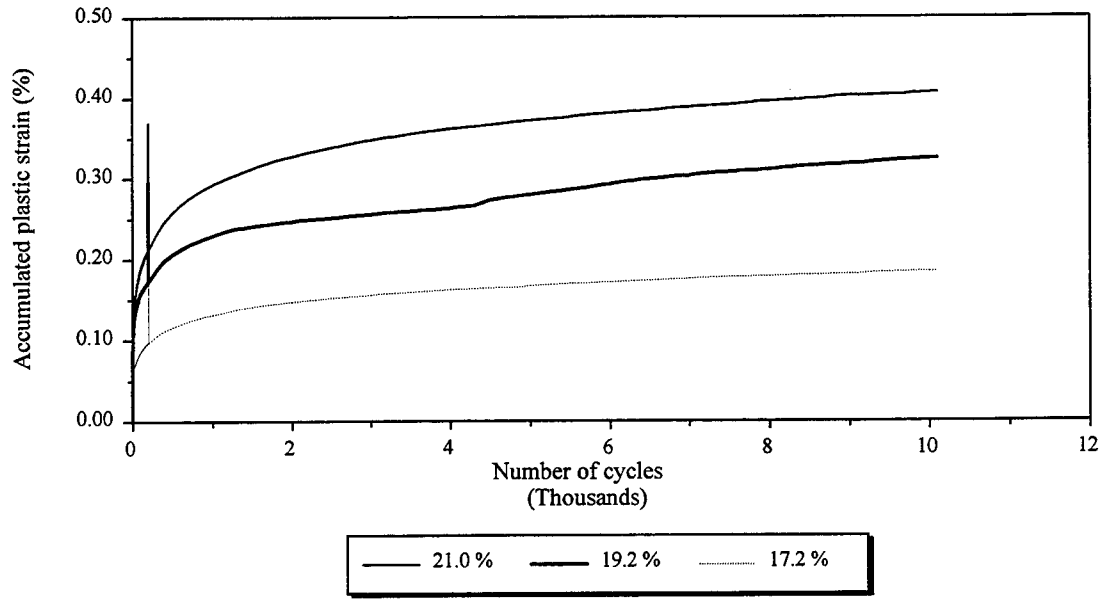

Figure C4. Influence of Moisture Content on Accumulated Plastic Strain in Clay (41.4 kPa Confining Pressure, 96.6 kPa Deviatoric Stress).

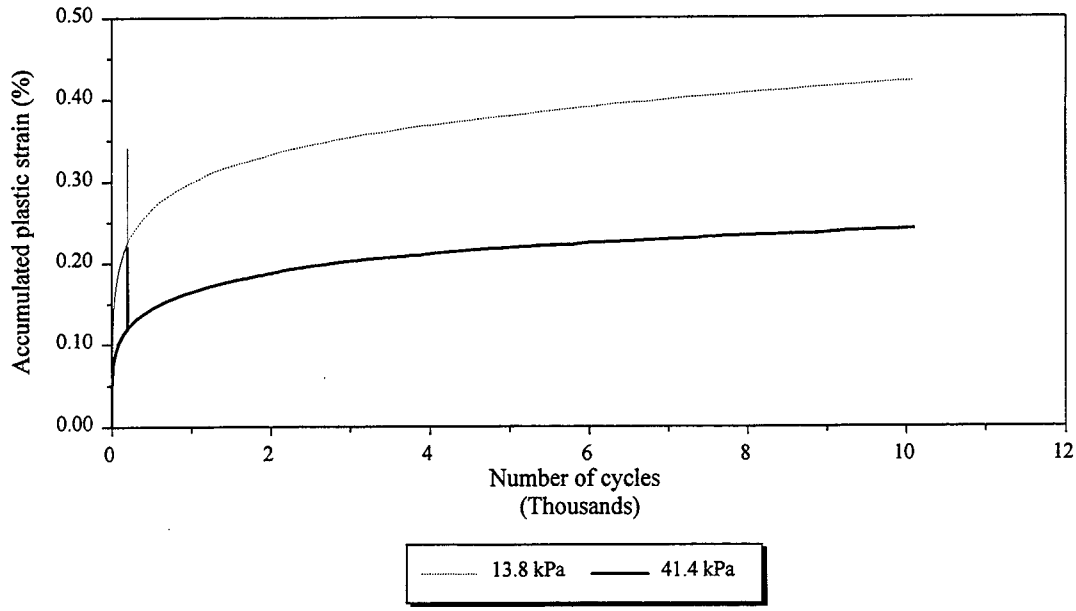

Figure C5. Effect of Confining Pressure on Accumulated Plastic Strain in Clay (48.3 kPa Deviatoric Stress and at Wet of Optimum Moisture Content).

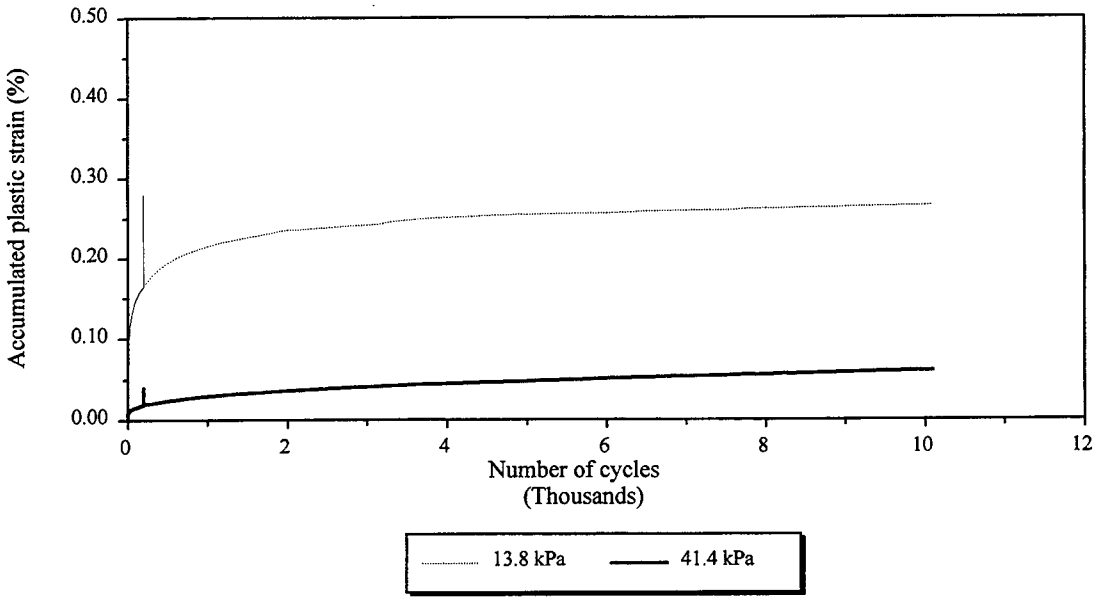

Figure C6. Effect of Confining Pressure on Accumulated Plastic Strain in Clay (48.3 kPa Deviatoric Stress and at Optimum Moisture Content).

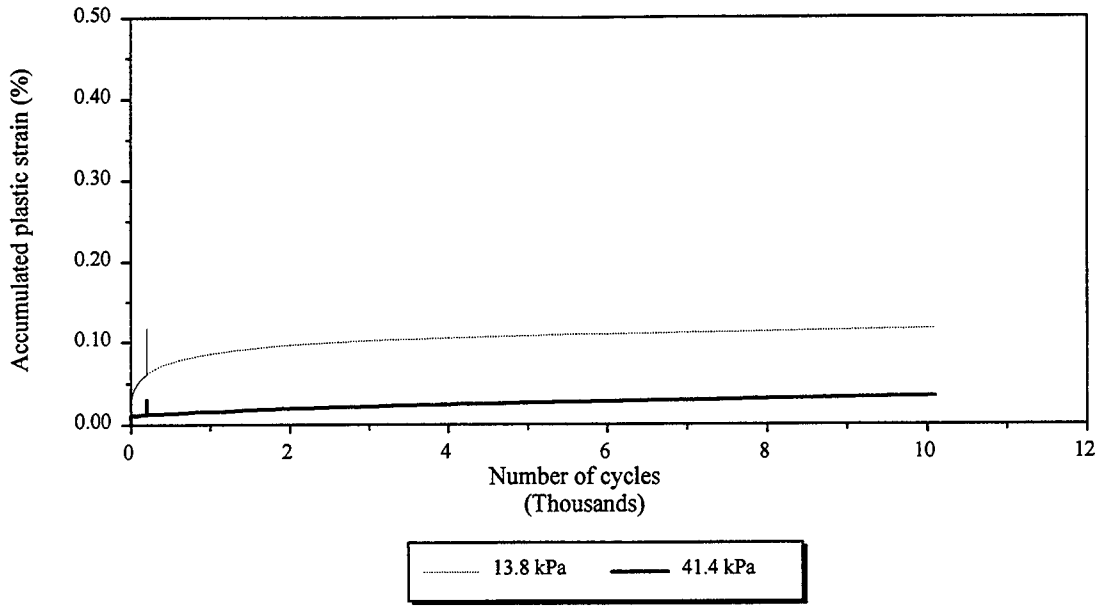

Figure C7. Effect of Confining Pressure on Accumulated Plastic Strain in Clay (48.3 kPa Deviatoric Stress and at Dry of Optimum Moisture Content).

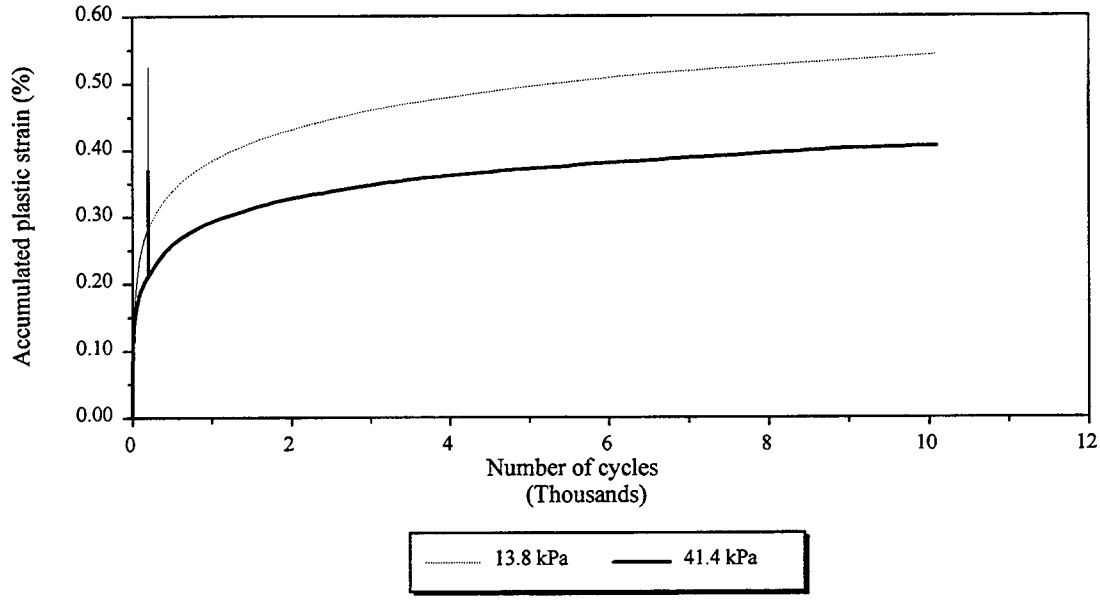

Figure C8. Effect of Confining Pressure on Accumulated Plastic Strain in Clay (96.6 kPa Deviatoric Stress and at Wet of Optimum Moisture Content).

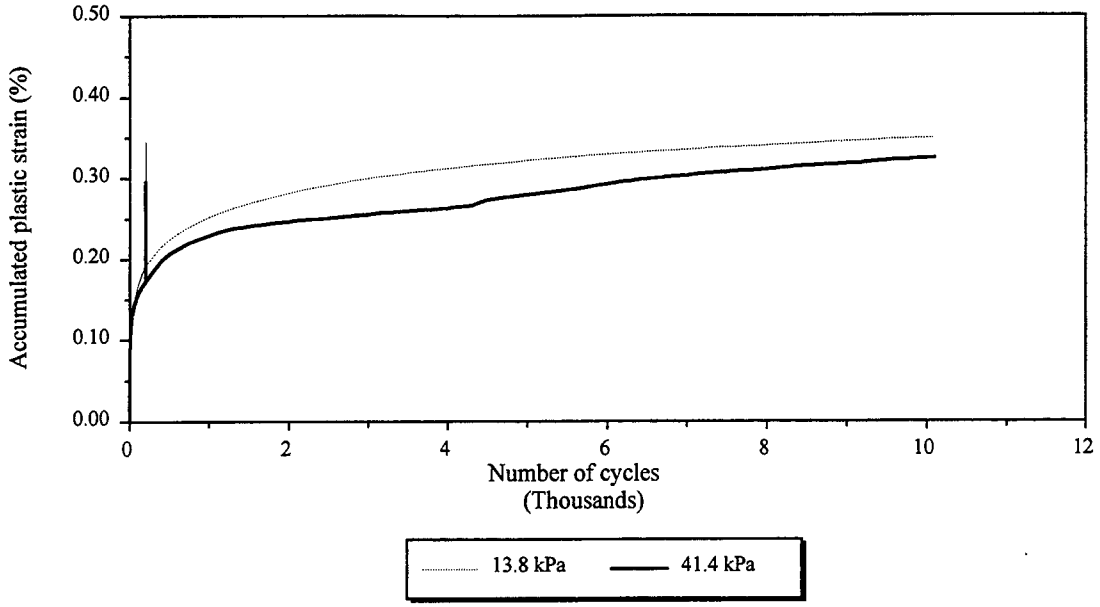

Figure C9. Effect of Confining Pressure on Accumulated Plastic Strain in Clay (96.6 kPa Deviatoric Stress and at Optimum Moisture Content).

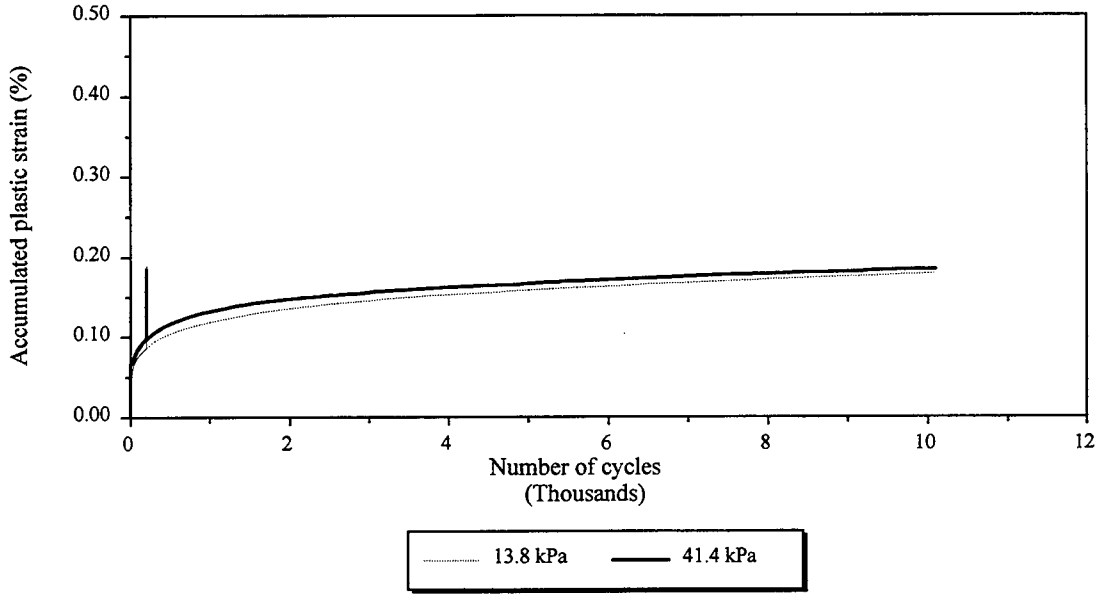

Figure C10. Effect of Confining Pressure on Accumulated Plastic Strain in Clay (96.6 kPa Deviatoric Stress and at Dry of Optimum Moisture Content).

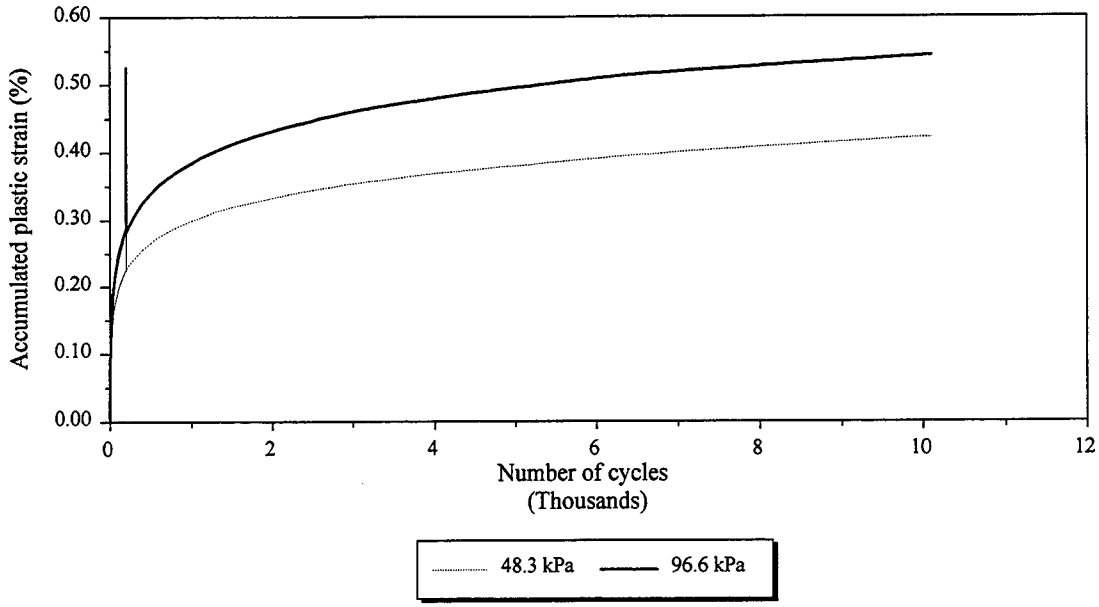

Figure C11. Effect of Deviatoric Stress on Accumulated Plastic Strain in Clay (13.8 kPa Confining Pressure and at Wet of Optimum Moisture Content).

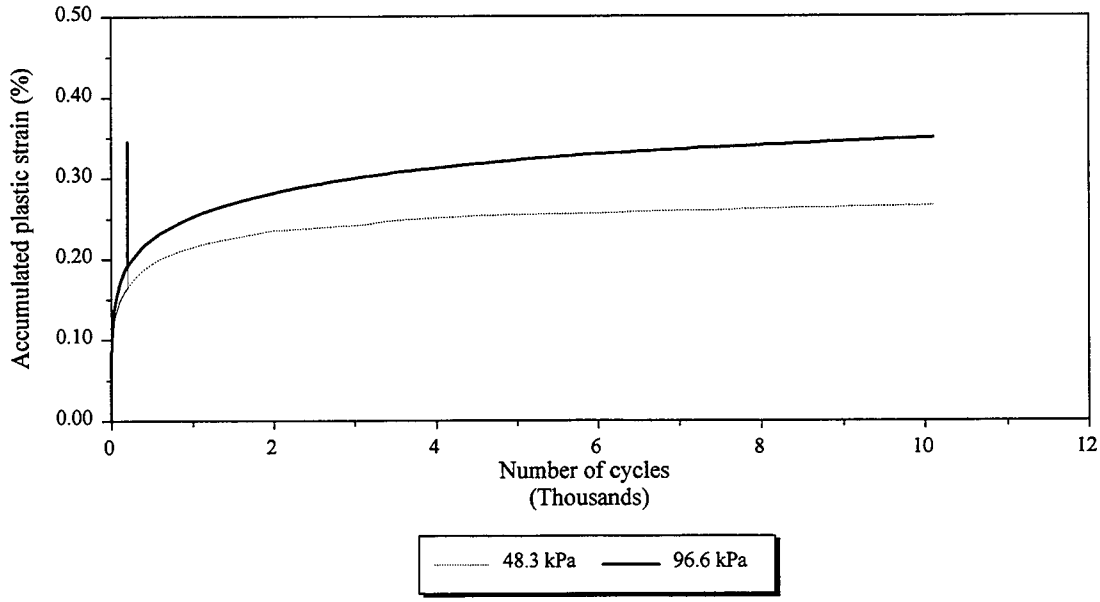

Figure C12. Effect of Deviatoric Stress on Accumulated Plastic Strain in Clay (13.8 kPa Confining Pressure and at Optimum Moisture Content).

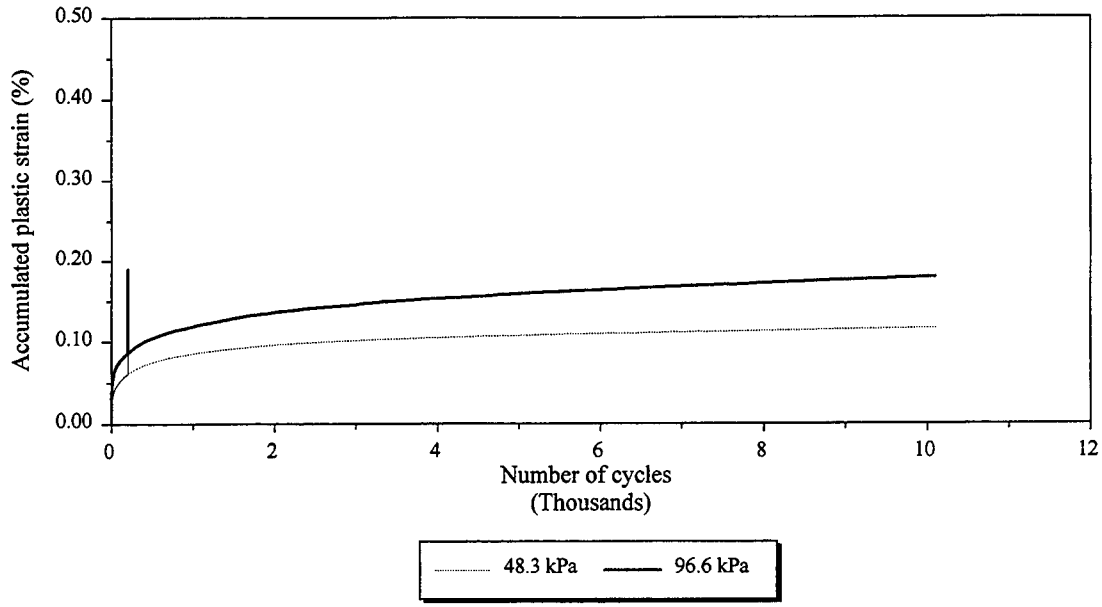

Figure C13. Effect of Deviatoric Stress on Accumulated Plastic Strain in Clay (13.8 kPa Confining Pressure and at Dry of Optimum Moisture Content).

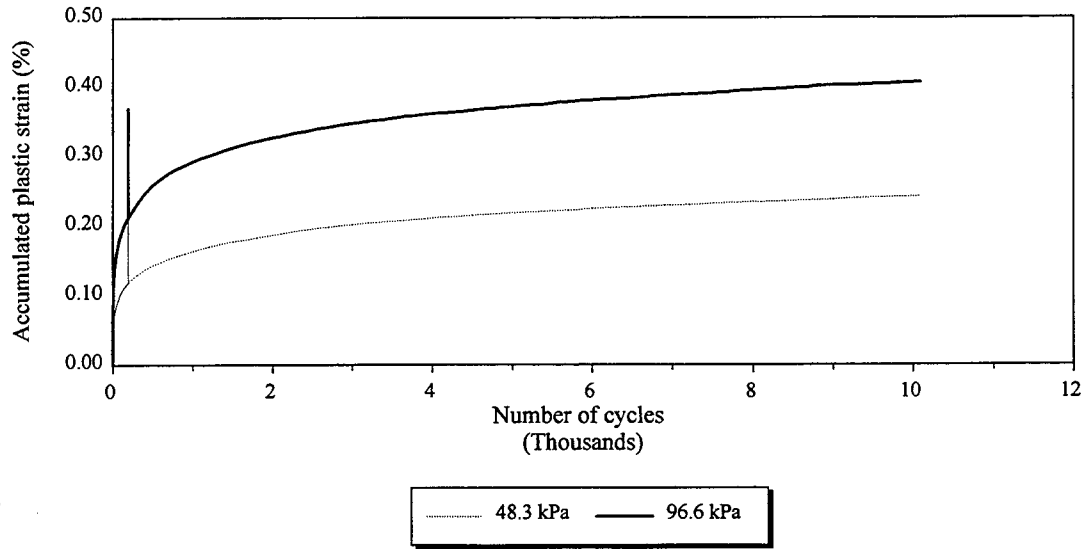

Figure C14. Effect of Deviatoric Stress on Accumulated Plastic Strain in Clay (41.4 kPa Confining Pressure and at Wet of Optimum Moisture Content).

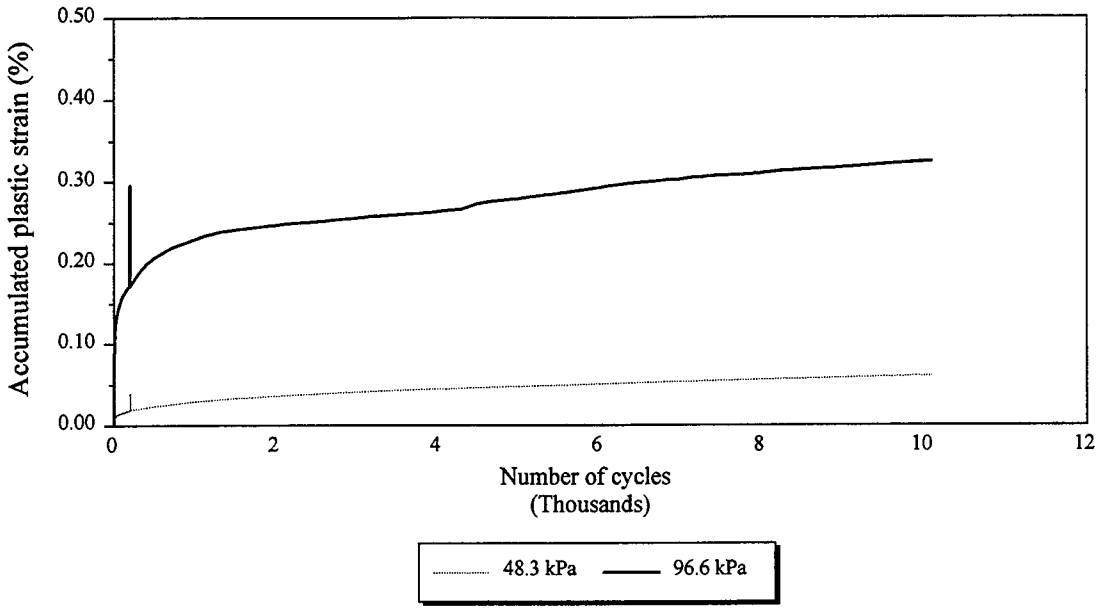

Figure C15. Effect of Deviatoric Stress on Accumulated Plastic Strain in Clay (41.4 kPa Confining Pressure and at Optimum Moisture Content).

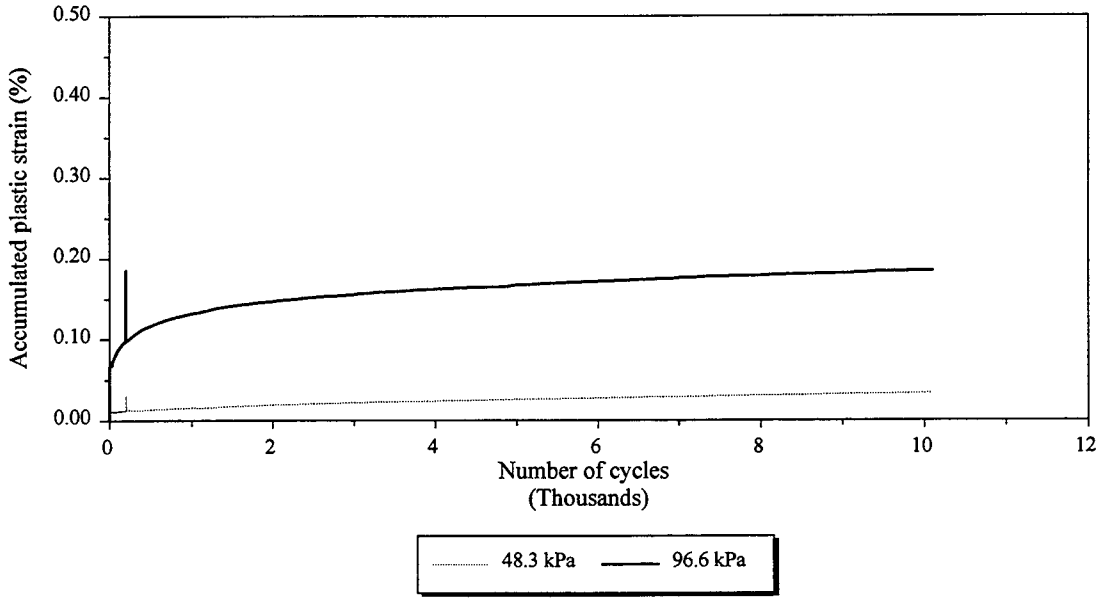

Figure C16. Effect of Deviatoric Stress on Accumulated Plastic Strain in Clay (41.4 kPa Confining Pressure and at Dry of Optimum Moisture Content).

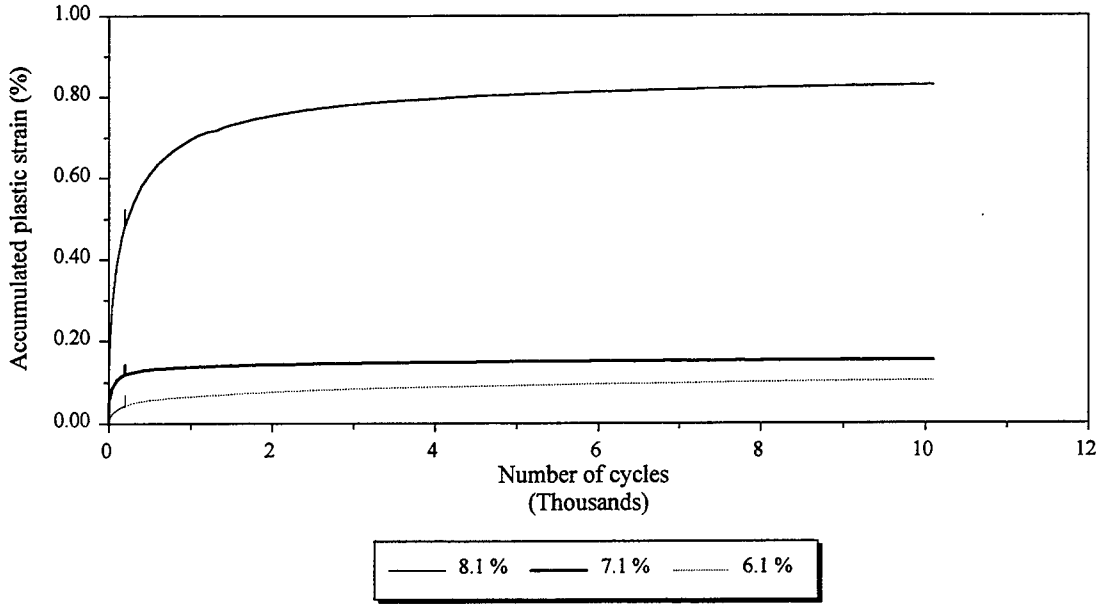

Figure C17. Effect of Moisture Content on Accumulated Plastic Strain in Limestone (34.5 kPa Confining Pressure and 172.5 kPa Deviatoric Stress).

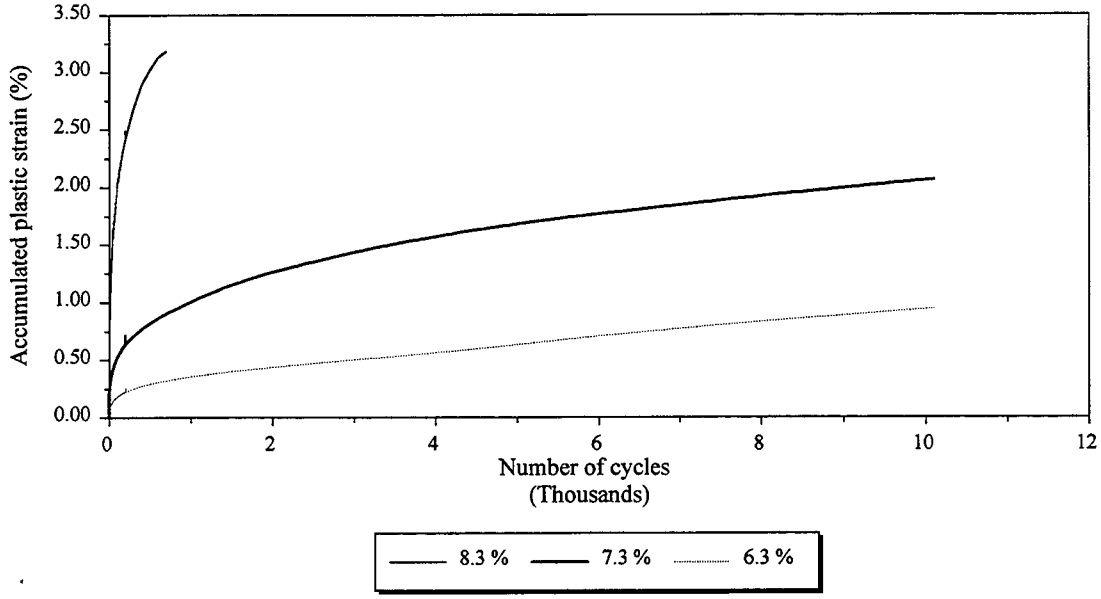

Figure C18. Effect of Moisture Content on Accumulated Plastic Strain in Limestone (34.5 kPa Confining Pressure and 345.0 kPa Deviatoric Stress).

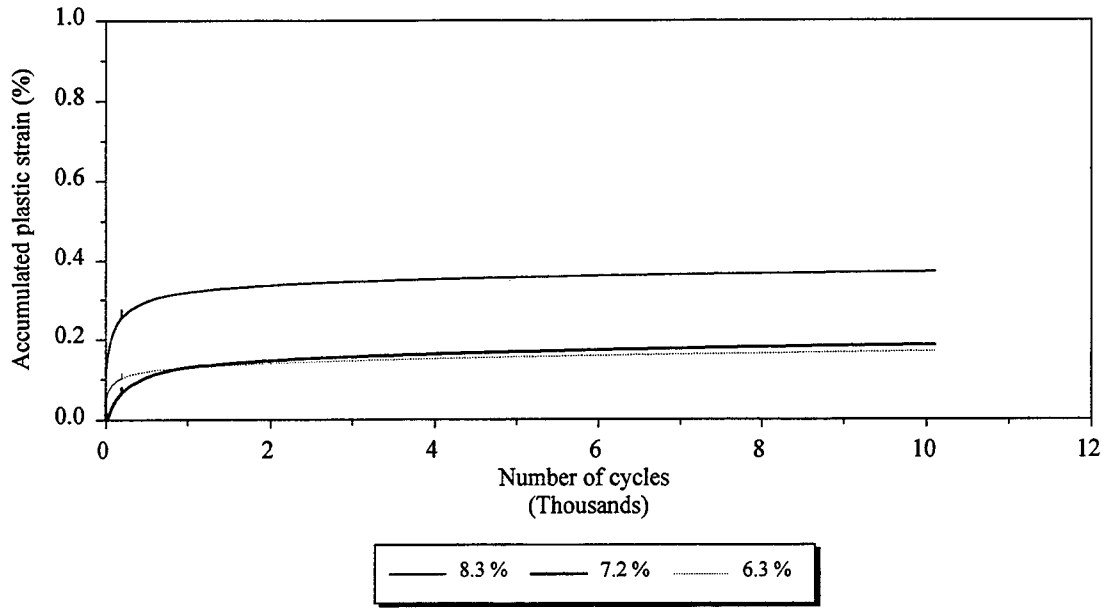

Figure C19. Effect of Moisture Content on Accumulated Plastic Strain in Limestone (103.5 kPa Confining Pressure and 172.5 kPa Deviatoric Stress).

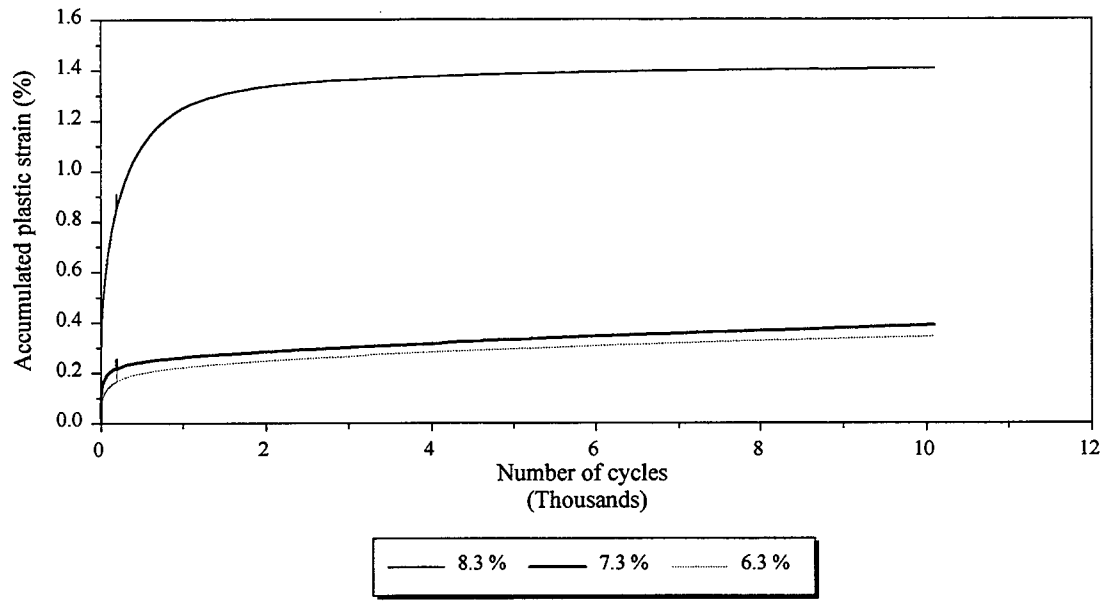

Figure C20. Effect of Moisture Content on Accumulated Plastic Strain in Limestone (103.5 kPa Confining Pressure and 345.0 kPa Deviatoric Stress).

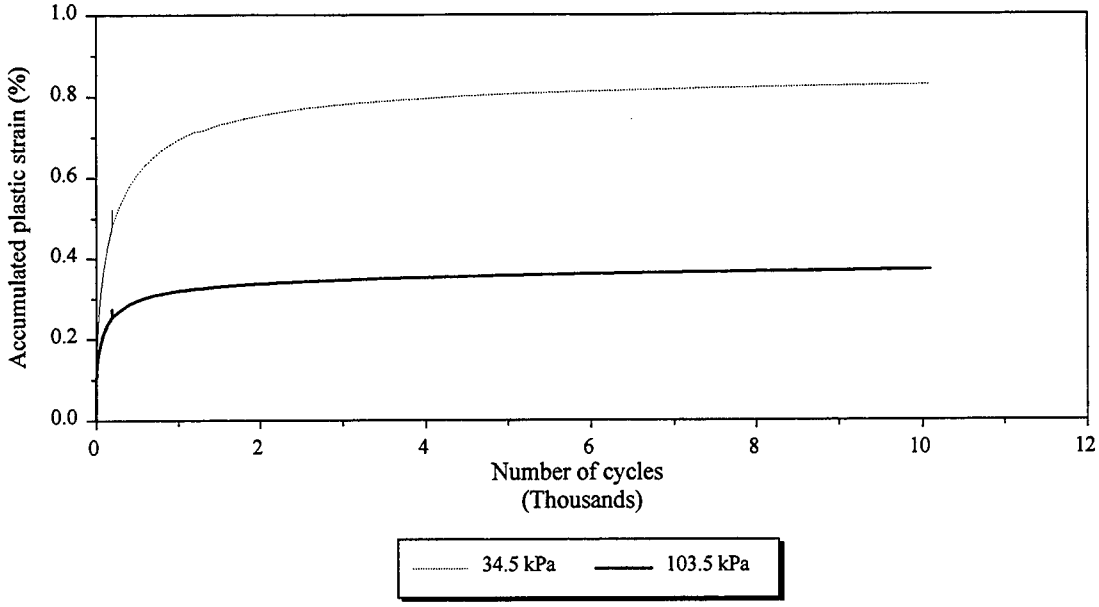

Figure C21. Effect of Confining Pressure on Accumulated Plastic Strain in Limestone (172.5 kPa Deviatoric Stress and at Wet of Optimum Moisture Content).

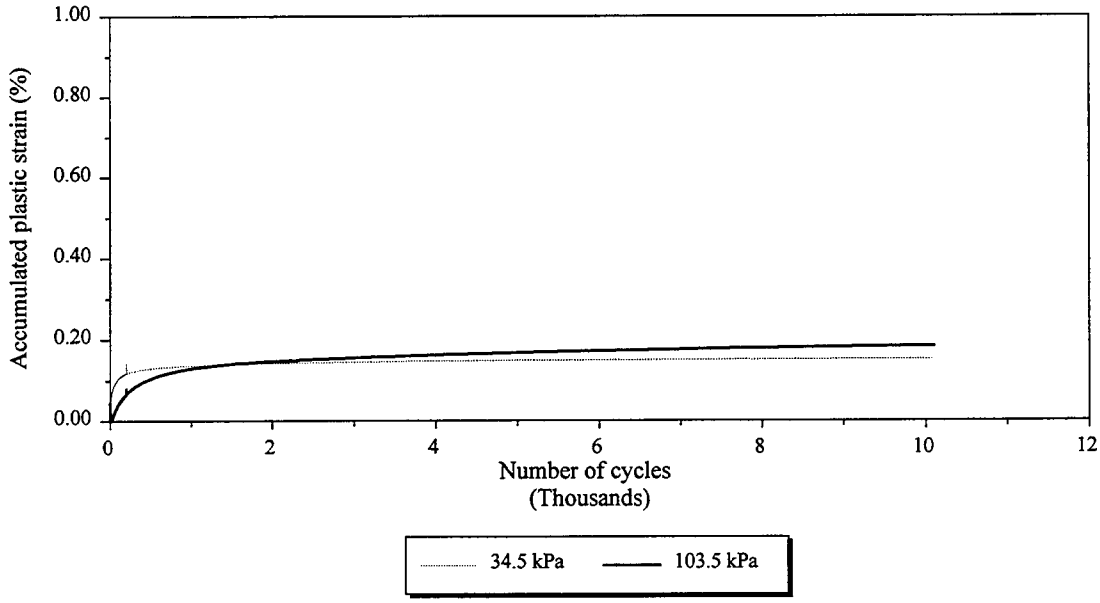

Figure C22. Effect of Confining Pressure on Accumulated Plastic Strain in Limestone (172.5 kPa Deviatoric Stress and at Optimum Moisture Content).

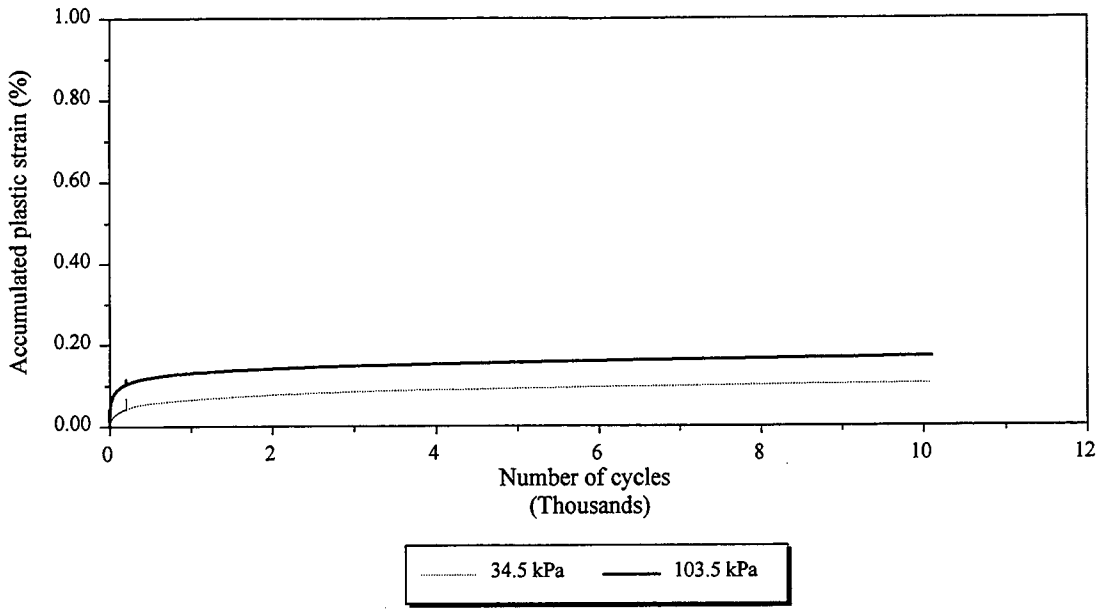

Figure C23. Effect of Confining Pressure on Accumulated Plastic Strain in Limestone (172.5 kPa Deviatoric Stress and at Dry of Optimum Moisture Content).

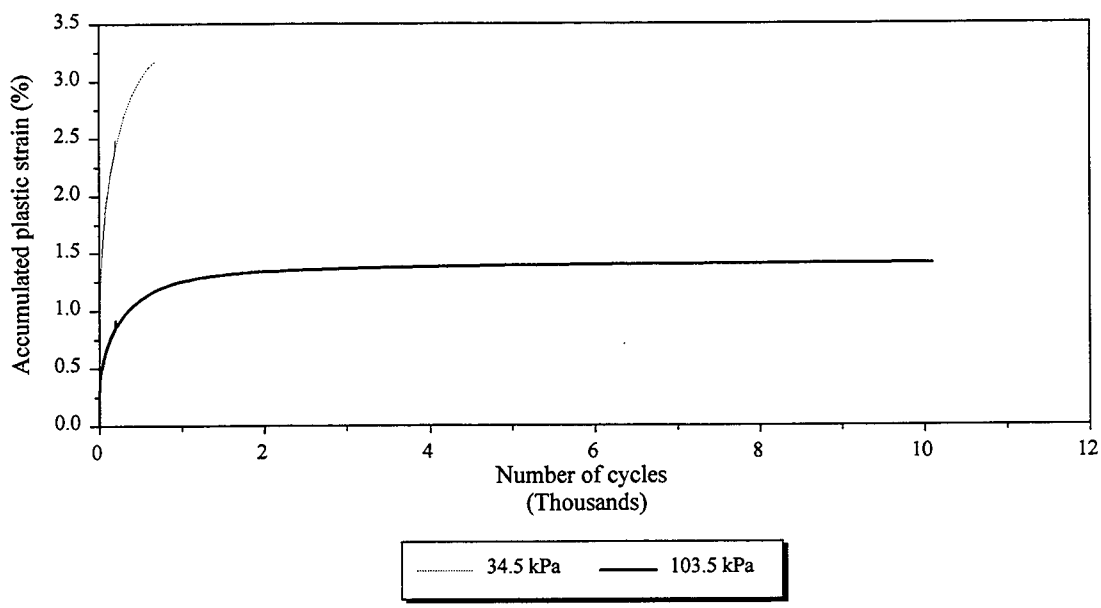

Figure C24. Effect of Confining Pressure on Accumulated Plastic Strain in Limestone (345.0 kPa Deviatoric Stress and at Wet of Optimum Moisture Content).

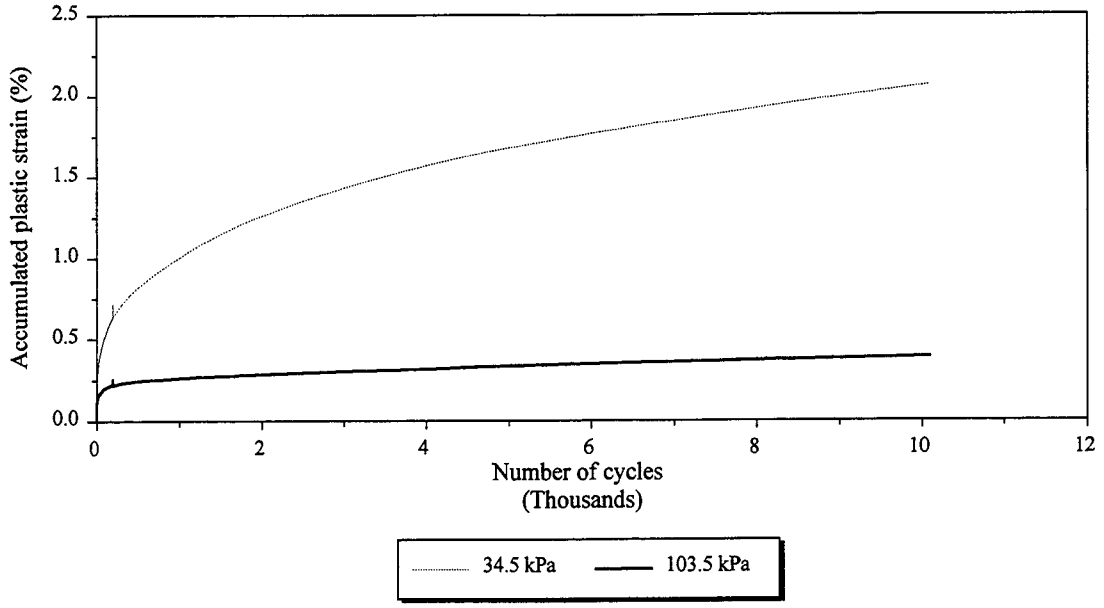

Figure C25. Effect of Confining Pressure on Accumulated Plastic Strain in Limestone (345.0 kPa Deviatoric Stress and at Optimum Moisture Content).

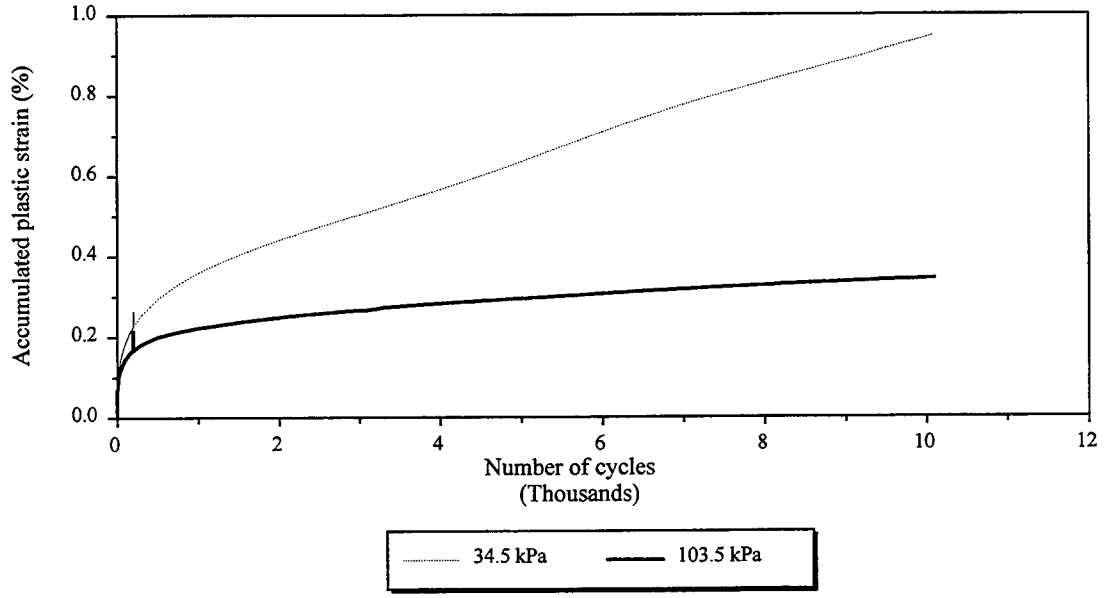

Figure C26. Effect of Confining Pressure on Accumulated Plastic Strain in Limestone (345.0 kPa and at Dry of Optimum Moisture Content).

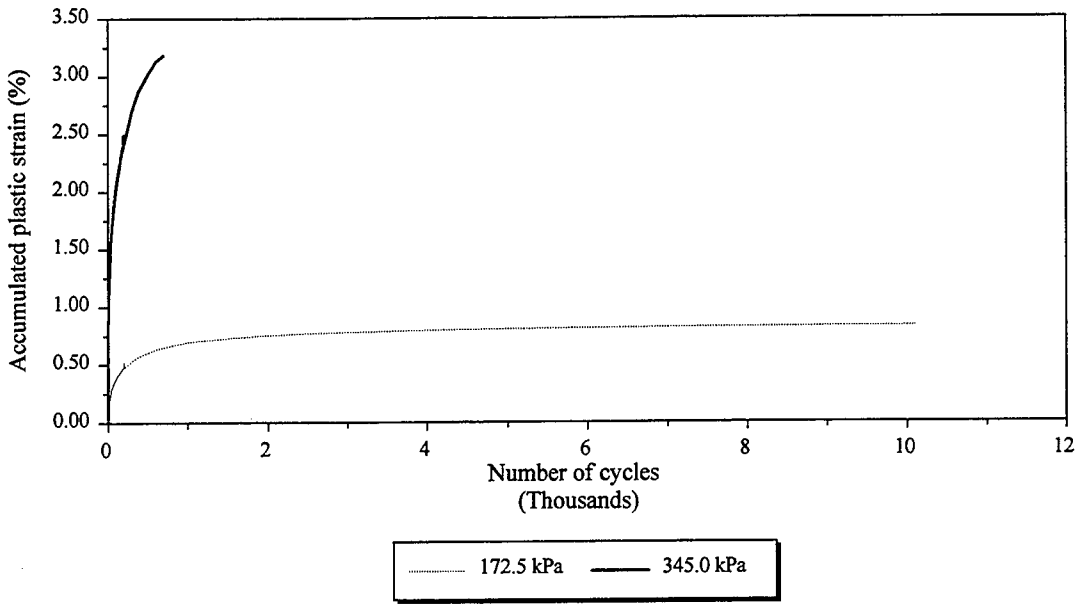

Figure C27. Effect of Deviatoric Stress on Accumulated Plastic Strain in Limestone (34.5 kPa Confining Pressure and at Wet of Optimum Moisture Content).

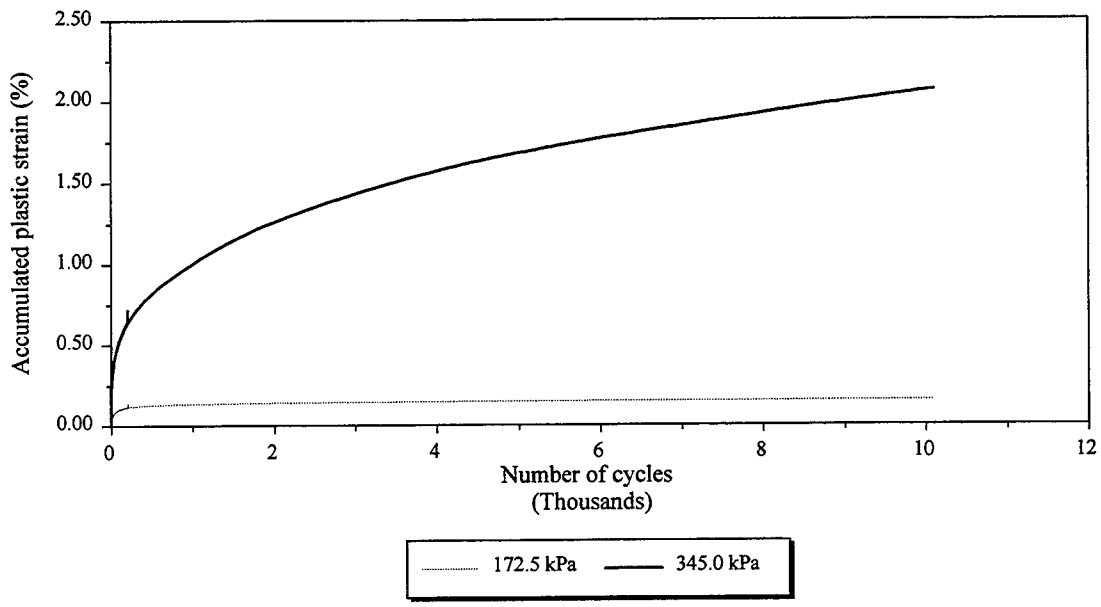

Figure C28. Effect of Deviatoric Stress on Accumulated Plastic Strain in Limestone (34.5 kPa Confining Pressure and at Optimum Moisture Content).

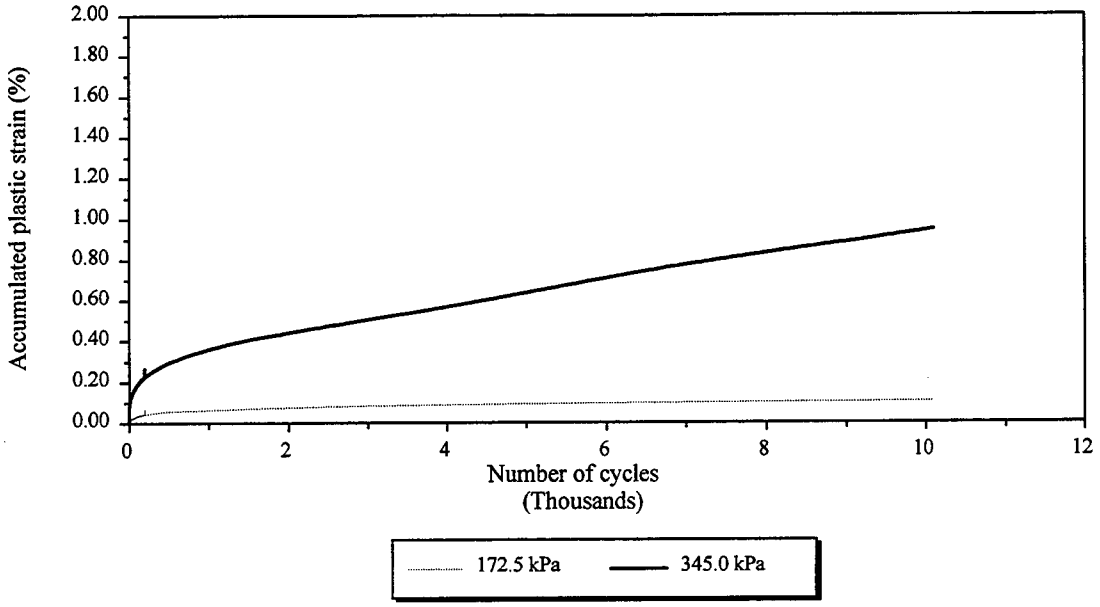

Figure C29. Effect of Deviatoric Stress on Accumulated Plastic Strain in Limestone (34.5 kPa Confining Pressure and at Dry of Optimum Moisture Content).

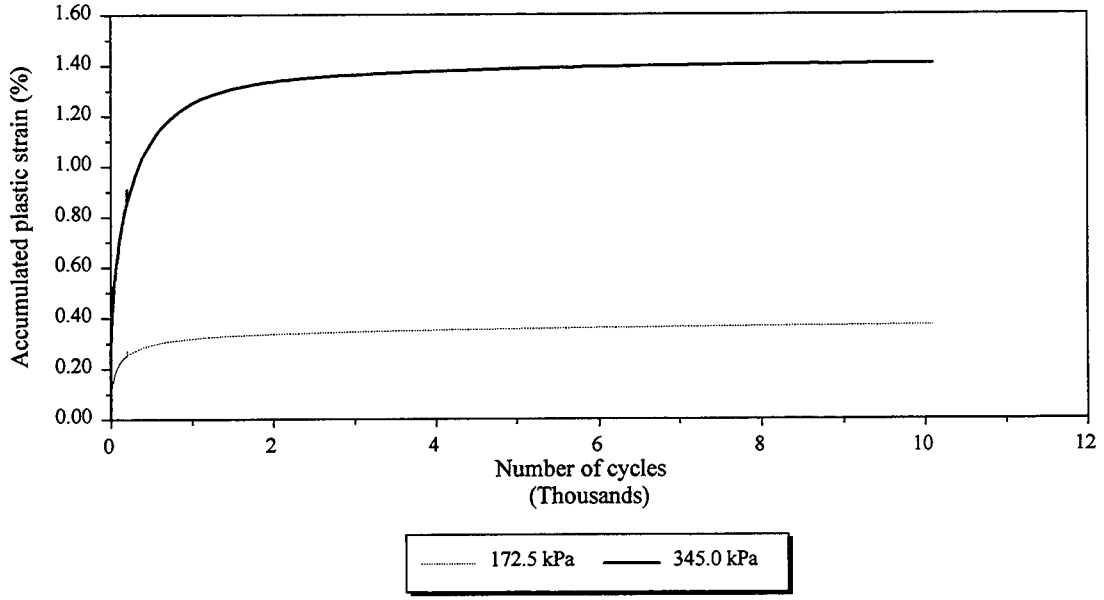

Figure C30. Effect of Deviatoric Stress on Accumulated Plastic Strain in Limestone (103.5 kPa Confining Pressure and at Wet of Optimum Moisture Content).

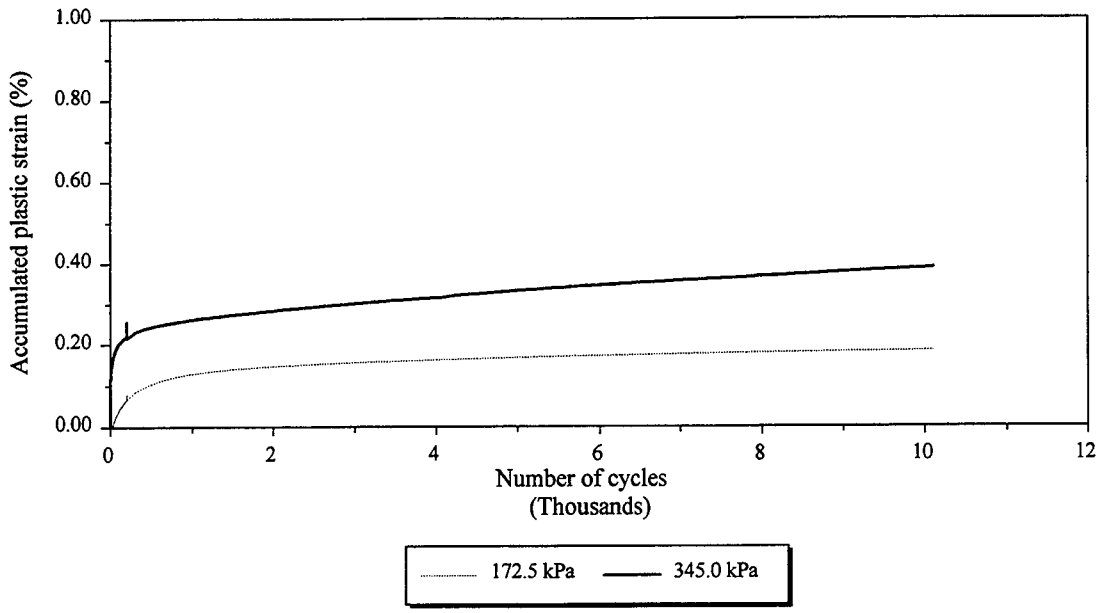

Figure C31. Effect of Deviatoric Stress on Accumulated Plastic Strain in Limestone (103.5 kPa Confining Pressure and at Optimum Moisture Content).

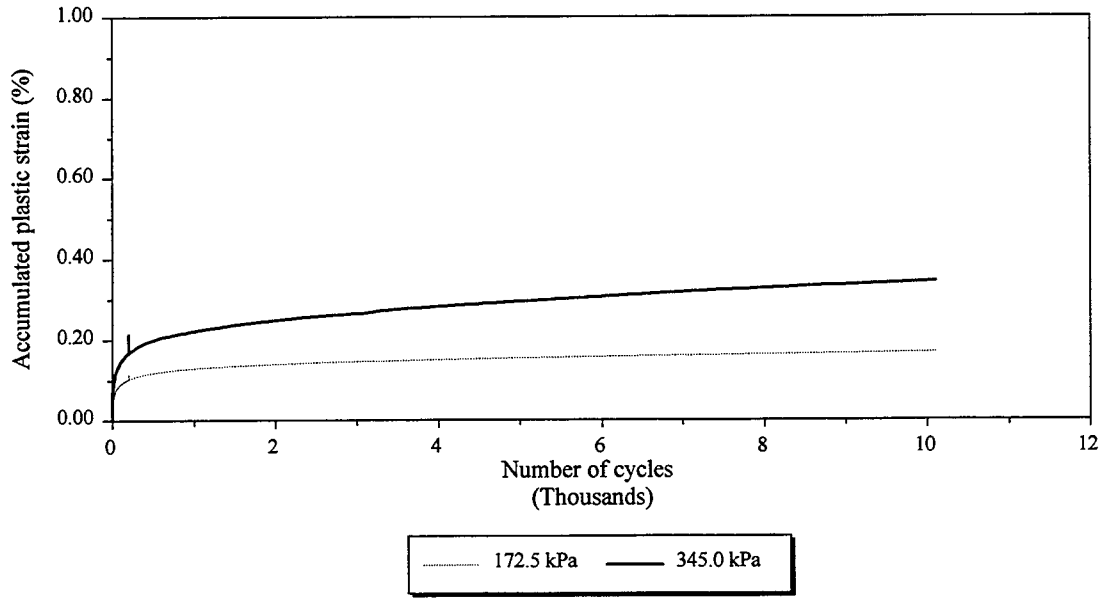

Figure C32. Effect of Deviatoric Stress on Accumulated Plastic Strain in Limestone (103.5 kPa Confining Pressure and at Dry of Optimum Moisture Content).

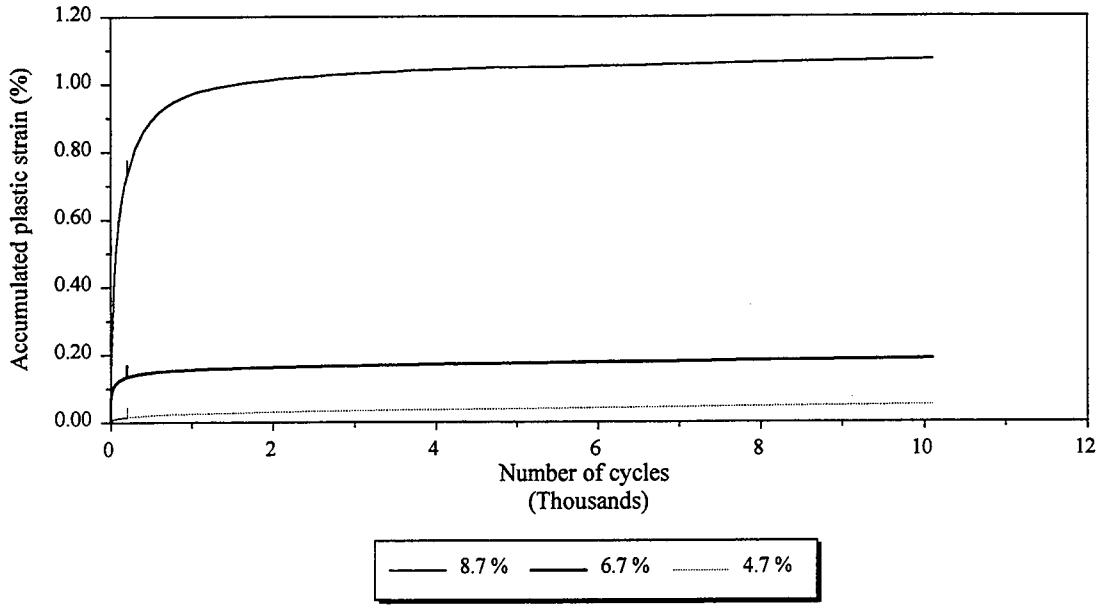

Figure C33. Effect of Moisture Content on Accumulated Plastic Strain in Caliche (34.5 kPa Confining Pressure and 172.5 kPa Deviatoric Stress).

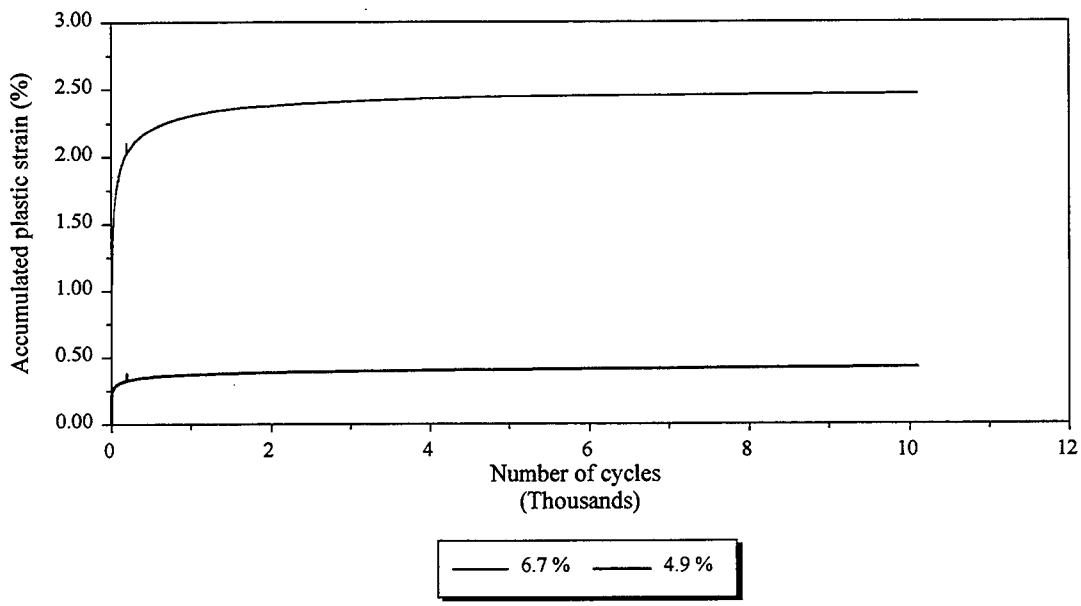

Figure C34. Effect of Moisture Content on Accumulated Plastic Strain in Caliche (34.5 kPa Confining Pressure and 345.0 kPa Deviatoric Stress).

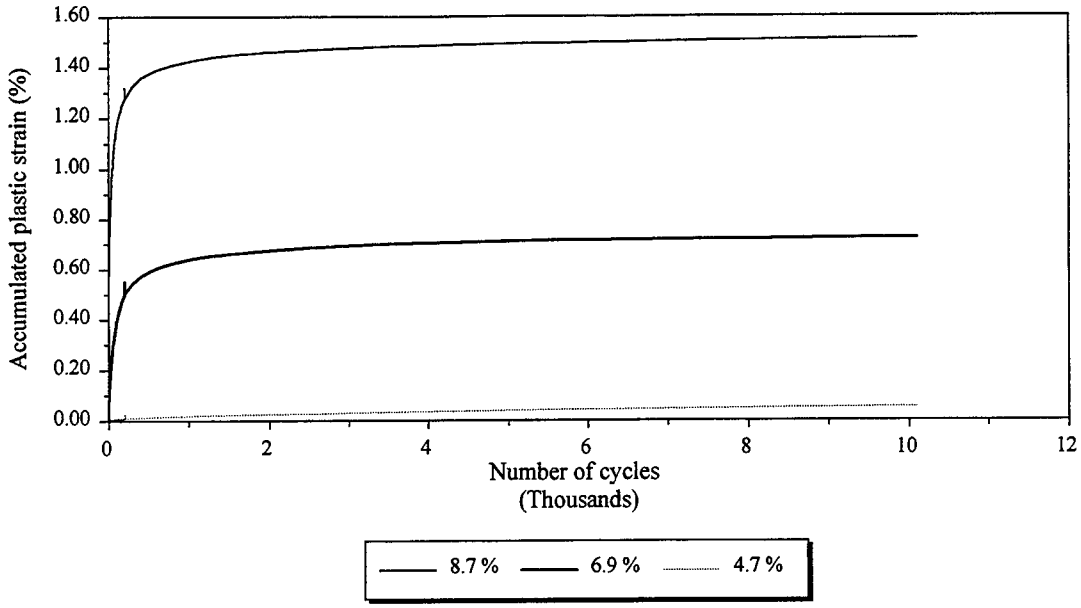

Figure C35. Effect of Moisture Content on Accumulated Plastic Strain in Caliche (103.5 kPa Confining Pressure and 172.5 kPa Deviatoric Stress).

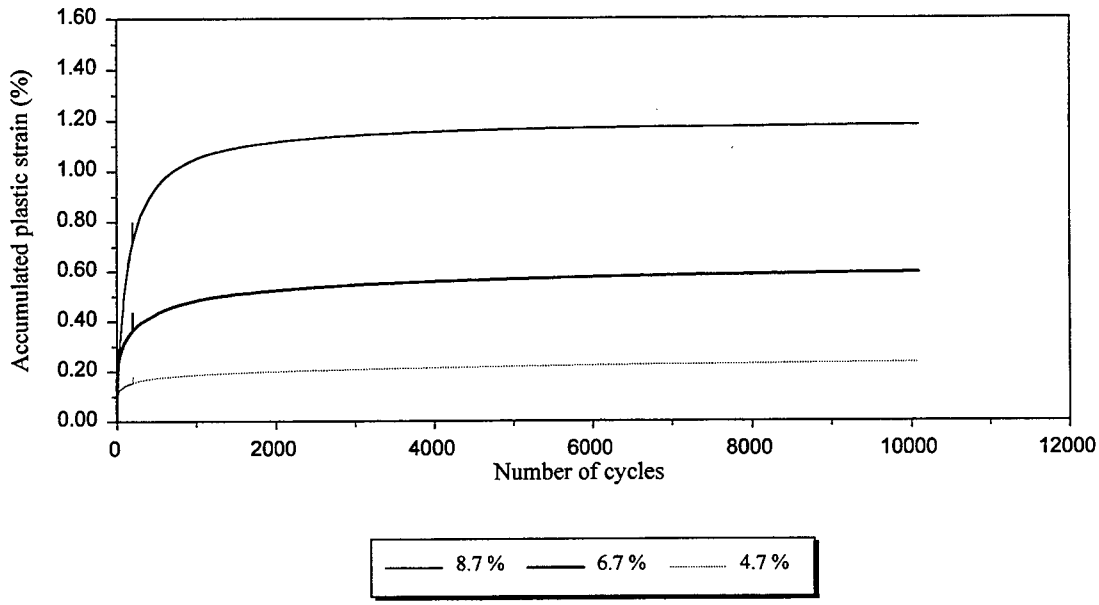

Figure C36. Effect of Moisture Content on Accumulated Plastic Strain in Caliche (103.5 kPa Confining Pressure and 345.0 kPa Deviatoric Stress).

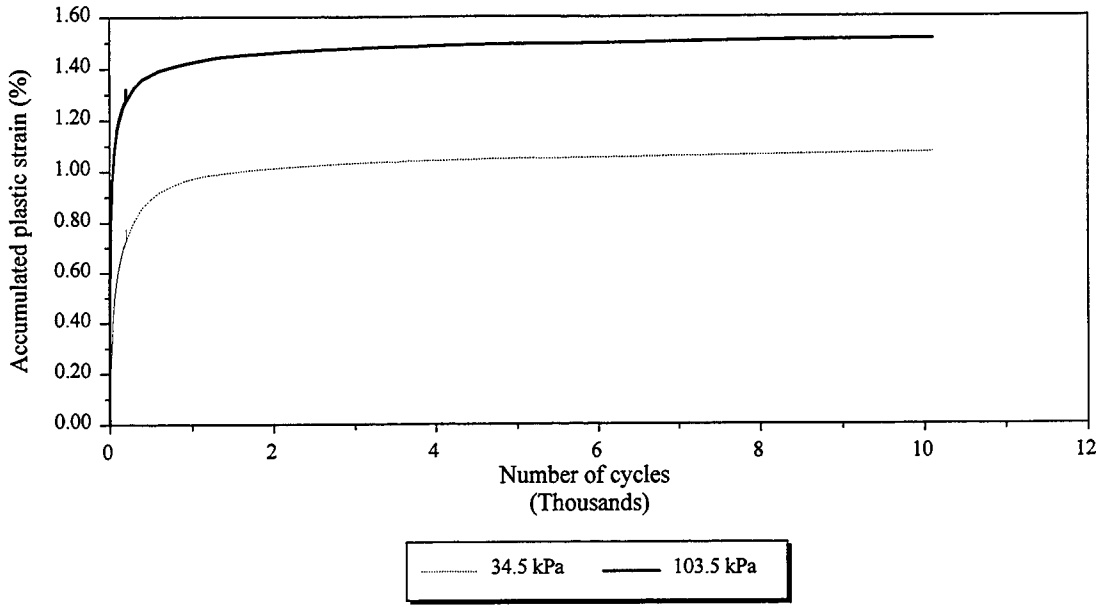

Figure C37. Effect of Confining Pressure on Accumulated Plastic Strain in Caliche (172.5 kPa Deviatoric Stress and at Wet of Optimum Moisture Content).

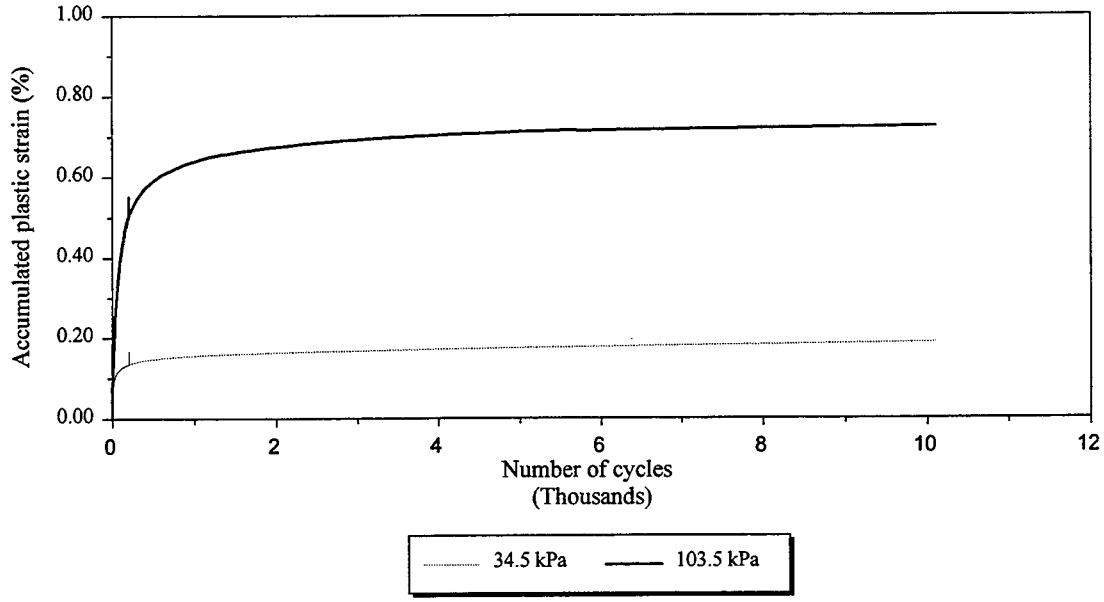

Figure C38. Effect of Confining Pressure on Accumulated Plastic Strain in Caliche (172.5 kPa Deviatoric Stress and at Optimum Moisture Content).

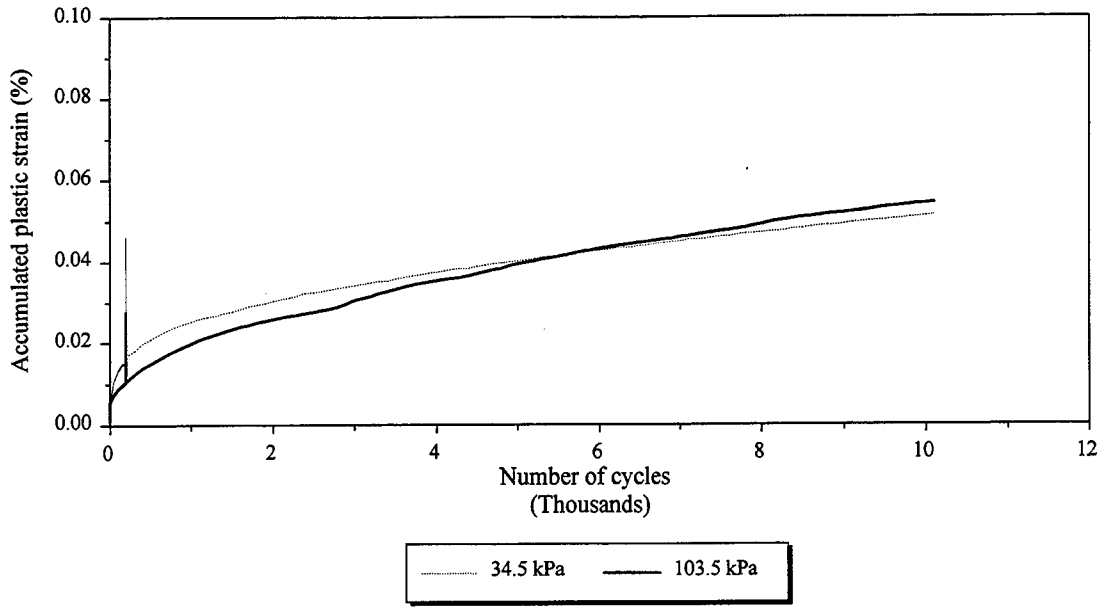

Figure C39. Effect of Confining Pressure on Accumulated Plastic Strain in Caliche (172.5 kPa Confining Pressure and at Dry of Optimum Moisture Content).

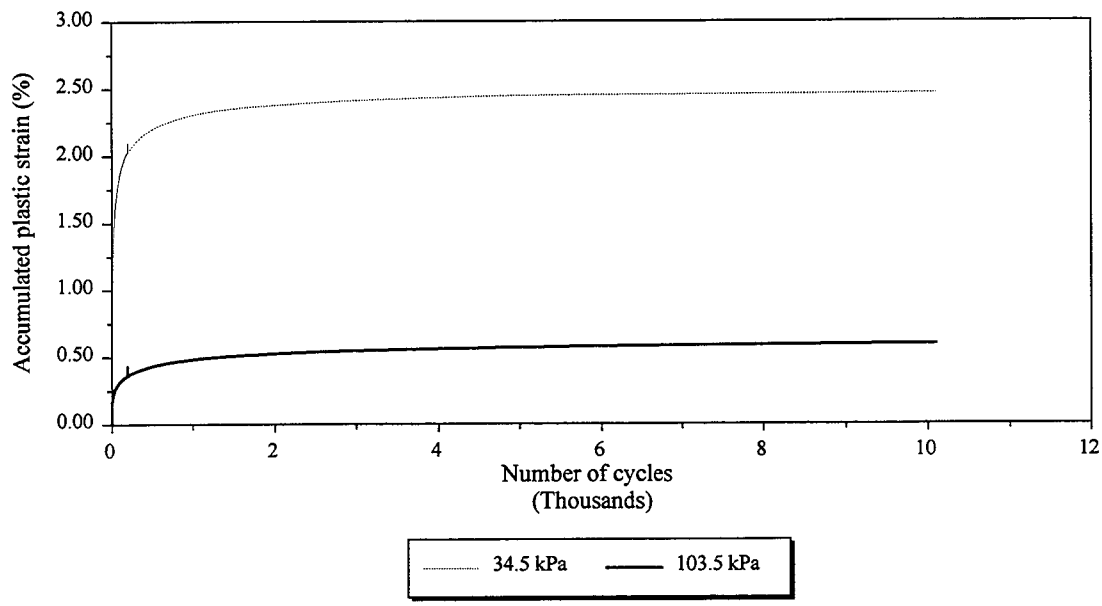

Figure C40. Effect of Confining Pressure on Accumulated Plastic Strain in Caliche (345.0 kPa Deviatoric Stress and at Optimum Moisture Content).

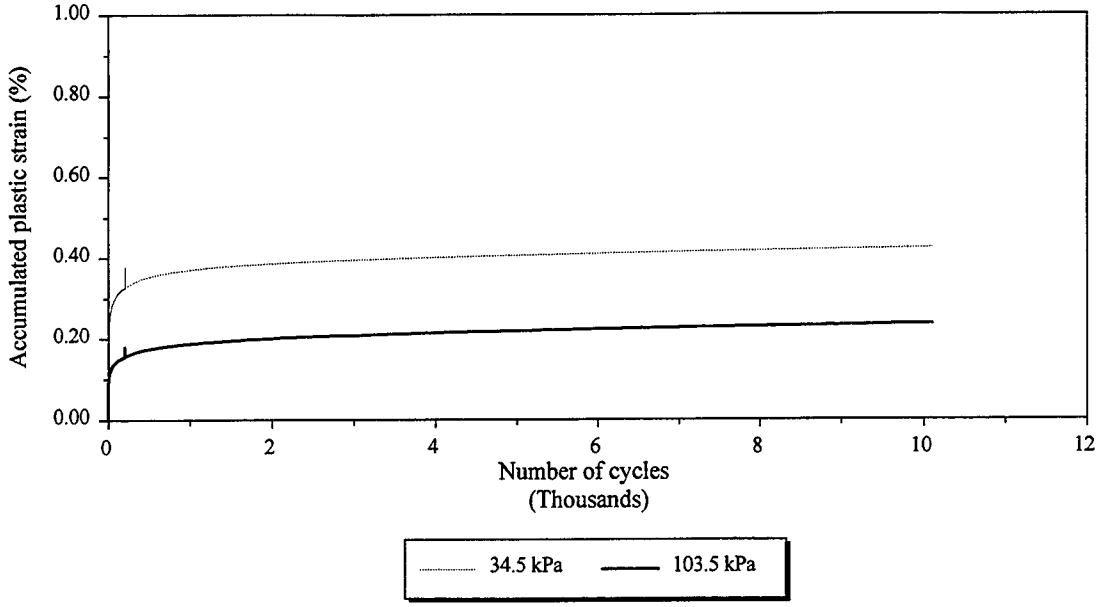

Figure C41. Effect of Confining Pressure on Accumulated Plastic Strain in Caliche (345.0 kPa Deviatoric Stress and at Dry of Optimum Moisture Content).

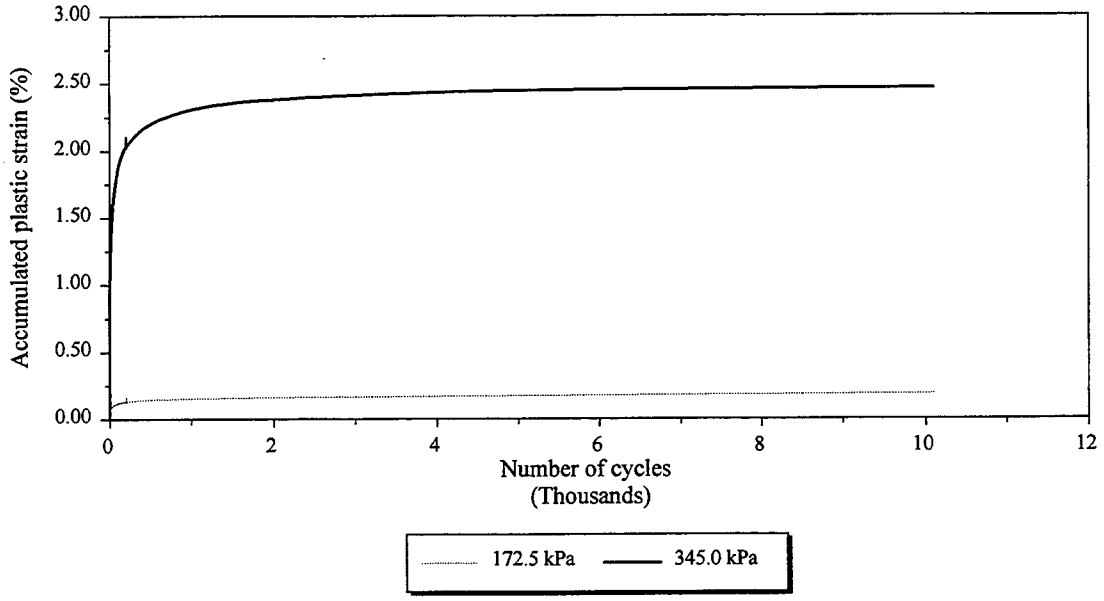

Figure C42. Effect of Deviatoric Stress on Accumulated Plastic Strain in Caliche (34.5 kPa Confining Pressure and at Optimum Moisture Content).

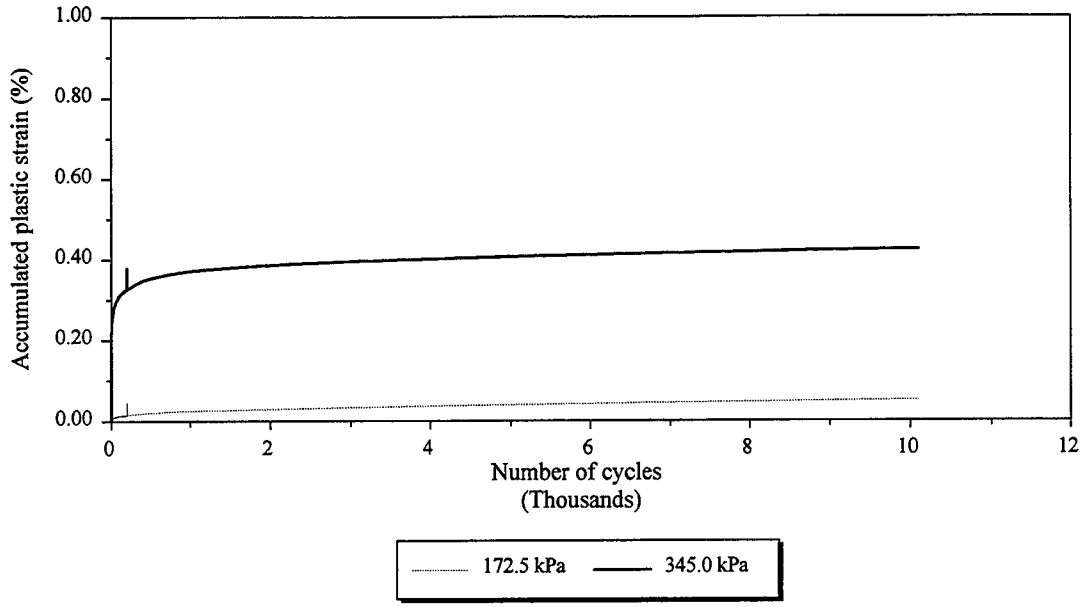

Figure C43. Effect of Deviatoric Stress on Accumulated Plastic Strain in Caliche (34.5 kPa Confining Pressure and at Dry of Optimum Moisture Content).

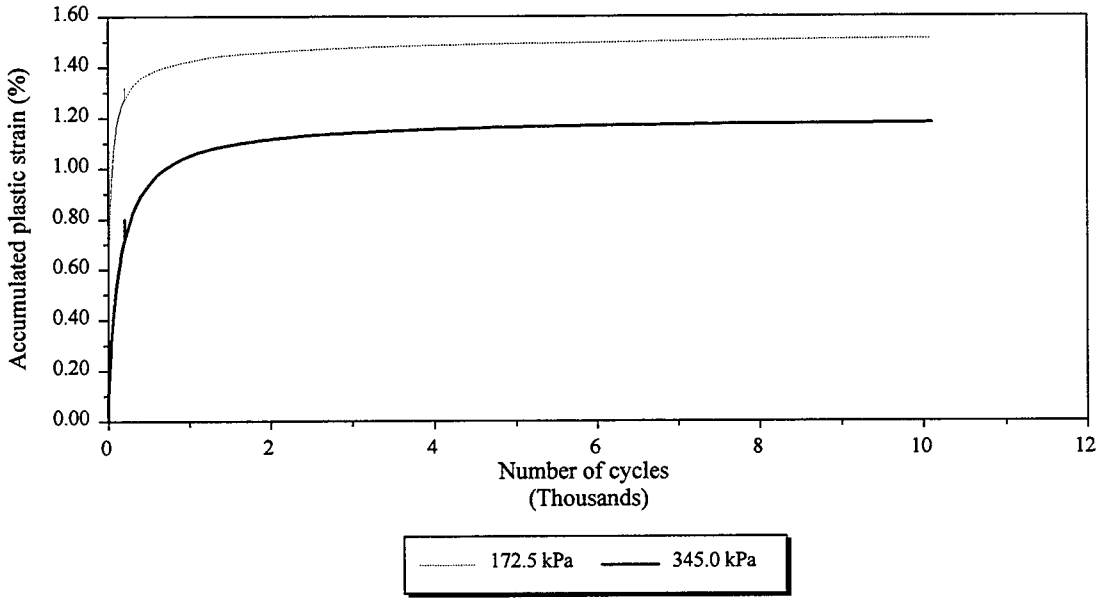

Figure C44. Effect of Deviatoric Stress on Accumulated Plastic Strain in Caliche (103.5 kPa Confining Pressure and at Wet of Optimum Moisture Content).

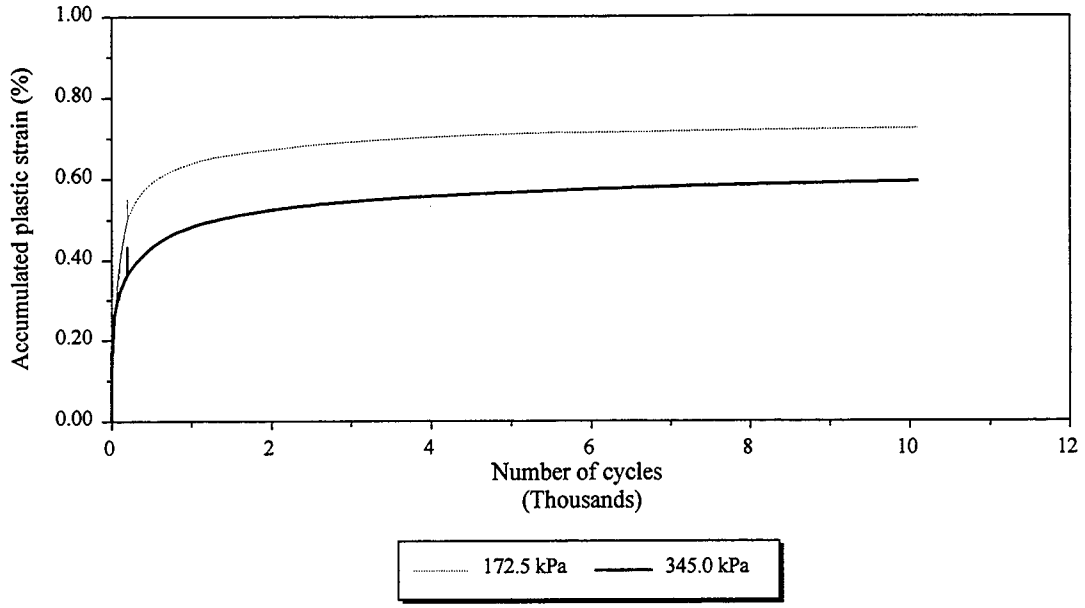

Figure C45. Effect of Deviatoric Stress on Accumulated Plastic Strain in Caliche (103.5 kPa Confining Pressure and at Optimum Moisture Content).

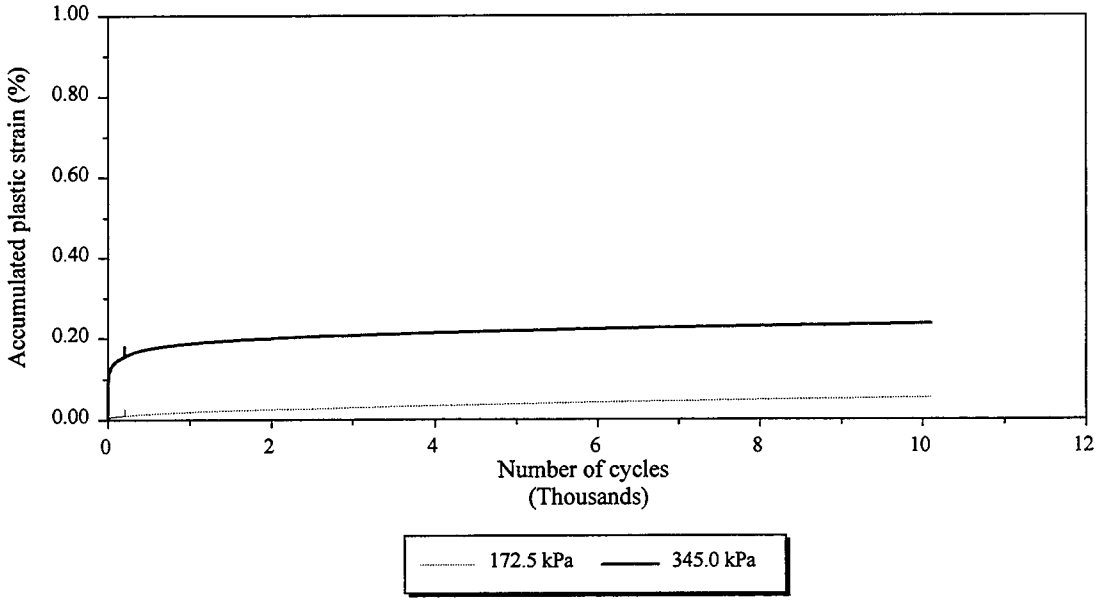

Figure C46. Effect of Deviatoric Stress on Accumulated Plastic Strain in Caliche (103.5 kPa Confining Pressure and at Dry of Optimum Moisture Content).

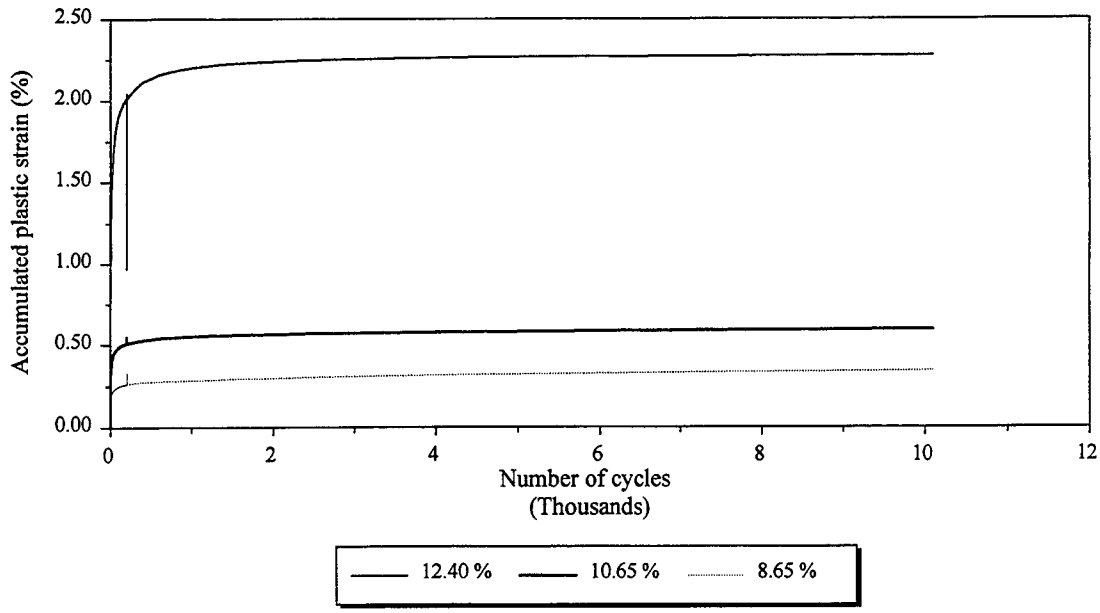

Figure C47. Effect of Moisture Content on Accumulated Plastic Strain in Iron Ore Gravel (34.5 kPa Confining Pressure and 172.5 kPa Deviatoric Stress).

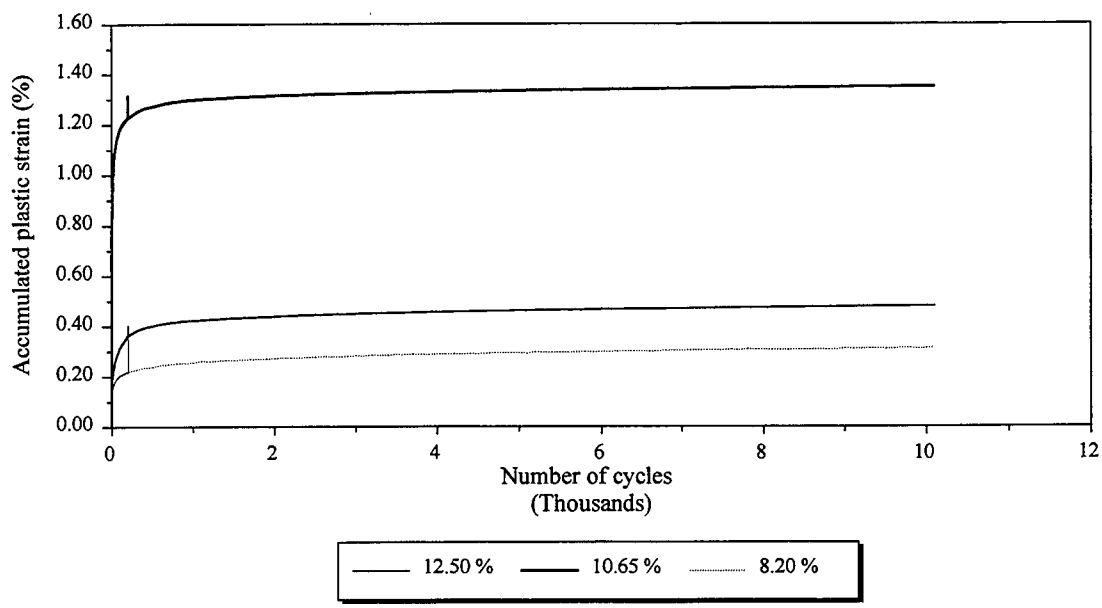

Figure C48. Effect of Moisture Content on Accumulated Plastic Strain in Iron Ore Gravel (34.5 kPa Confining Pressure and 345.0 kPa Deviatoric Stress).

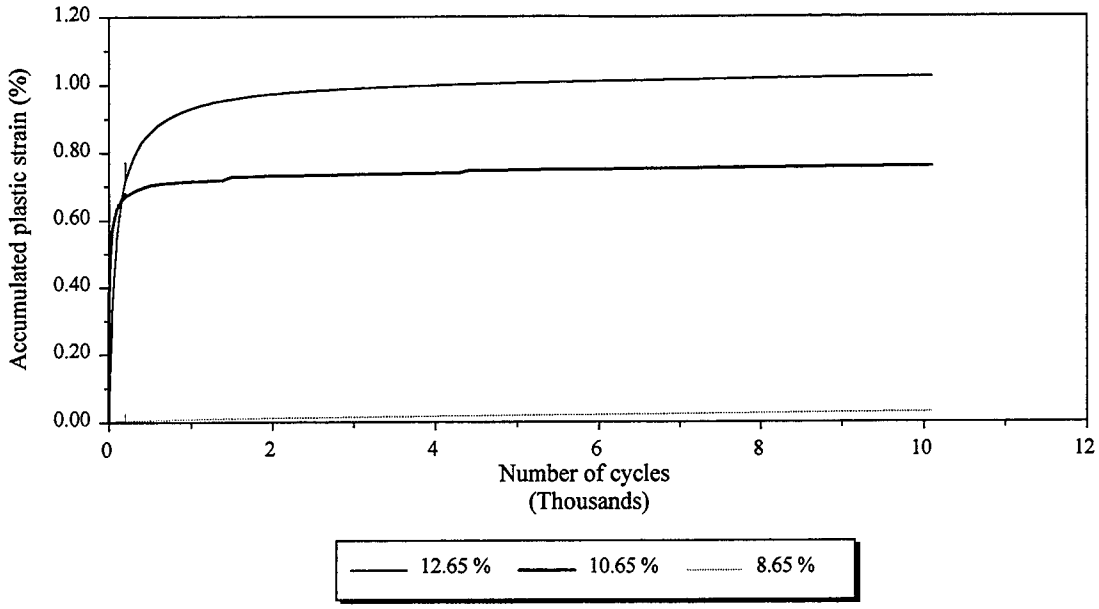

Figure C49. Effect of Moisture Content on Accumulated Plastic Strain in Iron Ore Gravel (103.5 kPa Confining Pressure and 172.5 kPa Deviatoric Stress).

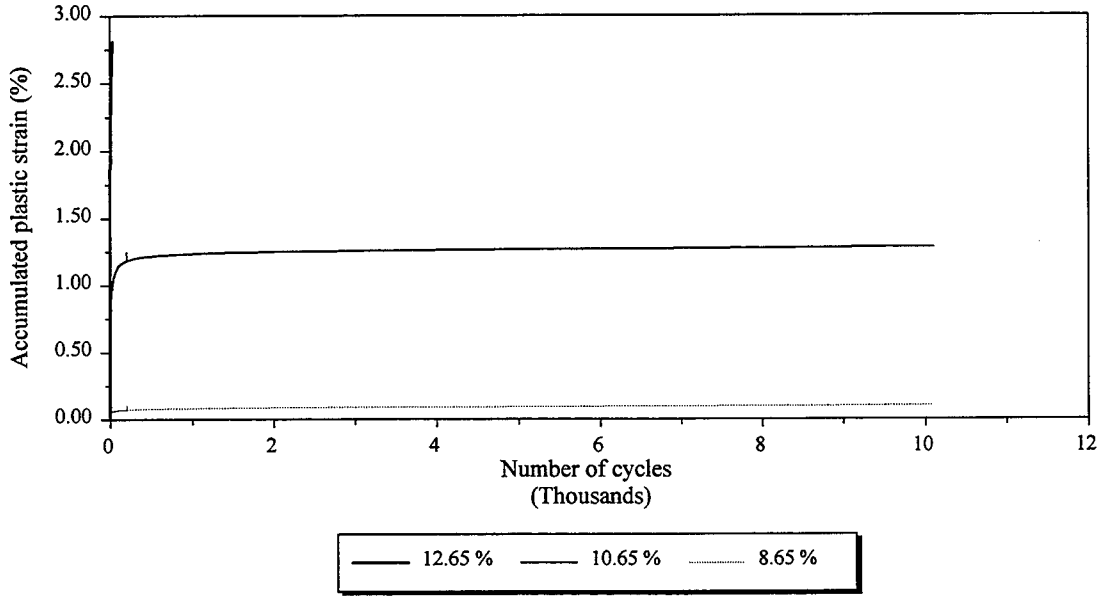

Figure C50. Effect of Moisture Content on Accumulated Plastic Strain in Iron Ore Gravel (103.5 kPa Confining Pressure and 345.0 kPa Deviatoric Stress).

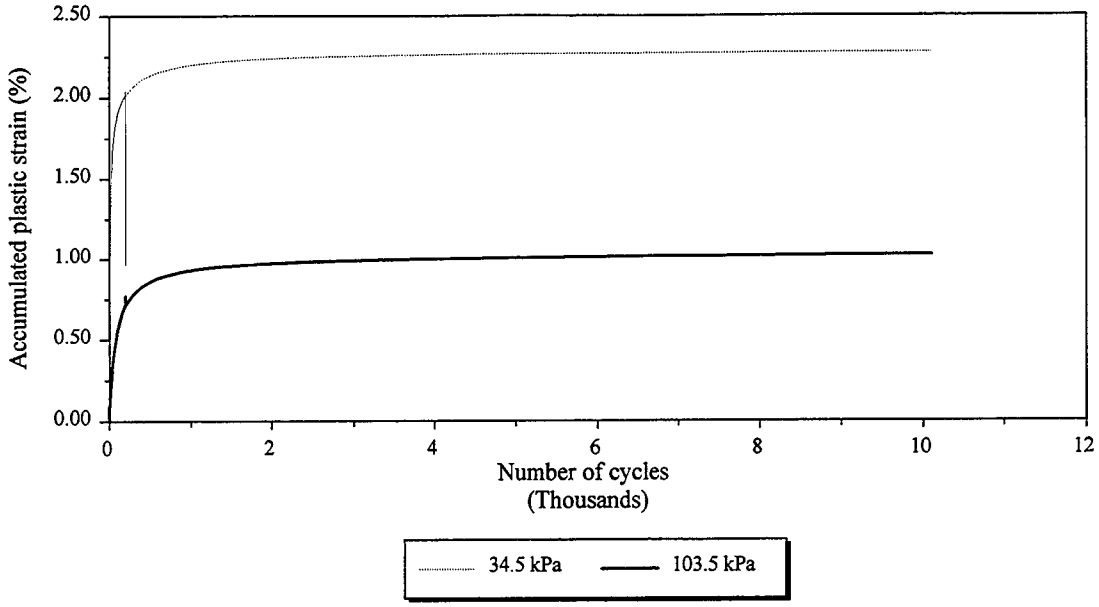

Figure C51. Effect of Confining Pressure on Accumulated Plastic Strain in Iron Ore Gravel (172.5 kPa Deviatoric Stress and at Wet of Optimum Moisture Content).

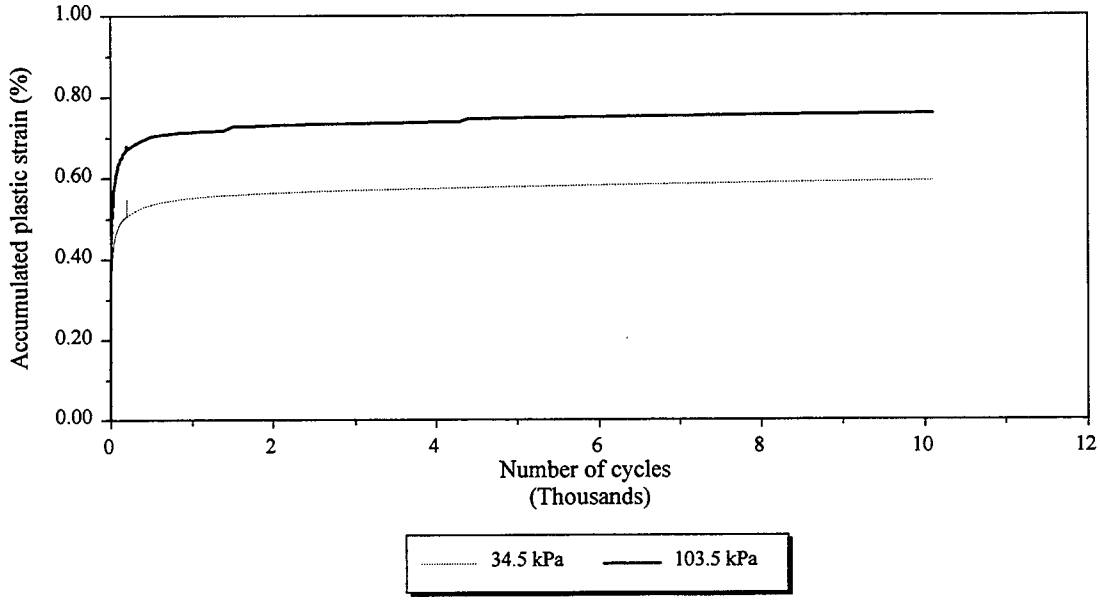

Figure C52. Effect of Confining Pressure on Accumulated Plastic Strain in Iron Ore Gravel (172.5 kPa Deviatoric Stress and at Optimum Moisture Content).

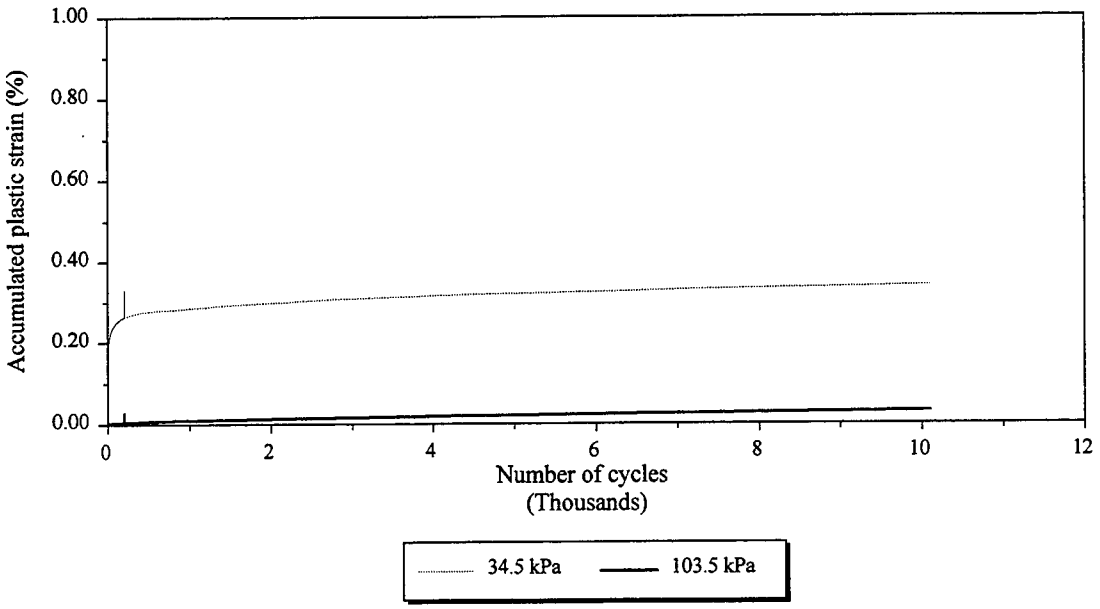

Figure C53. Effect of Confining Pressure on Accumulated Plastic Strain in Iron Ore Gravel (172.5 kPa Deviatoric Stress and at Dry of Optimum Moisture Content).

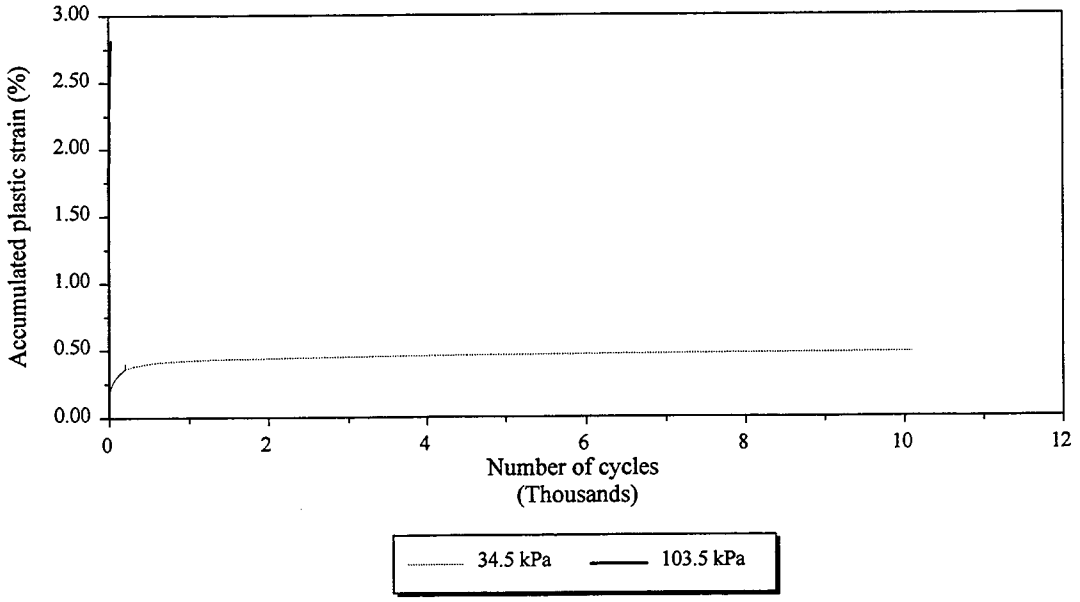

Figure C54. Effect of Confining Pressure on Accumulated Plastic Strain in Iron Ore Gravel (345.0 kPa Deviatoric Stress and at Wet of Optimum Moisture Content).

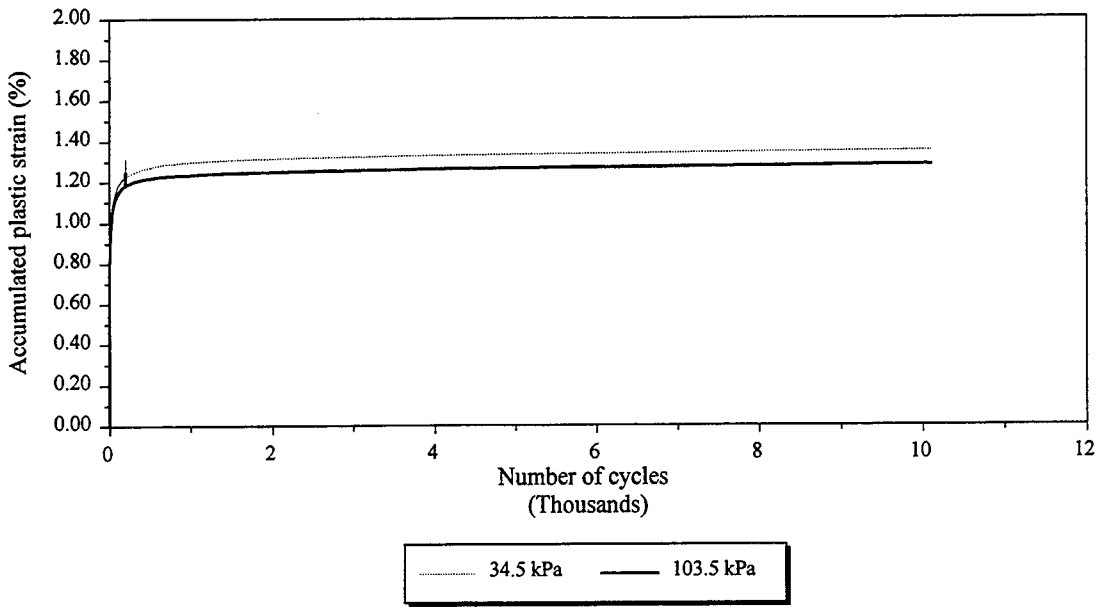

Figure C55. Effect of Confining Pressure on Accumulated Plastic Strain in Iron Ore Gravel (345.0 kPa Deviatoric Stress and at Optimum Moisture Content).

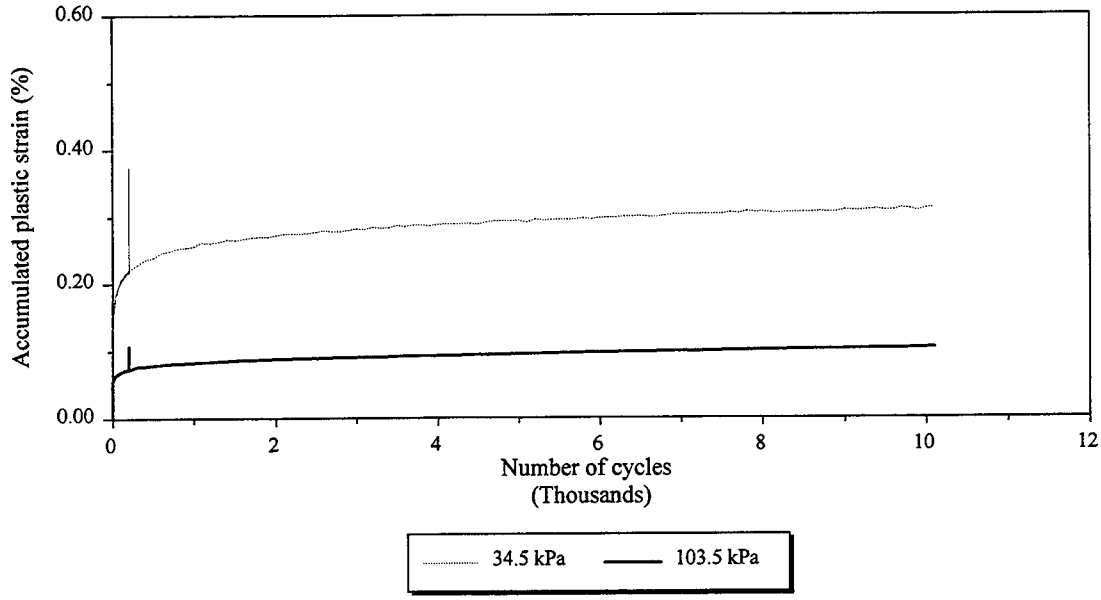

Figure C56. Effect of Confining Pressure on Accumulated Plastic Strain in Iron Ore Gravel (345.0 kPa Deviatoric Stress and at Dry of Optimum Moisture Content).

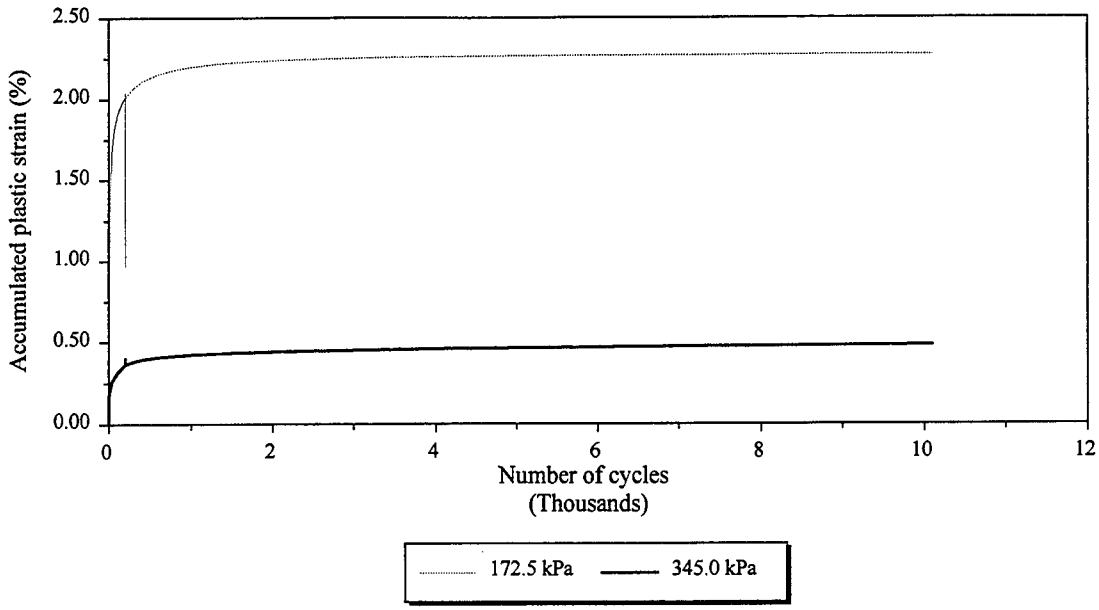

Figure C57. Effect of Deviatoric Stress on Accumulated Plastic Strain in Iron Ore Gravel (34.5 kPa Confining Pressure and at Wet of Optimum Moisture Content).

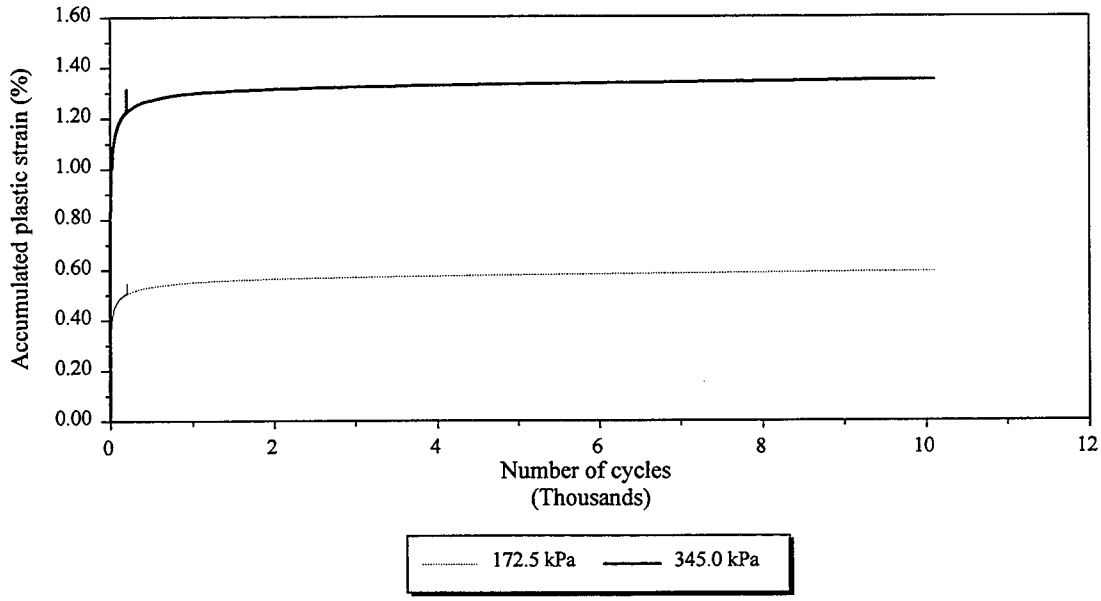

Figure C58. Effect of Deviatoric Stress on Accumulated Plastic Strain in Iron Ore Gravel (34.5 kPa Confining Pressure and at Optimum Moisture Content).

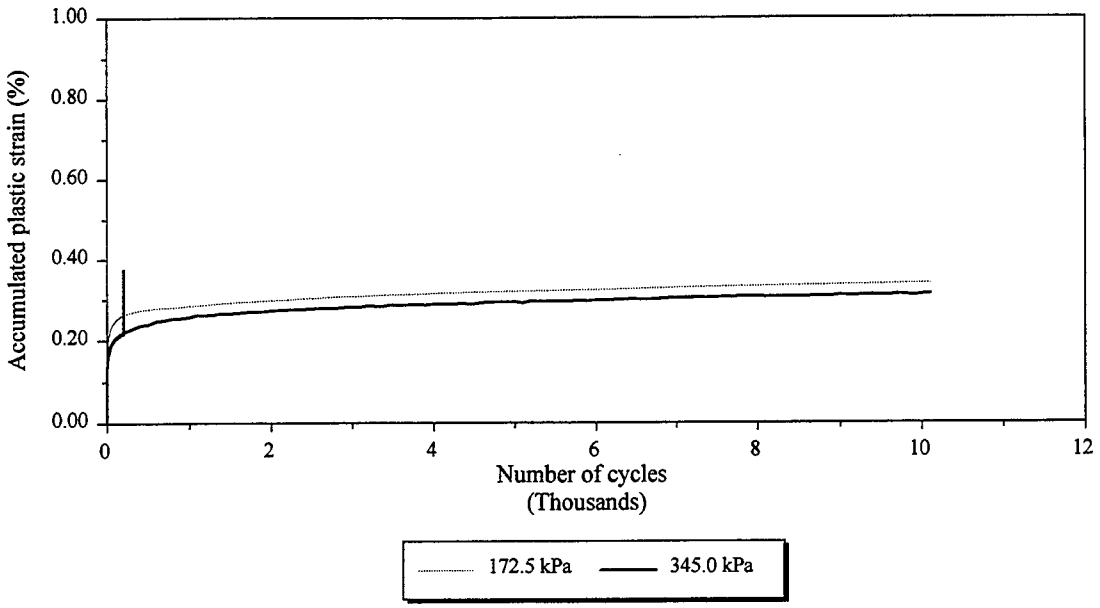

Figure C59. Effect of Deviatoric Stress on Accumulated Plastic Strain in Iron Ore Gravel (34.5 kPa Confining Pressure and at Dry of Optimum Moisture Content).

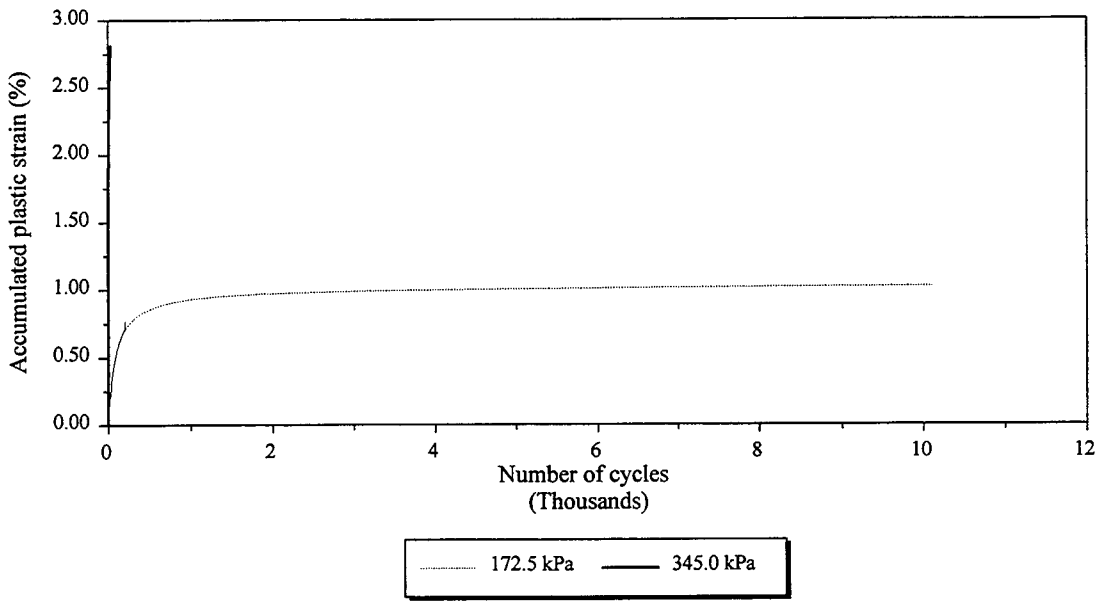

Figure C60. Effect of Deviatoric Stress on Accumulated Plastic Strain in Iron Ore Gravel (103.5 kPa Confining Pressure and at Wet of Optimum Moisture Content).

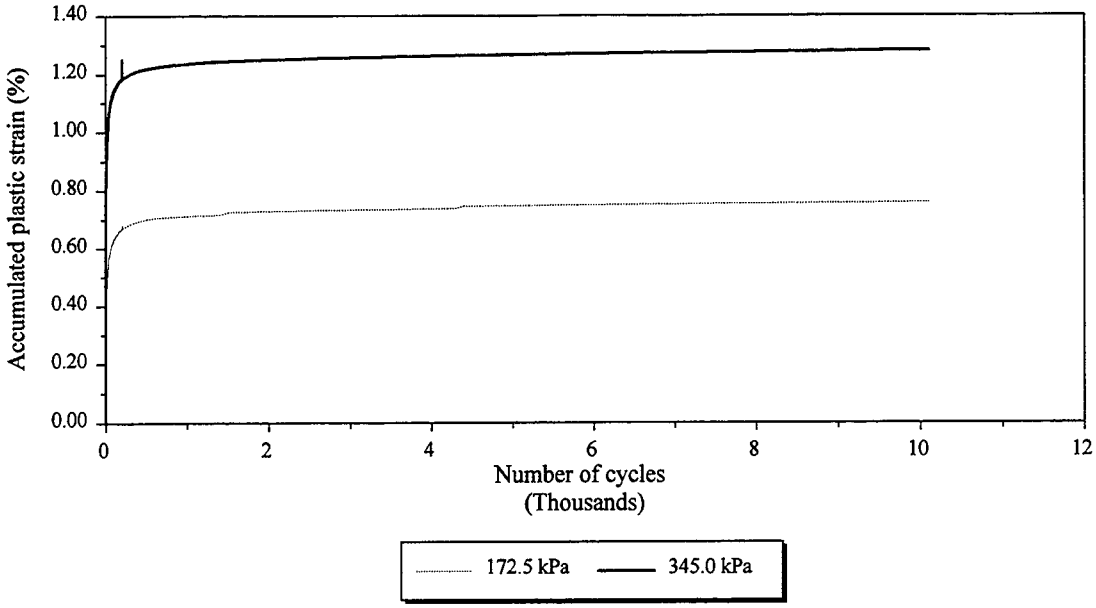

Figure C61. Effect of Deviatoric Stress on Accumulated Plastic Strain in Iron Ore Gravel (103.5 kPa Confining Pressure and at Optimum Moisture Content).

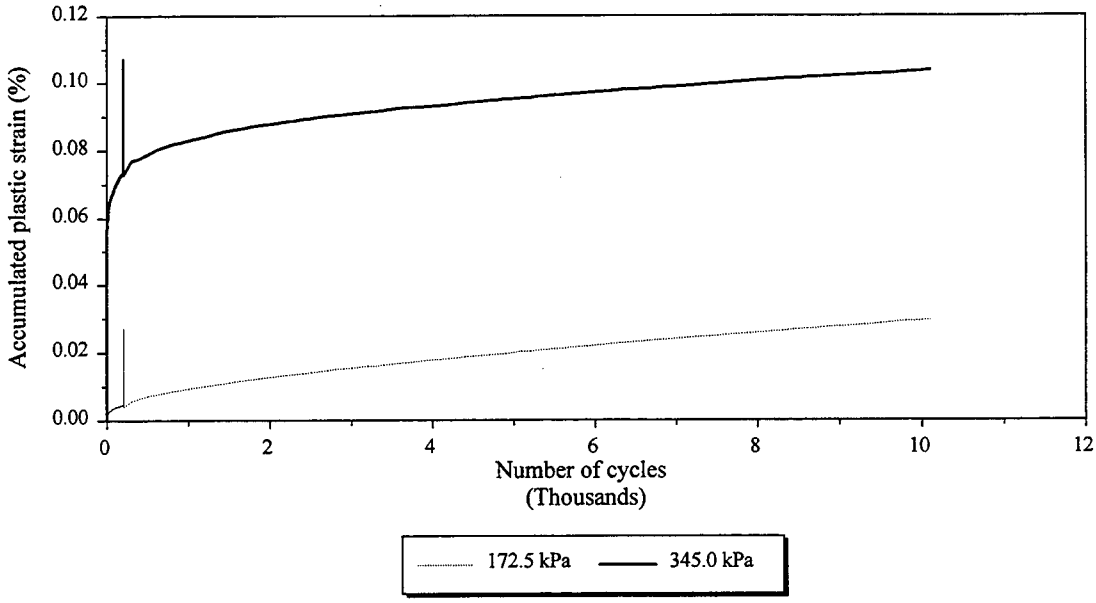

Figure C62. Effect of Deviatoric Stress on Accumulated Plastic Strain in Iron Ore Gravel (103.5 kPa Confining Pressure and at Dry of Optimum Moisture Content).